Characterization of amino acid ammonia lyases & aminomutases for the production of chiral α- and β-amino acids

Alana Dreßen

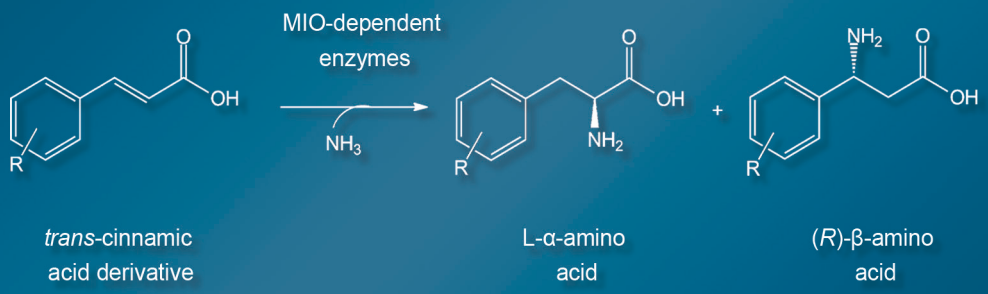

Schlüsseltechnologien / Key Technologies
Band / Volume 133
ISBN 978-3-95806-176-7

JÜLICH FORSCHUNGSZENTRUM

Member of the Helmholtz Association

Schriften des Forschungszentrums Jülich
Reihe Schlüsseltechnologien / Key Technologies Band / Volume 133

Forschungszentrum Jülich GmbH
Institute of Bio- and Geosciences
Biotechnology (IBG-1)

Characterization of amino acid ammonia lyases & aminomutases for the production of chiral α- and β-amino acids

Alana Dreßen

Schriften des Forschungszentrums Jülich
Reihe Schlüsseltechnologien / Key Technologies Band / Volume 133

ISSN 1866-1807 ISBN 978-3-95806-176-7

Bibliographic information published by the Deutsche Nationalbibliothek.
The Deutsche Nationalbibliothek lists this publication in the Deutsche
Nationalbibliografie; detailed bibliographic data are available in the
Internet at http://dnb.d-nb.de.

Publisher and Distributor:	Forschungszentrum Jülich GmbH Zentralbibliothek 52425 Jülich Tel: +49 2461 61-5368 Fax: +49 2461 61-6103 Email: zb-publikation@fz-juelich.de www.fz-juelich.de/zb
Cover Design:	Grafische Medien, Forschungszentrum Jülich GmbH
Printer:	Grafische Medien, Forschungszentrum Jülich GmbH
Copyright:	Forschungszentrum Jülich 2016

Schriften des Forschungszentrums Jülich
Reihe Schlüsseltechnologien / Key Technologies, Band / Volume 133

D 61 (Diss. Düsseldorf, Univ., 2016)

ISSN 1866-1807
ISBN 978-3-95806-176-7

The complete volume is freely available on the Internet on the Jülicher Open Access Server (JuSER)
at www.fz-juelich.de/zb/openaccess.

List of abbreviations

aa	amino acid
ACN	acetonitrile
AI	autoinduction
AL	ammonia lyase
AM	aminomutase
*At*PAL	phenylalanine ammonia lyase from *Arabidopsis thaliana*
bp	base pair
CA	*trans*-cinnamic acid
CCE	crude cell extract
*Cc*TAM	tyrosine aminomutase from *Chondromyces crocatus*
CDS	coding sequence
CFU	colony forming units
CLEA	cross linked enzyme aggregates
DCW	dry cell weight
ddH_2O	double deionized water
DNA	deoxyribonucleic acid
DSP	downstream processing
E. coli	*Escherichia coli*
ee	enantiomeric excess
FDC	ferulic acid decarboxylase
fw	forward
HAL	histidine ammonia lyase
His_6	hexahistidine fusion tag
IMAC	immobilized metal ion affinity chromatography
kb	kilobases

kDa	kilo Dalton
LB	Lysogeny broth
L-Phe	L-phenylalanine
L-Tyr	L-tyrosine
min	minutes
NMR	nuclear magnetic resonance
ORF	open reading frame
*Pc*PAL	phenylalanine ammonia lyase from *Petroselinum crispum*
PCR	polymerase chain reaction
PKU	phenylketonuria
PMMA	polymethylmethacrylate
*Rc*TAL	tyrosine ammonia lyase from *Rhodobacter capsulatus*
rpm	rotations per minute
*Rs*TAL	tyrosine ammonia lyase from *Rhodobacter sphaeroides*
RT	room temperature
*Rt*PAL	phenylalanine ammonia lyase from *Rhodosporidium toruloides*
rv	reverse
SDS-PAGE	sodium dodecyl sulfate polyacrylamide gel electrophoresis
*Sg*TAM	tyrosine aminomutase from *Streptomyces globisporus*
STY	space-time-yield
*Tca*PAM	phenylalanine aminomutase from *Taxus canadensis*
*Tch*PAM	phenylalanine aminomutase from *Taxus chinensis*
U	unit
v/v	volume/volume
w/v	weight/volume
wt	wild type

Table of contents

1 Abstract

1.1 English

Enantiopure non-natural amino acids are valuable building blocks for the production of chemicals and pharmaceuticals or are themselves pharmacologically active. Examples are 2-chloro-phenylalanine, a precursor for the production of a hypertension pharmaceutical and L-Dopa, which is used for the treatment of Parkinson desease or (*R*)-β-phenylalanine, which is part of the side chain of the antitumor drug Taxol. To get access to this class of compounds, a toolbox of MIO-dependent ammonia lyases and aminomutases was generated including four wild-type phenylalanine and tyrosine ammonia lyases (PAL/TAL), one variant with altered substrate specificity, and three wild-type phenylalanine and tyrosine aminomutases (PAM/TAM) from plants, yeast, and bacteria.

All ammonia lyases were comparatively characterized with respect to kinetic parameters, pH- and T-optima for the deamination reaction of their natural substrates. Scince the focus of this thesis was on the stereoselective amination of cinnamic acid (CA) derivatives to yield enantiopure α- and β-amino acids, the investigation of the substrate ranges and reaction parameters was the main goal. Among the tested ammonia lyases in the toolbox PAL from *Arabidopsis thaliana* (*At*PAL2), an enzyme which was not characterized in detail yet, performed best, compared to the enzymes from *Petroselinum cripsum* and *Rhodosporidium toruloides*, which are well studied and industrially applied. *At*PAL2 shows significant faster conversion of 3-F-CA (91.2 %), 4-F-CA (84.7 %) and 2-Cl-CA (96.4 %) in batch reactions. Due to the importance of 2-Cl-L-Phe as key intermediate for the production of hypertension drugs, this reaction was further investigated in larger scale using different reactor types and reaction modes. With a continuous enzyme membrane reactor the space-time-yield (STY) and productivity per catalyst (cell dry weight: CDW) could be enhanced from 11.8 g/L*d and 10.8 g/g_{DCW} in batch to 67.8 g/L*d and 46.8 g/g_{DCW}. The product 2-Cl-L-Phe could be isolated by simple volume reduction and crystallization with a yield of 57 % and high purity.

To improve the reusability of the *At*PAL2 an immobilization strategy using cellulose binding modules (CBMs) from *C. fimi* was investigated. *At*PAL2 fused with a C-terminal CBM immobilized on Avicel showed 81.5 % remaining activity in the amination of 2-Cl-CA after eleven 1 h batch reaction cycles. Furthermore *At*PAL2-CBM was immobilized on Avicel in a plug-flow reactor by simply pumping the *E. coli* crude cell extract containing the enzyme through a column filled with Avicel, which was afterwards directly used for biotransformation by pumping the substrate through the column. The STY reached 248.6 g/L*d and the productivity was 18.5 g/g_{DCW}.

The substrate range of the TAM from *Chondromyces crocatus* (*Cc*TAM), which was not described in detail until now, was investigated and compared to the PAMs from *Taxus canadensis* (*Tca*PAM) and the well-studied enzyme from *Taxus chinensis* (*Tch*PAM). Whole cells containing *Tca*PAM are less active compared to whole cells containing *Tch*PAM, due to

a lower expression level and produced more side-products. Both PAMs lead to the formation of a mixture of α- and β-amino acids, which is difficult to separate. *Cc*TAM has a less broad substrate range compared to PAMs, but produced only the desired (*R*)-β-amino acids in initial measurements. Therefore *Cc*TAM was investigated for immobilization studies to improve the handling of the enzyme by fusing the enzyme to the C-terminal CBM from *C. fimi*, but due to a strongly decreased soluble expression the fusion protein *Cc*TAM-CBM was not used for futher experiments.

1.2 Deutsch

Enantiomerenreine unnatürliche Aminosäuren sind wichtige Bausteine für die Herstellung von Chemikalien und Pharmazeutika oder sind selber pharmakologisch aktiv. Beispiel sind 2-chloro-Phenylalanin, eine Vorstufe für die Produktion von Blutdrucksenkern und L-Dopa, das zur Behandlung der Parkinson-Krankheit eingesetzt wird oder (*R*)-β-Phenylalanin, welches Bestandteil der Seitenkette des Antitumor-Medikaments Taxol ist. Um Zugang zu dieser Substanzklasse in unsere Arbeitsgruppe zu erhalten, wurde eine Toolbox mit Ammoniaklyasen (AL) und Aminomutasen (AM) erstellt werden, die den Kofaktor MIO enthalten. Diese Toolbox besteht aus vier Wildtyp Phenylalanin und Tyrosine Ammoniaklyasen (PAL/TAL), einer Variante mit geänderter Substratspezifität und drei Wildtyp Phenylalanin und Tyrosine Aminomutasen aus Pflanzen, Hefe und Bakterien.

Alle Ammoniaklyasen wurden vergleichend bezüglich der kinetischen Parameter, pH- und Temperaturoptima für die Deaminierung der natürlichen Substrate charakterisiert. Der Fokus dieser Arbeit liegt auf der stereoselektiven Aminierung von Zimtsäure (CA)-Derivaten zur Herstellung von enantiomeren reinen α- und β-Aminosäuren, daher war die Untersuchung des Substratspektrums und der Reaktionsparameter das Hauptziel. Von den getesteten Ammoniaklyasen zeigte die PAL aus *Arabidopsis thaliana*, welche bisher noch nicht näher charakterisiert wurde, die besten Umsätze verglichen mit den Enzymen aus *Petroselinum crispum* und *Rhodosporidium toruloides*, welche gut charakterisiert sind und industriell eingesetzt werden. *At*PAL2 zeigt schnellere Umsätze mit 3-F-CA (91.2 %), 4-F-CA (84.7 %) and 2-Cl-CA (96.4 %) in Batch Reaktionen verglichen mit den Referenzenzymen. Da 2-Cl-L-Phe ein wichtiges Intermediat für die Synthese von ACE Inhibitoren (Blutdrucksenkern) ist, wurde diese Reaktion im größeren Maßstab in verschiedenen Reaktoren und mit verschiedenen Betriebsweisen untersucht. Mit einem kontinuierlich betriebenen Enzym-Membranreaktor (EMR) konnten die Raum-Zeit-Ausbeute und die Katalysator-Produktivät von 11,8 g/L*d und 10,8 g Produkt pro g Katalysator im Batch, auf 67.8 g/L*d und 46.8 g/g im EMR erhöht werden. Das Produkt 2-Cl-L-Phe konnte durch einfache Volumenreduktion und Kristallisation mit einer Ausbeute von 57 % und hoher Reinheit isoliert werden.

Um die Wiederverwendbarkeit der *At*PAL2 zu erhöhen, wurde eine Immobilisierung an Cellulose über Cellulose-Binde-Module (CBMs) aus *C. fimi* untersucht. Das auf Avicel immobilisierte Fusionsprotein der *At*PAL2 mit einer C-terminalen CBM zeigte nach elf einstündigen 2-Cl-CA Aminierungsreaktionen im Batchreaktor eine Restaktivität von 81,5 %. Außerdem konnte das Fusionsprotein in einem mit Avicel befüllten Strömungsrohr-Reaktor direkt aus dem Rohextrakt immobilisiert werden, indem der *E. coli* Rohzellextrakt mit dem

Enzym durch den Reaktor gepumpt wurde. Nach der Immobilisierung wurde der Reaktor für die Aminierung von 2-Cl-CA verwendet. Die erreichte Raum-Zeit-Ausbeute lag bei 248,6 g/L*d und die Produktivität bei 18,5 g/g.

Das Substratspektrum der TAM aus *Chondromyces crocatus* (*Cc*TAM), das ebenfalls bis jetzt nicht im Detail beschrieben wurde, wurde untersucht und mit den PAMs aus *Taxus canadensis* (*Tca*PAM) und dem gut charakterisiertem Enzym aus *Taxus chinensis* (*Tch*PAM) verglichen. *Tca*PAM ist als Ganzzellkatalysator weniger aktiv als *Tch*PAM, aufgrund eines geringeren Expressionsniveaus und führt zu mehr Nebenprodukten. Beide PAMs führen zur Bildung einer Mischung von α- und β-Aminosäuren, die nur schwer zu trennen ist. *Cc*TAM hat ein weniger breites Substratspektrum im Vergleich zu den PAMs, allerdings wurden akzeptierte Substrate in ersten Messungen nur zur gewünschten (*R*)-β-Aminosäure umgesetzt. Daher wurde die *Cc*TAM ebenfalls mit einer CBM fusioniert, um die Handhabbarkeit im Prozess zu verbessern. Das Fusionsprotein *Cc*TAM-CBM wurde nur zu einem sehr geringen Teil löslich exprimiert, daher wurden mit diesem Fusisonsprotein keine weitern Versuche durchgeführt.

2 Introduction

2.1 Biocatalysis

Biocatalysis, also termed bioconversion or biotransformation is the usage of natural or modified isolated enzymes, enzyme extracts or whole cells as catalysts for the production of a variety of compounds from bulk to fine chemicals [1–3]. The importance of biocatalysis is rising, owing to an increasing public pressure on the development of "green" technologies. With respect to environmental issues there is a strong demand to replace chemical processes by safer, cleaner, and more ecofriendly biocatalytic processes [4,5]. Biocatalysis is generally regarded as greener because it works under mild conditions (moderate temperature, ambient pressure and physiological pH), is therefore less energy intensive and therefore more economic. Often less reaction steps are required because the protection and deprotection of functional groups is not necessary, thereby reducing waste and time [6,7]. But the most important advantage of biocatalysts is the high specificity [8]:

Regioselectivity: the property to distinguish between functional groups in different positions of the substrate molecule.

Chemoselectivity: the ability to act only on a single type of functional group in presence of other reactive functional groups.

Stereoselectivity: the ability to transform a prochiral substrate into an optically active product or to react only on one isomer of a racemic mixture

Especially the high stereoselectivity makes biocatalysts interesting for synthetic chemists, due to the need for enantiomerically pure compounds as building blocks for chemistry, agrochemicals and specifically pharmaceuticals [2,9,10]. Since 1992, the U.S. Food and Drug Administration (FDA) recommends the characterization of the individual enantiomers of a drug with regard to pharmacological activity and *in vivo* interconversion and disposition [11]. Application of only the desired enantiomer increases the efficiency and decreases the dosage and possible side-effects [2]. Today biocatalysis is a proven technology for the production of substances in the chemical and pharmaceutical industry [4], but for each production process the optimal combination of the biocatalyst preparation and reactor type has to be found, depending on the properties of the catalyst.

2.1.1 Enzyme preparation

An important decision to be made with regard to the biocatalyst is whether to use whole cells or isolated enzymes, because both systems have advantages and disadvantages [12] (Table 1). A huge advantage of whole cells is that they are cheaper than purified enzymes. Furthermore the cell wall can protect the enzyme against harmful reaction conditions and, in case of cofactor-dependent reactions the cofactor can often be recycled by other cellular enzymes. But the use of whole cells can be hampered by diffusion limitations over the membrane or by side-product formation. To minimize side-reactions the usage of purified enzymes are preferred, which are often more productive. However, chromatographic enzyme purification may increase the production cost of a biocatalyst up to 10-fold [13]. Furthermore, without the protecting cell wall stability can become an issue. Enzyme immobilization can help to overcome such disadvantages by stabilizing the biocatalyst. Moreover reusability and simplified downstream processing (DSP) decrease overall process costs [14]. In Figure 1 a short overview about immobilization strategies is given.

Table 1: Advantages and disadvantages of different enzyme preparations (according to [12,15])

preparation	advantage	disadvantage
whole cells[1,2]	no external cofactor regeneration[1] no enzyme purification[1,2] cell envelope protects enzyme[1,2] cheap[1,2]	diffusion limitations over the membrane[1,2] dependence on metabolic activity[1] side-product formation[1,2] often low productivity[1,2] sometimes low selectivity [1,2] cell lysis may impair DSP[1,2]
isolated enzyme	high productivity less side-reactions	low stability laborious and costly purification cofactor regeneration required
immobilized enzyme	stabilizes biocatalyst reusability possible easier downstream processing	enzyme leaching possible usually decrease in activity diffusion limitations (encapsulation)

1= metabolic active cell; 2= resting cell

2.1.2 Enzyme immobilization techniques

An important decision to stabilize the catalyst is to choose an appropriate immobilization technique. Immobilization techniques can be divided into three main categories: binding to an insoluble carrier, entrapment, and cross-linking (Figure 1) [16–18].

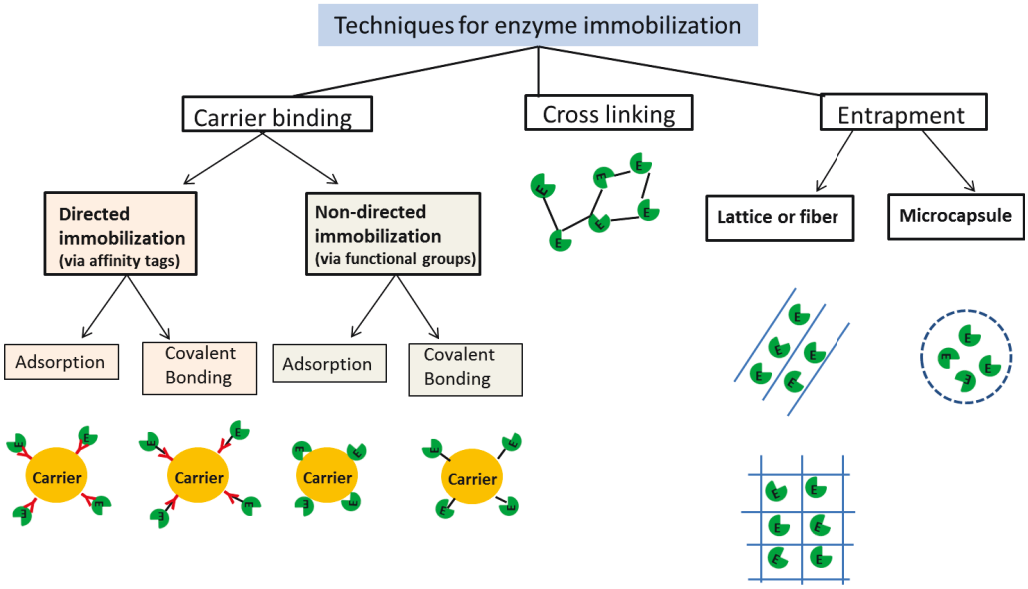

Figure 1: Overview about enzyme immobilization techniques

Cross-linking is a carrier-free immobilization technique, where the enzymes themselves are intermolecularily cross-linked via their side chains using a cross linking agent, for example glutaraldehyde. This ideally leads to insoluble enzyme preparations with concentrated activity in so-called cross-linked enzyme aggregates (CLEAS) [19–22]. The absence of carriers avoids costs and the dilution of the volumetric activity through the carrier, which can account for up to 99 % of the total weight of a carrier-immobilized biocatalyst. A drawback using CLEAs is the necessity to purify the enzymes before cross-linking to remove other proteins (as usual for many immobilization techniques) and the often low activity after cross-linking, when active site residues are involved [23–25]. Alternatively, enzymes or whole cells can be entrapped in different supports, like polymeric gels, fibers, lattice structures, and membranes [26–29]. Gelation of ionic polymers by adding counterions is the most common method to prepare these supports. Suitable polymers are for example alginate, collagen and gelatin [24,30]. The entrapment protects the biocatalyst from harmful environmental influences [25], improves its mechanical stability, but may also limit the mass transfer of the substrate to the active site. Further disadvantges are: enzyme leakage, abrasion of the support material, possible deactivation during the immobilization process, and low loading

capacity [24]. The third strategy is the catalyst binding to different carriers through directed immobilization (at a specific position in the enzyme, e.g. an affinity tag) or non-specific immobilization via functional groups present at the enzyme surface. Both techniques can be subdivided into covalent bonding or adsorption. Covalent immobilization is generally more stable and enables a better reusability than other methods, because enzyme leakage is prevented, but the correct orientation of the catalyst after binding on the carrier is crucial for activity. In case residues close or inside the active site are involved in matrix bonding the activity may be dramatically decreases. Physical adsorption through non covalent interactions is a simple, fast, but reversible immobilization [31]. When the catalyst activity decreases, the support can be regenerated and loaded with fresh enzyme. But the weak binding forces may also lead to enzyme desorption from the carrier during biocatalysis, which may contaminate the product. Furthermore, previous enzyme purification is necessary to ensure that only the desired enzyme binds to the carrier. More specific is here the binding via affinity tags. The interaction between the two binding partners is highly selective, minimizing the binding of other host proteins. The fixation leads to a controlled orientation of the catalyst on the surface, thereby retaining high activity. Depending on the carrier, this method is simple and cheap. Examples for affinity binding partners are glutathione S-transferase and glutathione, avidin and biotin, polyhistidine tag and metal ions [24,25,32] or carbohydrate-binding modules (CBM) and the respective carbohydrate, as described in the next chapter.

2.1.2.1 Carbohydrate-binding modules

CBMs are part of carbohydrate-active enzymes and mediate the binding of these enzymes to the cellulose-derived substrates. The close proximity to the substrate enhances the catalytic activity [33,34]. CBMs consist of 40-200 amino acids with molecular weights of 4-20 kDa [35,36]. CBMs can be divided into three binding types: type A (surface-binding), type B (glycan-chain-binding) and type C (small-sugar-binding). CBMs of type A exhibit a binding surface with a high content of aromatic amino acids, which bind via hydrophobic interactions to crystalline polysaccharides like cellulose and chitin [34]. Type A CBMs show low or no affinity towards soluble polysaccharides [37,38]. The fact that CBMs bind spontaneously to the respective carbohydrate makes them interesting as affinity tags, because no sample pretreatment is necessary [35], the binding is highly specific, and with less non-specific binding of other proteins [39]. Furthermore cellulose is a suitable carrier for immobilization because it is cheap, biodegradable, inert, commercial available in many different forms and general regarded as safe, because it is approved for pharmaceutical applications in medicine [36].

Therefore applications using CBM-fusions (tags) and cellulose as support for simultaneous purification and immobilization of enzymes directly from crude extract are on the rise. Wang *et al.* fused cis-epoxysuccinic acid hydrolase to five different CBMs and immobilized the

fusion proteins on Avicel (microcrystalline cellulose) within 5 minutes. All of them were active in the production of L-tartaric acid and the immobilization significantly increased the stability of the enzymes [40]. Velikodvorskaya *et al.* prepared lactase fusions with C- or N-terminal CBM, which were bound directly from crude cell extract on water swollen cellulose granules. The immobilized lactase with C-terminal CBM was applied in a small continuous-flow reactor. 10.000 column volumes substrate solution (150 mM lactose; 1 column volume per min) were hydrolyzed without a decrease in efficiency. And the fusion enzyme in the reactor was still active after six months storage at room temperature [41]. Kopka *et al.* fused a family 2 CBM from the exoglucanase/xylanase Cex from *C. fimi* to a hydroxynitrilase of *A. thaliana.* The fusion protein was bound to three different cellulose materials (Avicel, regenerated amorphous cellulose and cellulose acetate (CA)) directly from crude cell extracts and successfully used for the synthesis of (*R*)-mandelonitrile in micro-aqueous methyl *tert*-butyl ether [42].

2.1.3 **Reactor systems**

The second important decision to be made to set up a successful biocatalytic reaction is the selection of an appropriate reactor. Here the characteristic features of the biocatalyst have to be considered. Using metabolically active whole cells, the main purpose of the reactor is to ensure optimal conditions for the producing cell. For resting cells the main goal is to retain the cells and prevent inactivation and cell lysis. Whole cells are sensitive to shear forces and products of the cell metabolism may influence the biocatalyst. Besides, the biocatalytic activity strongly depends on external factors like temperature and concentrations of substrates and products. In case of substrate surplus or product inhibition, special reactor layouts have to be used. The three basic types of reactors are: stirred-tank reactor (STR, batch reactor), continuously operated stirred-tank reactor (CSTR), plug-flow reactor (PFR), and variations thereof [43]. These reactors are so-called “ideal chemical reactors”, simplified models of real reactors, with transport and mixing properties, which can be described mathematically exactly [44]. To generate a mathematical model for their quantitative description, mainly two major features have to be considered: the mode of operation (continuous or discontinuous) and the quality of mixing (ideal mixing or no mixing) [45].

Batch reactor

A batch reactor (Figure 2) is a closed system with a constant volume and no influent or effluent [44]. All substrates and the biocatalyst are added at the beginning of the reaction. During biotransformation the substrate concentration decreases and the product concentration increases over time. Due to the ideal mixing the substrate- and product concentration, at a defined timepoint t_1, is constant in each volume element. Because of the high substrate concentrations at the beginning and the high product concentration in the

end, a batch reactor is not suitable, in case of inhibition caused by the substrate or product [43].

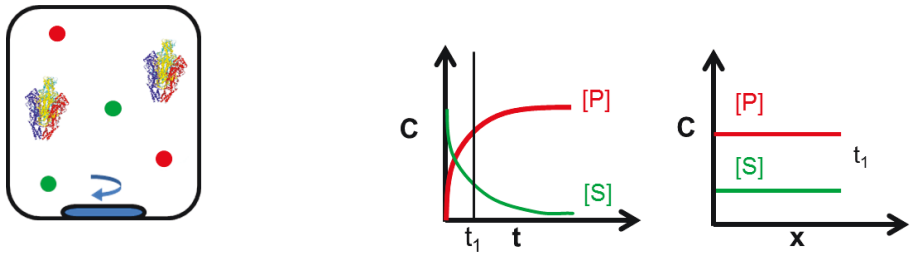

Figure 2: Schematic presentation of a batch reactor using isolated enzyme (left) and respective time- and space dependent concentration profils (right). t: time, C: concentration, x: space, [P] product concentration (red), [S] substrate concentration (green).

In case of substrate surplus inhibition a fed-batch reactor (Figure 3) is more suitable. Here only the biocatalyst is added with a part of the substrate solution at the beginning of the reaction to keep the substrate concentration below the inhibition constant. A concentrated substrate solution is feeded over time to compensate substrate depletion through the biotransformation. Owing to the ideal mixing and the substrate conversion, the substrate concentration in the reactor is low during the whole process, thereby ensuring maximal enzyme activity. In contrast to the batch reaction the volume increases continuously. The process is stopped when the maximum reactor volume is reached.

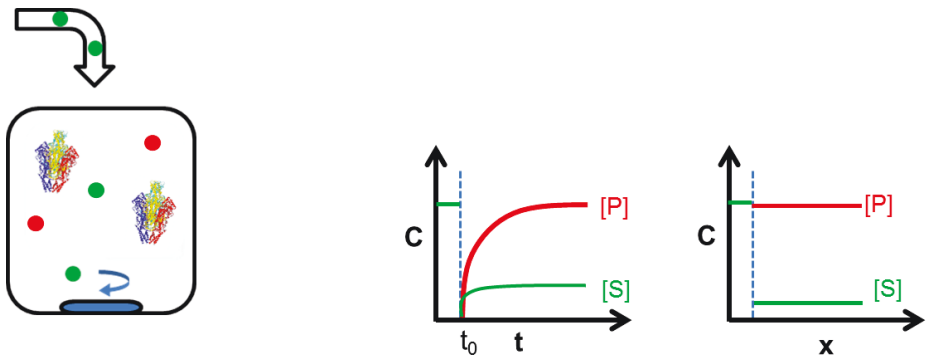

Figure 3: Schematic presentation of a fed-batch reactor using isolated enzyme (left) and respective time- and space dependent concentration profils (right). t: time, C: concentration, x: space, [P] product concentration (red), [S] substrate concentration (green).

Continuous enzyme membrane reactor

An enzyme membrane reactor (EMR; Figure 4) is a continuously operated stirred tank reactor adapted to biocatalysts. The biocatalyst (enzyme or whole cell) is retained by a membrane inside the reactor [46] whereas it is permeable for substrates and products.

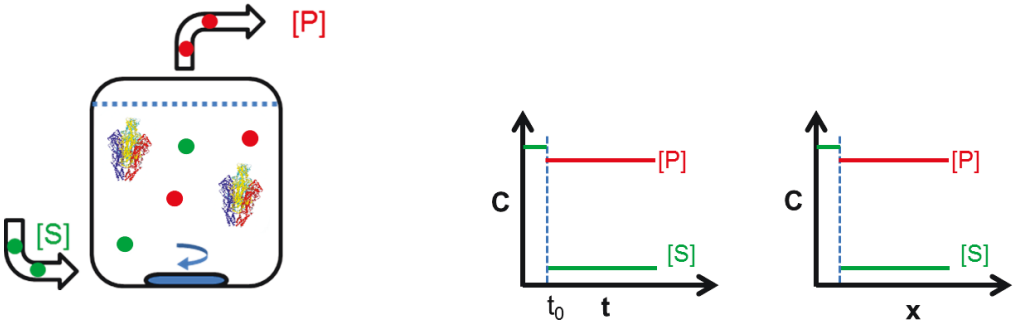

Figure 4: Schematic presentation of an enzyme membrane reactor using isolated enzyme. The biocatalyst is retained by a membrane (left, dotted line) and respective time- and space dependent concentration profils (right). t: time, C: concentration, x: space, [P] product concentration (red), [S] substrate concentration (green).

As in the fed-batch mode, a concentrated substrate solution is pumped into the EMR. Under ideal conditions (ideal mixing and constant biocatalyst activity) and at steady state the concentrations of substrate and product are constant at each time point and in each volume element. Continuous reactors work under efflux conditions, meaning that the concentrations of substrates and products at the outlet are the same as in each volume element in the reactor. The conversion in an EMR can be controlled by the catalyst amount or the residence time. Continuous reactors are specifically useful to overcome limitations caused by substrate surplus inhibition of the catalyst [43].

Plug-flow reactor

A plug-flow reactor contains a fixed catalyst bed (Figure 5) and is not mixed therefore the substrate concentration at the reactor inlet is high. The substrate concentration decreases over the length of the reactor and the product accumulates. At a defined place x_1 in an ideal reactor, product and substrate concentration are in steady state. A plug-flow reactor should not be used if substrate or product inhibition occurs [43].

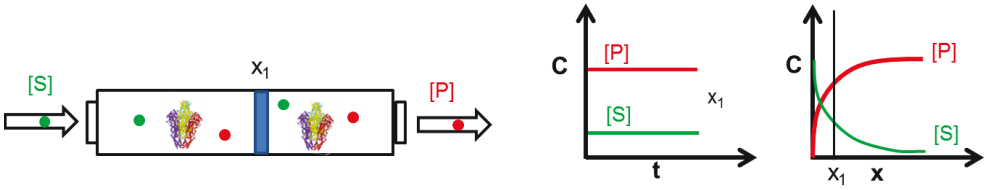

Figure 5: Schematic presentation of a plug-flow reactor using isolated enzyme (left) and respective time- and space dependent concentrations (right). t: time, C: concentration, x: space, [P] product concentration (red), [S] substrate concentration (green).

2.1.4 Productivity measures of biocatalytic processes

To compare different biocatalytic reactions in different reactors, several process performance indicators can be calculated such as: yield, final product concentration, space-time-yield (Equation 1), and catalyst productivity (Equation 2). According to Straathof *et al.* [47] successful product developments in the chemical industry involve on average a yield of 78 %, a volumetric productivity of 372 g/(L*d) and a final product concentration of 108 g/L. Another metric is the catalyst productivity, which according to Pollard and Woodley should reach at least 1000 for an enzyme and 15 for a whole-cell system (reflecting the different costs of each) [6].

Equation 1

$$space - time - yield\ [\frac{g}{L * d}] = \frac{mp}{Vr * t}$$

mp = mass of product produced [g]
Vr = reactor volume [L]
t = reaction time [h]

Equation 2

$$catalyst\ productivity\ [\frac{g}{g}] = \frac{mp}{mc}$$

mp = mass of product produced [g]
mc = mass of catalyst consumed [g]

2.2 Fine chemicals

Fine chemicals are high value products (> 10 $/kg) with several functional groups that are only produced in small scale (< 1000 t per year). Examples for fine chemicals are vitamins, agrochemicals, pigments, peptides, proteins, oligonucleotides, antibodies, glycoproteins, and amino acids [1]. They have only few applications and are mainly intermediates, which are further processed and therefore have to be of high purity [1,48]. In 2014 the total sales of the german chemical industry was 145.2 billion €, of which 27 % (39.7 billion €) accounted for fine- and speciality chemicals (Figure 6).

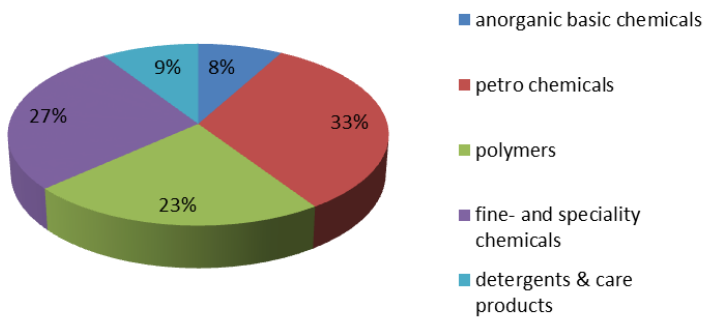

Figure 6: Shares of the total sales of the german chemical industry by sectors in 2014. (Source: VCI, "Chemiewirtschaft in Zahlen 2015") [49]

2.2.1 Biocatalytic synthesis of amino acids

The synthesis of enantiopure amino acids is an attractive target for the chemical industry, because amino acids are building blocks for a variety of products ranging from absorbents over pharmaceuticals to key components of human and animal nutrition. Best known are the 20 natural proteinogenic amino acids, which build up proteins. Natural amino acids are mainly produced by fermentation [50,51]. The main amino acids produced for animal nutrition are: L-lysine, L-threonine and L-tryptophan. Due to an increase in meat consumption in many countries there is the necessity for increased livestock production without waste of feed protein. L-lysine is often the first limiting amino acid in pig feed, and is therefore added to the feed [51,52]. L-lysine is mainly produced by the fermentation of *C. glutamicum* in fed-batch mode in fermenters with up to 500 m^3 volume and production capacities up to 100,000 tonnes. In similar quantities L-glutamic acid is produced for the food industry as flavoring agent (monosodium glutamate)[53], but also large amounts of L-Phe are needed for the production of the synthetic sweetener aspartame [54]. L-Phe is generally produced in *E. coli* [51,55], whereas L-Tyr is produced with *C. glutamicum* [51]. Even more important are dietary

supplements consisting of several amino acids, which are produced for performance athletes and body-builders or (together with vitamins, minerals and carbohydrates) as medical nutrition for artificial nutrition of patients [51].

All other non-proteinogenic amino acids are often referred to as non-natural amino acids, even if they were isolated from natural scources [50]. One example is the non-natural amino acid (*R*)-β-phenylalanine, which can be isolated from yew trees and is part of the side chain of Taxol, a potent drug for the treatment of breast, lung and ovarian cancer [56]. β-amino acids isolated from natural source are mainly derived from L-amino acids via intramolecular rearrangement of the α-amino group to the β-position, C–C-bond rearrangement of glutamate, decarboxylation, and Michael addition to dehydroalanine [57]. Further examples for pharmaceutical relevant amino acids are L-Dopa (3,4-dihydroxy-L-phenylalanine) for the treatment of Parkinson's disease [58–60] and 2-chloro-L-phenylalanine, which is further processed to yield (*S*)-2-indolinecarboxylic acid, a key intermediate for hypertension drugs [61]. Non-natural amino acids can be produced biocatalytically by several enzymes: aminopeptidases, nitrilases, acylases, lipases, hydantoinases [62,63], transaminases [64,65], ammonia lyases and aminomutases [66,67]. Some examples are are presented in Figure 7. All processes have their advantages and disadvantages. Using lipases and kinetic resolution starting from racemic substrates the yield is limited to 50 %, but the enzymes have a broad substrate range. Starting from hydantoin, two enzymes are involved, requiring product isolation after the first step or laborious cascade optimization. Transaminases act on cheap prochiral substrates, but require additional complex amine donors. Further, the yield is limited by the thermodynamic equilibrium.

Since several decades ammonia lyases and aminomutases are on the rise for the production of non-natural amino acids, especially those sharing the autocatalytically formed cofactor methylideneimidazole-5-one (MIO), which are in focus of this thesis and described in more detail in the next chapter. The MIO-cofactor is actually a prostetic group as it is covalently bound in the active site. This and the fact that no external cofactor regeneration is necessary make MIO-enzymes specifically useful for the application of enzyme immobilizates. They act on cheap achiral α,β-unsaturated carboxylic acids as substrates and use ammonia as a cheap ammonia source. Theoretically ammonia lyases can reach 100 % yield of the desired product, although the formation of amino acids is thermodynamically disfavoured.

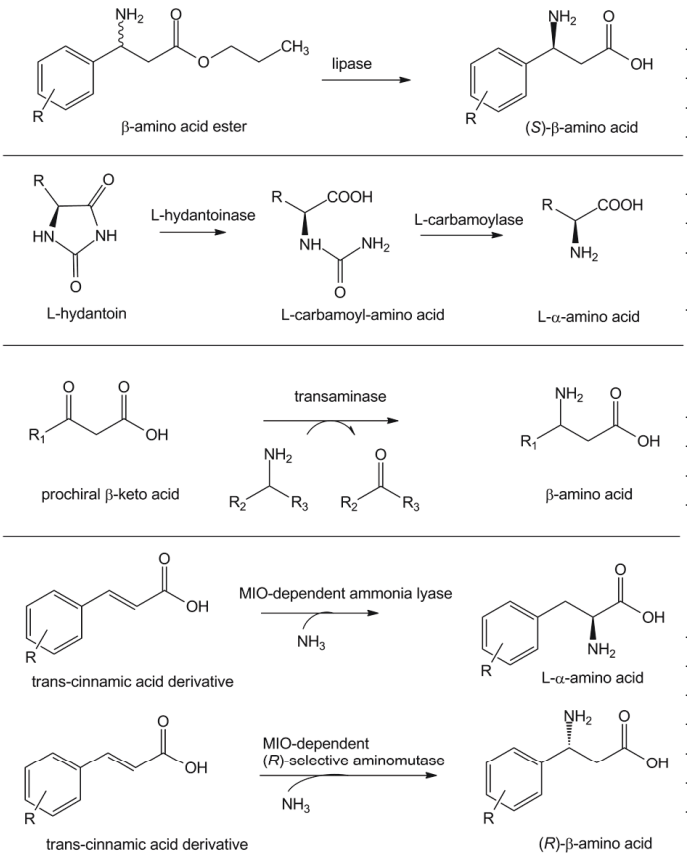

Figure 7: Different enzymatic routes to chiral non-natural amino acids and their advantages and disadvantages adapted from [63–66,68,69].

2.3 MIO enzymes

Ammonia lyases (AL) and aminomutases (AM) share the common cofactor methylidene-imidazole-5-one (MIO). Specifically those enzymes catalyzing the synthesis of aromatic α- and β-amino acids are important for green routes to the industrial production. The two enzyme classes share highly similar sequences and structures. The MIO-cofactor is formed autocatalytically after proteinbiosynthesis through the cyclization of a Ala-Ser-Gly tripeptide in the active site, by a condensation reaction (Figure 8) [66,70].

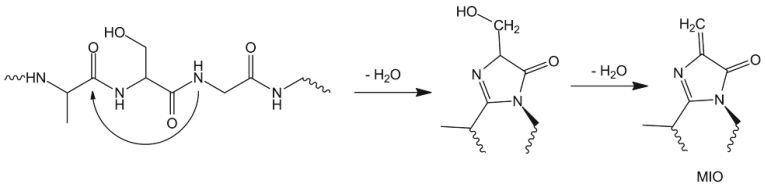

Figure 8: Formation of the MIO prosthetic group (adapted from [71]).

The cofactor serves as electrophile in the reaction mechanism. Because the mechanism is not clearly elucidated yet, two different reaction mechanisms are proposed for MIO-dependent enzymes [72,73]. In the E1cB mechanism (Figure 9, a) the electrophilic cofactor attacks the amino group of the α-amino acid to form a MIO-amine adduct with *trans*-cinnamic acid (t-CA) as an intermediate. In case of ALs, t-CA and NH_3 are released as products. In the AM reaction readdition of NH_3 at the β-carbon atom occurs, yielding the respective β-amino acid [74]. In the second proposal, a Friedel Craft-type mechanism (Figure 9, b), the aromatic ring is attacked by MIO and the proton in β-position is activated and abstracted. Subsequently, the ammonia elimination takes place. In the mutase reaction ammonia is afterwards bound stereospecific in β-position [75].

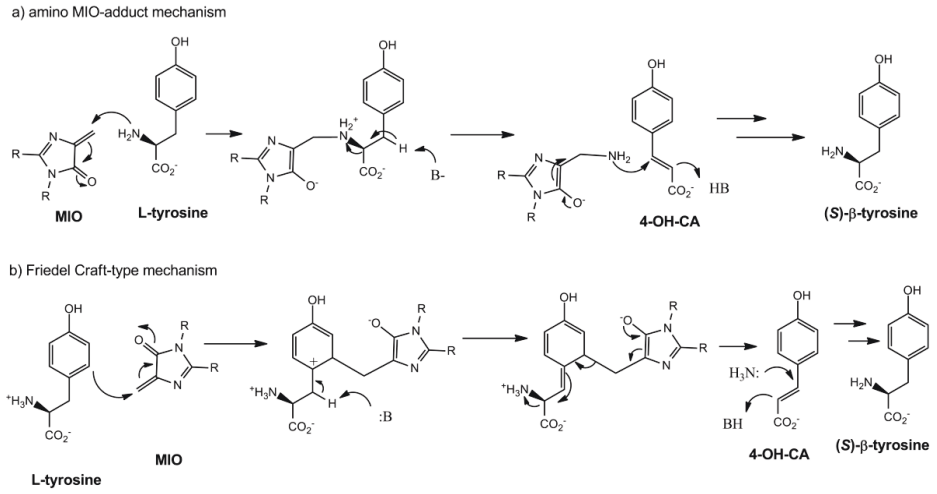

Figure 9: Proposed reaction mechanisms for MIO-enzymes (adapted from [74])

Following the properties of the MIO-enzymes PAL, TAL, PAM and TAM, which are studied in this thesis, are described in detail.

2.3.1 Phenylalanine ammonia lyases (PAL) and Tyrosine ammonia lyases (TAL)

PALs and TALs are found in plants, fungi, and prokaryotes. Their natural role is the deamination of L-phenylalanine or L-tyrosine to the corresponding cinnamic acid derivatives (Figure 10). In higher plants PAL is the key enzyme of the phenylpropanoid pathway where cinnamic acid is further metabolized to various phenylpropanoids [76]. Phenylpropanoids are a diverse group of compounds that are involved in plant defense, structural support, and survival [77]. Probably because of the importance of this reaction, plants can produce several PAL isoenzymes, which differ in sequence, but catalyze the same reaction. In *Arabidopsis thaliana* four PAL isoenzymes are known, all of them catalyze the deamination of L-Phe [78].

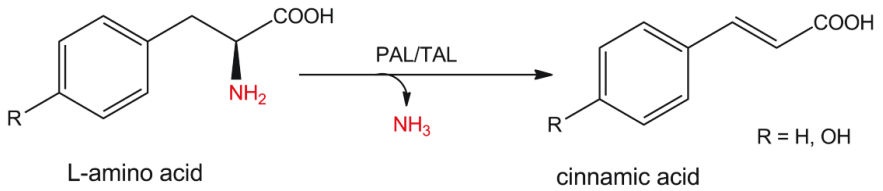

Figure 10: Physiological reaction of PALs and TALs.

(S)-α-phenylalanine (Cahn-Ingold-Prelog nomenclature) is a synonym for L-phenylalanine according to the Fischer nomenclature, which is still more common for amino acids and sugars until today.

The crystal structures of several ALs are known. PALs and TALs are similar in tertiary and quaternary structure. The sequence identity between TAL from *Rhodobacter sphaeroides* (*Rs*TAL) and PAL from *Rhodosporidium toruloides* (*Rt*PAL) for example is 30 %, but *Rs*TAL (523 amino acids (aa) per subunit) lacks an additional domain, which is present in the C-terminal region of *Pc*PAL and *Rt*PAL (both 716 aa). All PALs are homotetramers with four active sites consisting predominantly of α-helices. Three different monomers form one active site cavity [79]. As an example the active site of *Pc*PAL is shown in Figure 11 consisting of a hydrophobic pocket and a hydrophilic binding site. The hydrophobic pocket contains mainly non polar amino acids, which stabilize the aromatic ring of the substrate [80]. A key amino acid is phenylalanine in position 137. This amino acid points directly towards the aromatic ring and can be seen as selectivity switch. In TALs this position is occupied by a histidine forming a hydrogen bond to the *para*-hydroxy group of L-Tyr. By exchanging the respective histidine (His 89) in *Rs*TAL to a Phe, the preference of the enzyme could be switched from L-Tyr to L-Phe [79]. One exception is *Rt*PAL, a bifunctional enzyme converting both L-Tyr and L-Phe, and carrying a histidine in this position [81]. Besides, the hydrophilic carboxylic-acid and amine binding site contains hydrogene bond forming amino acids that are able to stabilize both functionalities of the substrate. The hydrogen bond network seems to be essential for activity and is sensitive to mutations [80]. The active site is covered by a lid-like loop, which contains a tyrosine that acts as the catalytic base [67].

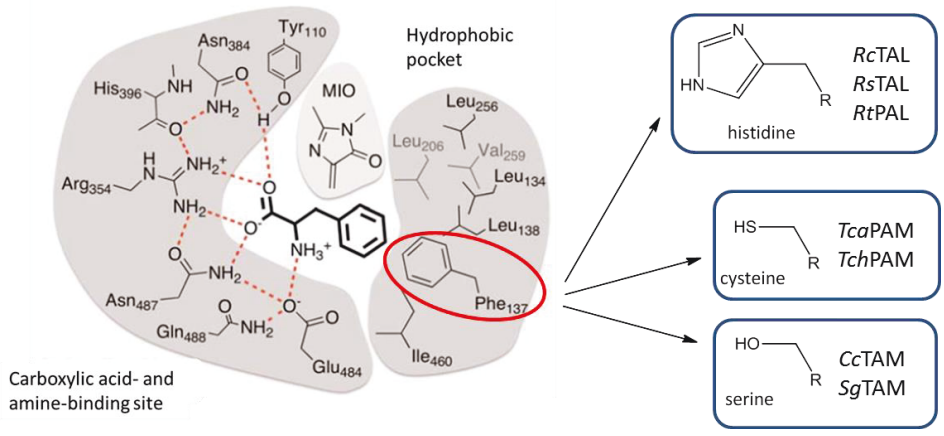

Figure 11: Active site of *Pc*PAL with bound substrate L-Phe (adapted from [80]) and differences in the selectivity switch region (Phe 137) in other MIO-dependent wt enzymes.

In 1968 the reversal of the physiological PAL reaction could be demonstrated for the first time. PAL can also be used for the synthesis of amino acids, but the equilibrium for L-Phe production is thermodynamically unfavorable. The equilibrium constant is 4.7 M, which makes it necessary to work at ammonia concentrations higher than 4.7 M to achieve good

conversions [82]. Further challenges working with ALs are low stability towards the harsh conditions during amino acid synthesis (high pH, high ammonia and substrate concentration), substrate inhibition, and a limited substrate range, mainly focusing on analogues closely related to the natural substrate [66,80,83]. One advantage of these enzymes is the asymmetric amination reaction, using cinnamic acids, which are cheap substrates with the possibility to reach 100 % yield and *ee*. Furthermore, no complex amine donors and no external cofactor recycling are necessary [67,80], which is especially interesting with regards to the application of these enzymes as immobilizates and in continuous reactions.

2.3.2 Phenylalanine aminomutase (PAM) and Tyrosine aminomutase (TAM)

Like the homologous ALs, PAMs and TAMs can be found in plants, bacteria, and fungi [67]. The physiological reaction is the reversible conversion of (*S*)-α-amino acids to ß-amino acids, by exchanging an amine substituent and a hydrogen atom residing on neighboring carbon atoms (Figure 12) [84,85]. β-amino acids are important precursors for the synthesis of several bioactive compounds with antibiotic and antitumor properties. In yews, for example *Taxus chinensis*, PAM catalyzes the synthesis of (*R*)-β-Phe, which is integrated in the side chain of the anticancer drug Taxol [86]. In the bacterium *Streptomyces globisporus* a TAM is involved in the synthesis of the (*S*)-3-chloro-4,5-dihydroxy-β-Phe moiety of the antitumor antibiotic C-1027 [87].

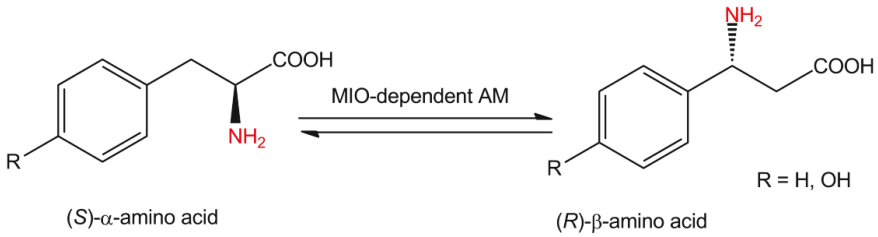

Figure 12: Physiological reaction of MIO-dependent aminomutases[84]. The stereochemistry of the β-amino acid depends on the enzyme used and can also be *S*-selective.

The crystal structures of PAM from *Taxus canadensis* (*Tca*PAM) and TAM from *Streptomyces globisporus* (*Sg*TAM) show homotetramers, which strongly resemble those of the AL structures [88,89]. PAM from *Taxus chinensis* (*Tch*PAM) shows a sequence identity of 97 % to *Tca*PAM [67] and therefore its crystal structure is likely also highly similar. Most of the residues forming the active site of AMs are highly conserved in all known MIO enzymes [88]. But as already shown for the ALs, the enzymes differ in selectivity switch region in the hydrophobic binding pocket (Figure 11) [90]. In most PALs this position is occupied by a phenylalanine residue, TALs contain a histidine in this position, whereas in PAMs a cysteine and in TAMs a serine is present [81,91–93]. Wu *et al.* demonstrated that the substrate selectivity of *Tch*PAM can be changed by single point mutations in this position. The variant

C107S showed still full activity towards (*S*)-α-phenylalanine but gained activity towards (S)-α-tyrosine with an excellent stereoselectivity for the product (*R*)-β-tyrosine (*ee* > 99 %) [93].

Similar to PAL and TAL, AMs can be used for the direct amination of cinnamic acid derivatives, because cinnamic acid occurs also as an intermediate in their reaction mechanism (Figure 9). In presence of high ammonia concentrations in the solution, the ammonia can be added directly to the cinnamic acid to give the respective α- and β-amino acids. The ratio of α- and β-amino acids depends on the substituent at the aromatic ring. Wu *et al*. investigated different *para*-substituted cinnamic acid derivatives as substrates for *Tch*PAM and discovered that an electron-donating group like methyl shifted the regioselectivity to the β-position (only 4 % α-amino acid), while a strongly electron-withdrawing nitro group promoted ammonia addition to the α-position (98 % α-amino acid) [94].

Challenges hampering the widespread application of aminomutases at large scale are: low activities (k_{cat} < 0.1 s^{-1}), reduced yields caused by the equilibrium between α- and β-amino acids, and the difficult separation of the desired product from a mixture of products [95,96]. Especially in case of TAMs, which show a β-Tyr racemase activity after prolonged incubation during the isomerization of L-Tyr, leading to a mixture of both β-amino acid isomers and up to 30 % of the corresponding cinnamic acid [97].

2.3.3 **Application of MIO enzymes**

The industrial application of MIO-dependent enzymes focusses mainly on ALs, which is reflected in the big number of patent applications. Following some examples for the production of amino acids are shown. DSM for example is using a PAL from *R. glutinis* in a chemoenzymatic process for the production of (*S*)-2-indolinecarboxylic acid, which is an intermediate for the production of hypertension pharmaceuticals (Figure 13) [61].

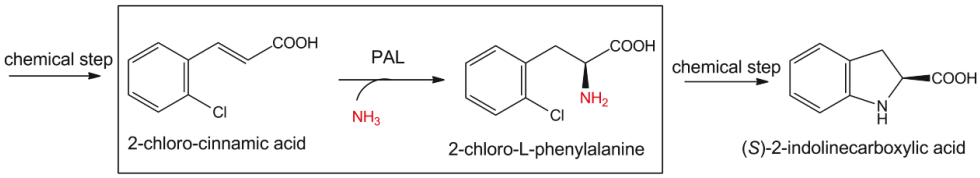

Figure 13: Process for the production of (*S*)-2-indolinecarboxylic acid by DSM

Already in 1985 Genex established a large scale process for the production of L-phenylalanine from cinnamic acid using PAL containing *R. rubra* cells in ammonium carbonate. This buffer can be removed from the product by evaporation and reused after condensation [98]. Mitsui Chemicals Inc. manufactures (*S*)-β-Phe from the corresponding (S)-α-amino acid with several recombinant aminomutases (*Sg*TAM, *Cc*TAM, *Tch*PAM) [99]. In

2011 the hydroamination of C-C double bonds with *Pc*PAL and *Rg*PAL for the production of aromatic amines was investigated and patented by BASF, although detailed information on the respective mutations is missing. Also the usage of several PALs, TALs, and HALs for the production of bulk and fine chemicals for industrial, agricultural and medical application was recently patended by BASF [100,101].

Also the natural deamination activity of ALs is used in several processes. Phytogene Inc. produces styrene (a building block used for the production of plastic, rubber, automobile, and boat parts) from renewable sources like glucose, using fusion proteins of PAL1, PAL2 or PAL4 from *A. thaliana* and a cinnamic/ferulic acid decarboxylase (FDC) from *S. cerevisiae*. A phenylalanine overproducing strain is transformed with a vector containing the gene encoding a PAL-FDC fusion protein and after expression the strain is cultured in a medium containing a carbon source to produce phenylalanine. The phenylalanine is deaminated by PAL to cinnamic acid and afterwards the cinnamic acid is decarboxylated by FDC to styrene [102]. Eviagenics S.A. developed recombinant yeast host cells, containing a PAL in a multienzyme complex for the biosynthetic production of vanillin, one of the most important aromatic flavor compounds used in perfumes, foods, and beverages. PAL catalyzes the deamination of phenylalanine to cinnamic acid, which is further metabolized using cinnamic acid hydroxylase (C4H), cytochrome P450 reductase (CPR), a CoA ligase, a crotonase, a 3-monooxygenase, and a methyltransferase to yield vanillin. According to the website of Eviagenics (www.eviagenics.com), the process was sold in June 2015 to a large industrial partner [103]. In a similar manner Evolva is manufacturing Resveratrol with yeast, fungi or bacteria containing a multienzyme complex with PAL, cinnamate 4-hydroxylase (C4H), 4-coumarate-CoA ligase (4CL) and resveratrol synthase (VST). Resveratrol has antifungal, cardioprotective- and cancer chemopreventive activities [104].

In medicine PAL and TAL are investigated as enzyme substitution therapy in patients with phenylketonuria (PKU) and tyrosinemia. PKU is a metabolic genetic disorder in which the phenylalanine-converting enzyme phenylalanine hydroxylase is not functional, leading to high L-Phe concentrations in the blood. If PKU is not treated early, significant medical problems including intellectual disability, microcephaly and seizures occur. Similar to PKU tyrosinemia is characterized by elevated blood levels of tyrosine, due to the deficiency of an enzyme required for the catabolism of tyrosine in the liver. Codexis Inc. engineered ALs from different organisms including *R. toruloides* and *A. variabilis*, to generate enzymes with enhanced catalytic activity, reduced sensitivity towards human proteases, and increased tolerance towards acidic pH present in the stomach. Different AL formulations were tested ranging from oral administration including pills, emulsions, chewing gums to implants, patches, sprays, and injection [105]. The Sydney Children's Hospital Network recently patented genetically modified probiotics for the treatment of PKU. Lactic acid bacteria expressing PAL, for example from parsley, were admistered to mice and lowered phenylalanine concentrations in blood. This may be a promising approach for treating PKU in humans in the future [106,107].

2.4 Aim of the work

The aim of this thesis was to create a toolbox for ammonia lyases and amino mutases, which are new enzymes for our working group, in order to access aromatic α- and β-amino acids. Chiral amino acids are important precursors for pharmaceuticals or are themselve pharmaceutically active. Therefore appropriate enzymes from different organism had to be selected from literature, produced in *Escherichia coli*, purified, and characterized. Therefore, Assays and HPLC analytics to monitor enzyme activity, substrate and product concentrations, and product *ee* must be established to compare the properties of already well studied and new enzymes.

The characterization included the investigation of pH- and temperature optima as well as kinetic data to identify optimal reaction conditions for the production of valuable amino acids. Afterwards a thorough characterization of the substrate spectra starting with different substituted α,β-unsaturated aromatic cinnamic acids should be performed to identify interesting targets. MIO-enzymes exhibit a comparatively low activity and the reactions are hampered by non-favourable equilibria. As a thorough comparison of reactor types and reaction conditions was not yet performed in literature, a further task of this thesis was to analyze the preformance of selected enzymes in preparative synthesis of selected target compounds including downstream processing.

In order to ease the enzyme application, immobilization of the enzymes was a further important subject of this project. An immobilization strategy using CBMs for the direct immobilization from crude cell extracts onto cellulose carrier should be investigated. This technique was selected, because cellulose is a green and ecofriendly carrier. Furthermore the immobilization of PAL on cellulose could be also a promising technique for the treatment of phenylketonuria, a metabolic disorder. PAL is already extensively investigated for the treatment of phenylketonuria in different pharmaceutical formulations. Applicability of the immobilizates in biocatalytic amination reactions and their reusability should be examined.

3 Material & Methods

3.1 Material

3.1.1 **Chemicals**

Table 2: Chemicals used in this thesis

name	**manufacturer**
acetic acid	Merck
acetonitrile	Biosolve
agar-agar	Roth
agarose	Roth
ammonia 32%	Merck
ammonium carbonate ($(NH_4)_2CO_3$)	Sigma
ampicillin disodium salt	Roth
Avicel PH-101	Sigma
bovine serum albumin (BSA)	Sigma
calcium chloride dihydrate ($CaCl_2$*2 H_2O)	Merck
chloramphenicol	Merck
cOmplete ULTRA Tablets, Mini, EDTA-free, Easypack	Roche
Coomassie Blue G-250	Fluka
D-glucose	Roth
diethylamine	Sigma
dipotassium hydrogen phosphate (K_2HPO_4)	Roth
EDTA	Serva
ethanol (EtOH)	Roth
ethidium bromide	Merck
FastRuler High Range DNA Ladder	Thermo Fisher Scientific
formic acid	Sigma
GelPilot DNA Loading Dye (5x)	Qiagen
glycerol	Roth
imidazole	Roth
isopropyl β-D-1-thiogalactopyranoside (IPTG)	Roth
kanamycine sulphate	Roth
lactose monohydrate	Roth
L-arabinose	Sigma
magnesium chloride	Sigma
methanol (MeOH)	Biosolve
Ni-NTA Superflow	Qiagen
NuPAGE LDS sample buffer (4 x)	Thermo Fisher Scientific
NuPAGE MES SDS buffer (20 x)	Thermo Fisher Scientific
NuPAGE Reducing Agent (10 x)	Thermo Fisher Scientific
NuPAGE® Novex® 4-12 % Bis-Tris Mini Gel	Thermo Fisher Scientific
ortho-phosphoric acid (H_3PO_4)	Roth
PageRuler™ (Plus) Prestained Protein Ladder	Thermo Fisher Scientific

peptone	Roth
potassium dihydrogen phosphate (KH_2PO_4)	Roth
Sephadex G-25	GE Healthcare
Simply BlueTM SafeStain	Invitrogen
sodium chloride (NaCl)	Roth
sodium hydroxid (NaOH)	Roth
sulfuric acid 95-97%	Merck
tetracycline	Applichem
tris(hydroxymethyl)aminomethane (TRIS)	Merck
yeast extract	Roth
trans-cinnamic acid and derivatives	
trans-cinnamic acid	Sigma
trans-2-Methoxycinnamic acid; 99%	ABCR
3-Methoxycinnamic acid, predominantly *trans*, 98%	ABCR
4-Methoxycinnamic acid, predominantly *trans*; 98%	ABCR
2-Fluorocinnamic acid; 98%	ABCR
3-Fluorocinnamic acid; 98%	ABCR
4-Fluorocinnamic acid; 99%	ABCR
2-Hydroxycinnamic acid; 98%	ABCR
3-Hydroxycinnamic acid; 99%	ABCR
p-Coumaric acid ≥98.0%	Sigma
2-Chlorocinnamic acid, predominantly *trans*, 99%	Alfa
3-Chlorocinnamic acid, predominantly *trans*; 98%	ABCR
4-Chlorocinnamic acid, predominantly *trans*; 99%	ABCR
trans-2,3-Dimethoxycinnamic acid, 97 %	Sigma
3,4-Dimethoxycinnamic acid, predominantly *trans* 99%	Sigma
trans-2,4-Dimethoxycinnamic acid, 98%	Sigma
trans-Ferulic acid, 99%	Sigma
α-amino acids	
L-phenylalanine	Fluka
D-phenylalanine	Fluka
2-Fluoro-DL-phenylalanine; 98%	ABCR
3-Fluoro-DL-phenylalanine; 98%	ABCR
4-Fluoro-DL-phenylalanine; 98%	ABCR
2-Chloro-L-phenylalanine, 98+%	Alfa
3-Chloro-L-phenylalanine; 95%	ABCR
4-Chloro-DL-phenylalanine; 98+%	ABCR
DL-o-Tyrosine	TCI Europe
DL-m-Tyrosine	TCI Europe
L-tyrosine	Fluka
D-tyrosine	Fluka
2-Methoxy-L-phenylalanine; 95%	ABCR
3-Methoxy-DL-Phenylalanine	chemos
4-Methoxy-L-phenylalanine	Sigma
3-(3,4-Dimethoxyphenyl)-L-alanine 97%	Sigma
3-Methoxy-L-tyrosine monohydrate	Sigma
β-amino acids	
(*R*)-3-Amino-3-phenylpropionic acid, 98 %	ABCR
(*S*)-3-Amino-3-phenylpropionic acid	ABCR
(*R*)-3-Amino-3-(2-chloro-phenyl)-propionic acid	Peptech
(*R*)-3-Amino-3-(3-chloro-phenyl)-propionic acid	Peptech

(*R*)-3-Amino-3-(4-chloro-phenyl)-propionic acid	Peptech
(*R*)-3-Amino-3-(2-fluoro-phenyl)-propionic acid	Peptech
(*R*)-3-Amino-3-(3-fluoro-phenyl)-propionic acid	Peptech
(*R*)-3-Amino-3-(4-fluoro-phenyl)-propionic acid	Peptech
(*R*)-3-Amino-3-(2-hydroxy-phenyl)-propionic acid	Peptech
(*R*)-3-Amino-3-(3-hydroxy-phenyl)-propionic acid	Peptech
(*R*)-3-Amino-3-(4-hydroxy-phenyl)-propionic acid	ABCR
(*R*)-3-Amino-3-(2-methoxy-phenyl)-propionic acid	Peptech
(*R*)-3-Amino-3-(4-methoxy-phenyl)-propionic acid	Peptech
(*R*)-3-Amino-3-(3,4-dimethoxy-phenyl)-propionic acid	Peptech
(*S*)-3-Amino-3-(2-chloro-phenyl)-propionic acid	Peptech
(*S*)-3-Amino-3-(3-chloro-phenyl)-propionic acid	Peptech
(*S*)-3-Amino-3-(4-chloro-phenyl)-propionic acid	Peptech
(*S*)-3-Amino-3-(2-fluoro-phenyl)-propionic acid	Peptech
(*S*)-3-Amino-3-(3-fluoro-phenyl)-propionic acid	Peptech
(*S*)-3-Amino-3-(4-fluoro-phenyl)-propionic acid	Peptech
(*S*)-3-Amino-3-(2-hydroxy-phenyl)-propionic acid	Peptech
(*S*)-3-Amino-3-(3-hydroxy-phenyl)-propionic acid	Peptech
(*S*)-3-Amino-3-(4-hydroxy-phenyl)-propionic acid	ABCR
(*S*)-3-Amino-3-(2-methoxy-phenyl)-propionic acid	Peptech
(*S*)-3-Amino-3-(4-methoxy-phenyl)-propionic acid	Peptech
(*S*)-3-Amino-3-(3,4-dimethoxy-phenyl)-propionic acid	Peptech

3.1.2 **Cultivation media, antibiotics and inductors**

All media and solutions, except of inductors and antibiotics, were prepared with dH_2O and autoclaved for 20 min at 2 Bar. Antibiotics and inductors were dissolved in ddH_2O and sterile filtered with a 0.2 µm syringe-filter.

Lysogeny broth (LB)- medium		**LB agar plates**	
peptone	10 g/L	peptone	10 g/L
yeast extract	5 g/L	yeast extract	5 g/L
NaCl	10 g/L	NaCl	10 g/L
		agar	15 g/L
inductor stock solutions		**antibiotic stock solutions**	
IPTG (1000 x)	1 M	ampicillin (1000 x)	100 mg/ml
L-arabinose (500 x)	250 mg/ml	kanamycin (1000 x)	75 mg/ml
tetracycline (5000 x)	25 µg/ml	chloramphenicol (1000 x) in EtOH	20 mg/ml
KPi-buffer for AI-medium		**media component AI-medium**	
1 M KH_2PO_4-solution	39 % (v/v)	peptone	12 g/L
1 M K_2HPO_4-solution	61 % (v/v)	yeast extract	24 g/L
final media-conc.: 90 mM		fill up to 790 ml	

AI-media additives stock
(separately autoclaved)

glucose (100 x)	1.5 g/L
lactose (10 x)	2.2 g/L
glycerol (100 x)	50 %

3.1.3 Equipment

Table 3: Equipment used in this thesis

centrifuges	
Avanti J-20 XP Centrifuge	Beckmann Coulter
J-LITE® JLA-8.1000 Rotor, Fixed Angle	Beckmann Coulter
Allegra 6KR Centrifuge	Beckmann Coulter
Centrifuge 5417R and 5424	Eppendorf
Universal 32 R	Hettich
scales	
Precision scale CPA22S	Satorius
Analytical scale BP2100S	Satorius
HPLC	
ASTEC Chirobiotic T (25 cm x 4.6 mm), 5 µm	Supelco, Sigma-Aldrich
CHIRALPAK Zwix (+) (150 x 4.0mm) 3µm	Daicel
HPLC analysis system Series 1100	Agilent/Hewlett Packard
G1315A diode array detector	Agilent/Hewlett Packard
enzyme purification	
ÄKTApurifier system	GE Healthcare
XK 16/20 Column	GE Healthcare
XK 50/100 Column	GE Healthcare
spectroscopy	
UV-1601 and UV-1800 Spectrophotometer	Shimadzu
Quartz cuvettes QS 10 mm	Hellma
BioPhotometer plus	Eppendorf
µCuvette G1.0	Eppendorf
others	
XCell SureLock Mini-Cell Electrophoresis System	Thermo Scientific
Ultrasonification processor UP 200S	Hielscher
Sonotrodes: S1, S3 and SD14	Hielscher
pH-Meter	Metrohm
Autoclav Systec DX-65	Systec
Alpha 1-4 LD plus Freeze Dryer	Christ
TProfessional Thermocycler	Biometra
Multitron Standard shaking incubator	INFORS
Hera cell 150 CO_2 incubator	Thermo Scientific
Incubator genie	Scientific industries
Rotavapor R114	Büchi
Vac V513 vacuum pump	Büchi
Water bath B480	Büchi

Circulation chiller WKL 230	Lauda
Water bath C6CS	Lauda
High Precision Pump P-500	Amersham Biosciences
kits	
QIAprep Spin Miniprep Kit	QIAGEN
QIAquick Gel Extraction Kit	QIAGEN
Rapid DNA Ligation Kit	Thermo Scientific
KOD HotStart Polymerase Kit	Novagen
DNA Clean & Concentrator 5 Kit	Zymo Research
BC Assay Protein Quantitation Kit	INTERCHIM UPTIMA

3.1.4 **Plasmids**

The coding sequences for the selected wild-type (wt) enzymes were extracted from GenBank database. Synthetic genes were synthesized by GeneArt (Table 4), a gene synthesis service from Thermo Fisher Scientific. All genes were codon optimized for *E. coli* and delivered in pMA-RQ vectors containing the *bla* gene (ampicillin resistance). The plasmids containing the genes for *Pc*PAL1, *At*PAL2 and *Rs*TAL were kindly provided by Dr. Jan Marienhagen (IBG-1, Forschungszentrum Jülich). The *Rs*TAL used in this thesis contains an additional glycine in position 2 compared to the amino acid sequence of the wt enzyme (GB code ABA81174.1), due to the insertion of three bases to generate an NcoI restriction site.

Table 4: Synthetic genes in shipping vectors produced by GeneArt

encoded enzyme	GenBank entry CDS	GeneArt shipping vector	genetic features
*Pc*PAL1	Y07654.1	pETDuet-1-*Pc*PAL (MP 30.1.1)	P_{T7}, *lacI*, pBR322 *ori*, *ampR*, 2148 bp *pcpal1* (NcoI, BamHI)
*At*PAL2	NM_115186	pETDuet-1-*At*PAL (MP 30.2.1)	P_{T7}, *lacI*, pBR322 *ori*, *ampR*, 2151 bp *atpal2* (NcoI, BamHI)
*Rt*PAL	X51513.1	pMA-RQ-*Rt*PAL (MP 30.3.1)	ColE1 *ori*, *ampR*, 2148 bp *rtpal* (NdeI, XhoI)
*Rs*TAL Gly2ins	ABA81174.1 (annotated as HAL)	pETDuet-1-*Rs*TAL (MP 30.4.1)	P_{T7}, *lacI*, pBR322 *ori*, *ampR*, 1572 bp *rstal* (NcoI, BamHI)
*Rc*TAL	NC_014034.1 (annotated as HAL, compartment 1143930..1145525)	pMA-RQ-*Rc*TAL (MP 30.5.1)	ColE1 *ori*, *ampR*, 1593 bp *rctal* (NdeI, XhoI)
*Sg*TAM	AY048670 (ORF24)	pMA-RQ-*Sg*TAM (MP 31.4.1)	ColE1 *ori*, *ampR*, 1617 bp *sgtam* (NcoI, XhoI)
*Cc*TAM	AM179409.1 (compartment 40179..41774)	pMA-RQ-*Cc*TAM (MP 31.3.1)	ColE1 *ori*, *ampR*, 1593 bp *cctam* (NdeI, XhoI)
*Tch*PAM	AY724735	pMA-RQ-*Tch*PAM (MP 31.2.1)	ColE1 *ori*, *ampR*, 2061 bp *tchpam* (NcoI, XhoI)

*Tca*PAM	AY582743	pMA-RQ-*Tca*PAM (MP 31.1.1)	ColE1 *ori*, *ampR*, 2094 bp *tcapam* (NcoI, XhoI)

All synthetic genes were cloned into pET22b or pET28a expression vectors (Table 5) to generate enzymes with C-terminal His_6 tags. Genes in pETDuet1 vectors were amplified via PCR (3.2.6) with the respective primers (3.1.5), genes in pMA-RQ vectors were cloned by direct excision from the shipping vector.

Table 5: Expression vectors

plasmid	**genetic features**	**reference**
pET22b	P_{T7}, pBR322 *ori*, *lacI*, *ampR*	Novagen
pET28a	P_{T7}, pBR322 *ori*, *lacI*, *kanR*	Novagen
pET22b-*Pc*PAL1 (MP 30.1.2)	2148 bp *pcpal1* (NdeI, XhoI) cloned in pET22b	this thesis
pET22b-*At*PAL2 (MP 30.2.2)	2151 bp *atpal2* (NdeI, XhoI) cloned in pET22b	this thesis
pET22b-*Rt*PAL (MP 30.3.2)	2148 bp *rtpal* (NdeI, XhoI) cloned in pET22b	this thesis
pET22-*Rc*TAL (MP 30.5.2)	1593 bp *rctal* (NdeI, XhoI) cloned in pET22b	this thesis
pET28-*Rs*TAL (MP 30.4.2)	1572 bp *rstal* (NcoI, XhoI) cloned in pET28a	this thesis
pET22-*Cc*TAM (MP 31.3.2)	1593 bp *cctam* (NdeI, XhoI) cloned in pET22b	this thesis
pET28-*Sg*TAM (MP 31.4.2)	1617 bp *sgtam* (NcoI, XhoI) cloned in pET28a	this thesis
pET28-*Tca*PAM (MP 31.1.2)	2094 bp *tcapam* (NcoI, XhoI) cloned in pET28a	this thesis
pET28-*Tch*PAM (MP 31.2.2)	2061 bp *tchpam* (NcoI, XhoI) cloned in pET28a	this thesis
pET22b-*At*PAL2-F136H (MP 30.2.3)	2151 bp *atpal2* F136H (NdeI, XhoI) cloned in pET22b	Hilberath, 2015 [108]
pET28a-n*At*PAL-CBM (MP 30.2.6.1)	2151 bp *atpal2* (NcoI, XhoI) cloned in pET28a with integrated cbm	Hilberath, 2015
pET28a-*Cc*TAM-CBM (MP 31.3.3)	1593 bp *cctam* (NcoI, XhoI) cloned in pET28a with integrated cbm	this thesis

To enhance the amount of soluble *Tch*PAM and *Tca*PAM enzyme during expression, the PAM genes were coexpressed with genes encoding chaperones according to the manual from TAKARA BIO INC., who provide a respective plasmid toolbox (Table 6).

Table 6: Commercial available chaperone plasmids from TAKARA BIO INC.

no.	plasmid	chaperone	promotor	inducer	resistence
1	pG-KJE8	dnaK-dnaJ-grpE-groES-groEL	araB, Pzt1	L-arabinose tetracycline	chloramphenicol
2	pGro7	groES-groEL	araB	L-arabinose	chloramphenicol
3	pKJE7	dnaK-dnaJ-grpE	araB	L-arabinose	chloramphenicol
4	pG-Tf2	groES-groEL-tig	Pzt1	tetracycline	chloramphenicol
5	pTf16	tig	araB	L-arabinose	chloramphenicol

3.1.5 Oligonucleotides

Table 7: Oligonucleotides for the amplification of genes from pETDuet1 vectors, restriction sites are underlined. PCR primers were synthesized by Eurofins Genomics.

name	DNA sequence (5´- 3´)	Tm [°C]
*Pc*PAL_fw_NdeI	CGACAGCATATGGAAAATGGTAATGGTGCAACCACCAATGG	72.4
*Pc*PAL_rv_XhoI	GGATCCCTCGAGACAAATCGGCAGCGGTGCACCATTC	>75.0
*At*PAL_fw_NdeI	CCAGAGCATATGGATCAGATTGAAGCAATGCTGTGTGGTGGTGGTGAA	>75.0
*At*PAL_rv_XhoI	GTCACGCTCGAGGCAAATCGGGATCGGTGCACCATTCCATTC	>75.0
*Rs*TAL_fw_NcoI	GCATACCATGGGTCTGGCTATGAGTCCTCCTAAAC	71.8
*Rs*TAL_rv_XhoI	AATTCGGATCCCTCGAGAACTGGACTCTGTTGCAGCAGATGG	>75.0
*Cc*TAM pMARQ fw	GGCCGTCAAGGCCGCATCCCATGGAAATTACCG	65.0
*Cc*TAM pMARQ rv	GAAGGCACATGAGGCCCAGTTACTCGAGGCTGCTTG	75.0

3.1.6 Cloning enzymes

KOD HotStart Polymerase (Novagen), FastDigest restriction endonucleases NdeI, NcoI, XhoI and BlpI and T4 DNA Ligase (Thermo Scientific).

3.1.7 Bacterial strains

Table 8: Commercial available bacterial strains from Invitrogen and Agilent Technologies

strain	genotype
One Shot® BL21 (DE) chemically competent *E. coli*	F^- *omp*T *hsdS*$_B$(r_B^- m_B^-) *gal dcm* (DE3)
Efficiency® DH5α^{TM} competent cells	F^- Φ80*lac*ZΔM15 Δ(*lac*ZY-argF) U169 *rec*A1 *end*A1 *hsd*R17 (r_K^-, m_K^+) *pho*A *sup*E44 λ^- *thi*-1 *gyr* A96 *rel*A1
BL21-Gold (DE3)	B F^- *omp*T *hsdS*(r_B^- m_B^-) *dcm*$^+$ Tet^R gal λ(DE3) endA Hte

3.2 Molecular biological methods

3.2.1 **Preparation of chemically competent *E. coli* cells**

The respective *E. coli* cells (3.1.7) were spread on a LB-agar plate without antibiotic and incubated for at least 16 h at 37 °C. 100 ml LB-medium were inoculated with one single colony and shaken at 150 rpm and 37 °C until the OD_{600} reached 0.6-0.7. The culture was poured in two iced 50 ml falcon tubes and stored for 10 min on ice. The falcon tubes were centrifuged for 10 min at 4000 rpm and 4 °C. The supernatant was discarded and the pellet resuspended in 30 ml iced $MgCl_2$/$CaCl_2$-solution. Afterwards the falcon tubes were centrifuged (10 min, 4000 rpm, 4 °C) and the supernatant was removed. The cells were resuspended in 2 ml iced 0.1 M $CaCl_2$ solution. Both cell solutions were combined. For storage 140 µl DMSO was added, and after 15 min incubation on ice, another 140 µl DMSO were added. Cells were stored in 200 µl aliquots at -70 °C.

3.2.2 **Transformation**

5-10 µl ligation sample or 1 µl plasmid DNA was added to 50 µl chemically competent *E. coli* cells (3.1.7). The reaction tube was incubated for 30 min on ice. Afterwards the cells were heated to 42 °C for 90 s. After 5 min cooling on ice, 500 µl sterile LB medium was added and the reaction tube was shaked for 1 h at 37 °C and 500 rpm. The cells were separated from the medium by centrifugation (1 min, 13000 rpm, RT) and 300 µl medium were removed. The cells were resuspended in the remaining medium and spread on an LB-agar plate containing 75-100 µg/ml of the respective antibiotic. The plates were incubated at 37 °C overnight.

3.2.3 **Liquid bacterial cultures**

A single colony from a LB-agar plate was transferred to 5 -20 ml LB-medium with 75-100 µg/ml of the respective antibiotic and incubated for at least 16 h at 150 rpm and 37 °C. *E. coli* DH5α was used for plasmid DNA isolation, whereas *E.coli* BL21 was used for enzyme production.

3.2.4 **Plasmid preparation**

Bacterial plasmid DNA was isolated from a 5 ml liquid culture using the "QIAprep Spin Miniprep Kit" (QIAGEN) according to the manufacturer´s manual.

3.2.5 **DNA concentration**

The plasmid DNA concentration was determined using the "BioPhotometer plus" (Eppendorf) equipped with a "µCuvette G1.0". After zeroing with 1.5 µl elution buffer, 1.5 µl of the sample was applied. The concentration was calculated from the absorbance at 260 nm.

3.2.6 **PCR**

To amplify the ammonia lyase genes from pETDuet1 vectors (Table 4) a PCR was conducted using the "KOD HotStart Polymerase Kit" (Novagen) and the respective primers (Table 7).The components for the reaction were mixed according to the manual:

component	volume [µl]	final concentration/final amount
template (10 ng/µl)	2.5	25 ng
2 mM dNTP´s	5.0	0.2 mM each
primer fw and rv (5 pmol/µl)	2.5 each	12.5 pmol each
$MgSO_4$	2.5	1.5 mM
10 x buffer	5.0	1 x
DMSO	2.5	
KOD Hot start Polymerase	1.0	0.02U/µl
PCR grade H_2O	26.5	
total volume:	**50.0 µl**	

PCR program:

step	temperature [°C]	time
heat lid	99	
initial denaturation	98	30 s
denaturation	98	10 s
annealing	74.5	30 s
elongation	72	1 min (2 kb)
final elongation	72	15 min
storage	15	∞

30 cycles

3.2.7 **Agarose gel electrophorese**

A solution with 1 % agarose in TAE buffer (composition see below) was prepared and poured into a gel chamber. After polymerization of the gel, one volume "GelPilot DNA Loading Dye 5x" (QIAGEN) was mixed with four volumes of the sample (from PCR or vector digestion). 12.5 -25 µl of the mixture were loaded onto the gel. As a reference 5 µl "FastRuler High Range DNA Ladder" (Thermo Scientific) was used. The separation was performed at 200 V, 60-100 mA, 15 W for 1 h. The gel was stained in a 0.25 µg/ml ethidium bromide solution and afterwards destained for 5 min in water. The DNA fragments were visualized under UV-light and the appropriate fragment (PCR product or the digested vector) was excised from the gel for extraction.

TAE buffer (50 x), pH 8.0	
Tris	2 M
Acetic acid	1 M
EDTA	50 mM

3.2.8 **DNA gel extraction**

The extraction of DNA fragments from agarose gels was performed using the "QIAquick Gel Extraction Kit" (QIAGEN) according to the manufacturer´s manual.

3.2.9 **DNA digestion**

PCR products or cloning and shipping vectors were digested before the ligation using the respective FastDigest restriction endonucleases (Thermo Scientific) according to the following scheme:

name	**amount [µl]**
DNA	x (up to 1 µg DNA)
10 x FastDigest buffer	2
FastDigest NcoI or NdeI	1
FastDigest XhoI	1
ddH_2O	fill up to 20 µl

The reactions were incubated at 37 °C for at least 2 h. PCR products were digested overnight. The reaction was terminated by heat inactivation of the enzymes at 80 °C for 5 min. Digested PCR products were purified using a purification kit (3.2.10), the digested pET cloning vectors or the shipping vectors with integrated target gene were purified by gel electrophorese (3.2.7). The desired fragment (vector backbone or target gene) was isolated by extraction (3.2.8).

To control the constructed expression vectors (Table 5) after ligation, 5 µl of the isolated construct were digested with BlpI, a FastDigest enzyme which cuts in the inserted target gene and in the vector backbone. The size of the DNA fragments was controlled on an agarose gel (3.2.7). Samples with the expected fragments were sequenced (3.2.12).

3.2.10 **PCR product purification**

The digested PCR products were purified using the "DNA Clean & Concentrator 5 Kit" (Zymo research). Two volumes binding buffer were added to one volume PCR sample and mixed. The mixture was applied to the binding column and centrifuged (30 s, 14000 rpm, RT). The flow through was discarded and the column washed twice with 200 µl washing buffer. ddH_2O (10 µl) was added and the column was incubated for 1 min. The PCR product was eluted by centrifugation for 30 s, and the DNA concentration determined (3.2.5).

3.2.11 **Ligation**

The ligation of PCR products or synthetic genes into pET-expression vectors was conducted with the "Rapid DNA Ligation Kit" from Thermo Scientific. 25 -52 ng vector DNA were used, depending on the concentration of the samples. The required amounts of insert DNA (vector/insert ratio 1:4) were calculated according Equation 3:

Equation 3

$$\boldsymbol{mass\ insert\ [ng]} = \frac{\boldsymbol{mass\ vector\ [ng] * size\ insert\ [bp]}}{\boldsymbol{size\ vector\ [bp]}} \boldsymbol{*4}$$

Ligation approach:

name	**amount [µl)**
vector DNA	x
insert DNA	x
5 x rapid ligation buffer	4
T4 DNA ligase	1
water (nuclease free)	fill up to 20

The ligation reactions were incubated for 2 h at 22 °C and afterwards directly used for transformation of *E. coli* DH5α (3.2.2). After plasmid isolation (3.2.4) and control digestion (3.2.9) samples with the expected fragments were sequenced.

3.2.12 **Sequencing**

20-40 µl of plasmid DNA with a concentration of at least 100 ng/µl were sent to LGC Genomics GmbH, Berlin, Germany. The appropriate primers which bind to the promotor and the terminator region of the pET-vector were synthesized and stored by LGC.

3.3 Enzyme production and purification

3.3.1 **Gene expression without chaperones**

All genes encoding ammonia lyases and the aminomutase *Cc*TAM were expressed without chaperones. Expression vectors (Table 5) with verified sequence were used to transform competent *E. coli* BL21 (DE) (3.2.2). Precultures in Lysogeny broth-medium (LB) were prepared from the agar plates (3.2.3). To identify the best expression conditions, the expression in LB medium and autoinduction medium (AI) was investigated in small scale. 200 ml medium in 1 L shaking flasks with the respective antibiotic was inoculated with the preculture to an OD_{600} of 0.1 and grown at 37 °C. After 2 h the shaking flask with autoinduction medium was further incubated at 20 °C for expression. When the culture in LB-medium reached OD_{600} of 0.4-0.6 gene expression was induced by adding Isopropyl β-D-1-thiogalactopyranoside (IPTG) to a final concentration of 1 mM, and the cultivation was continued at 20 °C. Both cultures were cultivated for 48 h at 20 °C in an INFORS Multitron shaking incubator. After 24 h and 48 h samples were taken for SDS-PAGE analysis (3.4.1). To track the total production of target enzyme, samples with OD_{600} 0.45/ml were prepared. To follow the production of soluble target enzyme after cell disruption samples of OD_{600} 5/ml were prepared.

When the optimal expression medium was identified, cultivation was conducted in this medium in a 5 L scale (5 L shaking flasks with buffels, each with 1 L medium) as described above. After 48 h the cells were harvested by centrifugation (40 min, 4 °C, 7000 rpm) in an Avanti J-20 XP centrifuge and stored at -20 °C.

3.3.2 **Gene expression with chaperones**

Both PAM genes were expressed in LB medium and in presence of chaperones to enhance the production of soluble enzyme. To identify the best expression conditions, chemically competent *E.coli* BL21 (DE) were transformed with five chaperone plasmids (Table 6) and prepared for a second transformation (3.2.1). PAM expression vectors (Table 5) with verified sequence were used to transform competent *E. coli* BL21 (DE) containing a chaperone plasmid. Precultures in LB medium containing 75 µg/ml kanamycin and 20 µg/ml chloramphenicol were prepared from the agar plates (3.2.3). 50 ml medium in 0.25 L shaking

flasks with the respective antibiotics was inoculated with the appropriate preculture to an OD_{600} of 0.1 and induced with the respective inducer (L-arabinose and/or tetracycline) according to the manufacturer´s manual to start chaperone expression. The cultures were incubated at 37 °C and 150 rpm until the OD_{600} reached 0.4-0.7, at this timepoint IPTG was added to a final concentration of 0.2 mM to start the PAM expression. Expression was conducted for 48 h at 20 °C. After 24 h and 48 h samples were taken for analysis. To investigate the soluble expression after cell disruption, samples of OD_{600} 5/ml were prepared.

Large scale PAM expression was conducted in 5 L scale (5 L shaking flasks with buffels each with 1 L LB-medium) in combination with chaperone plasmid no. 5 for 24 h as described above. After 24 h the cells were harvested by centrifugation and stored at -20 °C.

3.3.3 **Preparation of crude cell extract (CCE)**

E. coli BL21 (DE) cells containing the respective enzyme were resuspended in 50 mM TRIS-HCl, pH 8.8, to prepare a 12.5 % or 25 % (w/v) cell suspension, depending on the amount of recombinant target enzyme. For IMAC purification one protease inhibitor tablet per 10 ml suspension was added. The cells were disrupted with an Ultrasonification processor UP 200S (Hielscher) and the appropriate sonotrode (S3 or SD14, 10 x 30 s, 0.5 cycle, 40 % amplitude, on ice). Afterwards the solution was centrifuged for 30 min at 4 °C and 19000 rpm. Before IMAC the supernatant was filtered (0.22 µm, PES, Millex). Protein content (3.4.2.1) and activity (3.4.3) were measured.

For analysis of expression levels cell pellets with OD_{600} 5/ml were resuspended im 1 ml 50 mM TRIS-HCl buffer, pH 8.8, and disrupted on ice (sonotrode S1, 10 x 30 s, 0.5 cycle, 40 % amplitude). Samples were centrifuged at 4 °C and 4000 rpm for 30 min. The supernatant was collected and the pellet washed twice with 1 ml TRIS-HCl, residual liquid was removed by positioning the inverted falcon tube on a filter paper for 1 min, and finally the pellet was resuspended in 1 ml TRIS-HCl buffer. Supernatant and pellet fractions were analyzed with SDS-PAGE (3.4.1), to compare soluble and insoluble expression levels.

3.3.4 **Enzyme purification via IMAC**

To purify His_6-tagged enzymes, a XK16/20 column filled with Ni-NTA Superflow was connected to an ÄKTApurifier system. The column was flushed with ddH_2O and equilibrated with three column volumes equilibration buffer (see below). The filtered CCE (3.3.3) was loaded onto the column with a flow rate of 3 ml/min. Afterwards non-bound proteins were removed by washing with equilibration buffer until the UV absorption at 280 nm reached the baseline (< 200 mAU) again. Then unspecifically bound proteins were flushed with the

washing buffer containing 30 mM imidazole, and in the last step the target enzyme was eluted using the elution buffer with an imidazole concentration of 300 mM. Flow through, wash and elution fractions were collected, pooled and investigated regarding protein content (3.4.2.1), enzyme activity (3.4.3) und purity (3.4.1).

equilibration buffer, pH 8.8	
TRIS-HCl	50 mM
NaCl	300 mM

washing buffer, pH 8.8	
TRIS-HCl	50 mM
NaCl	300 mM
imidazole	30 mM

elution buffer, pH 8.8	
TRIS-HCl	50 mM
NaCl	300 mM
imidazole	300 mM

3.3.5 Desalting of purified enzymes

To remove imidazole and NaCl the purified enzyme was desalted after IMAC. An XK 50/100 column filled with Sephadex G-25 was connected to the ÄKTApurifier system and equilibrated with one column volume 10 mM TRIS-HCl buffer, pH 8.8. Afterwards the solution with the purified enzyme after IMAC was loaded and the column was flushed with 10 mM buffer until the conductivity reached the baseline. All steps were performed with a flow of 10 ml/min. Fractions containing enzyme were pooled. Samples were taken for protein content (3.4.2.1) and enzyme activity (3.4.3) measurements. The purified and desalted enzyme fraction was frozen and lyophilized (3.3.6).

desalting buffer, pH 8.8	
TRIS-HCl	10 mM

3.3.6 Lyophilization

Lyophilization was performed with an Alpha 1-4 LD plus Freeze Dryer (Christ). Wet whole cells or desalted enzyme solution spread in a crystallizing dish, was transferred from – 20 °C to the freeze dryer and dried under vacuum at -49 °C and 0.1 mbar.

3.4 Analytical methods

3.4.1 **SDS-PAGE**

Sodium dodecyl sulfate polyacrylamide gel electrophoresis (SDS-PAGE) was performed with a XCell SureLock™ Mini-Cell Electrophoresis System and NuPAGE™ Novex™ 4-12% Bis-TRIS Protein Gels, 1.5 mm (Thermo Scientific). The gel was embedded into the gel chamber. NuPAGE MES Running buffer (20x) was diluted with deionized water and poured into the chamber. Protein samples were diluted to a concentration of 1 mg/ml. Cell pellets of OD_{600} 0.45/ml were resuspended in 19.5 µl water. The samples for application were prepared as described below:

name	**amount [µl]**
sample	19.5
NuPAGE LDS Sample buffer (4x)	7.5
NuPAGE Reducing agent (10x)	3.0
Total volume:	30 µl

Samples were heated to 99 °C for 10 min. 10 µl of each sample was loaded onto the gel and 5 µl PAGE Ruler (Plus) Protein ladder as reference. The separation was performed at 200 V, 100 mA, 15 W for 1 h. Subsequently the gel was stained for at least 1 h with Coomassie Blue G-250 solution and destained in deionized water overnight. A picture of the gel was taken.

3.4.2 **Protein concentration assays**

Solutions with free enzyme were measured with the Bradford assay. For immobilized proteins the BCA assay was used. In this assay Cu^{2+} is reduced in a first step in presence of proteins to Cu^{+}, in the second step the Cu^{+}ion is chelated by two molecules of bicinchoninic acid resulting in a color change, which can be measured at 562 nm. Due to this, the solid cellulose carriers with immobilized protein can be removed before the photometric measurement.

3.4.2.1 Bradford assay

Bradford reagent

Coomassie Brilliant Blue G-250	100 mg/ml
ethanol (p. a)	50 mg/ml
ortho-phosphoric acid (85 %)	100 mg/ml

For one liter reagent 100 mg Coomassie Brilliant Blue were dissolved in 50 ml ethanol. After adding 100 ml phosphoric acid the solution was stirred for at least 1 h. Afterwards the solution was filled up to 1 L with water, boiled and filtered.

A calibration curve with bovine serum albumin (BSA) in the range of 0.01-0.1 mg/ml was prepared with the reagent. 100 µl of the sample were mixed with 900 µl reagent and incubated for 10-15 min in the dark. The absorbance was measured in PMMA cuvettes at 25 °C and 595 nm in an UV-1800 spectrophotometer (Shimadzu). Measurements were performed in triplicate. The protein content of the samples was calculated using the BSA calibration curve.

3.4.2.2 BCA assay

To determine the protein amount bound to the cellulose carrier Avicel, the "BC Assay Protein Quantitation Kit" (Uptima) was used. The assay reagent and the BSA standards with concentrations from 0.02-2 mg/ml were prepared according to the manufacturer`s manual. 50 µl of the respective standard were mixed with 1 ml reagent and incubated at 37 °C for 30 min. 900 µl were transferred to a cuvette and the absorbance was measured at 562 nm in an UV-1601 spectrophotometer (Shimadzu).

20 mg Avicel were resuspended in 500 µl deionized water containing 0.5 % Triton X-100. After mixing, 50 µl of the suspension were immediately added to 1 ml reagent and incubated at 37 °C for 30 min. During the incubation the reaction tube was mixed several times, to prevent the sedimentation of the carrier with the immobilized enzyme. After 30 min the reaction tube was centrifuged (1 min, 13000 rpm, RT) and 900 µl were transferred to a cuvette and measured. The protein amount on the carrier was calculated using the BSA calibration curve. Measurements were performed in duplicate.

3.4.3 Enzyme activity assays

The activity of ammonia lyases was determined with continuous photometric assays, following the deamination or amination of the natural substrate.

3.4.3.1 Deamination of L-phenylalanine with PAL (standard assay)

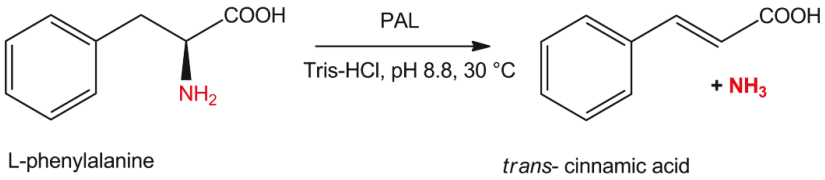

Figure 14: Deamination of L-phenylalanine to *trans*-cinnamic acid catalyzed by PALs.

A substrate solution containing 30 mM L-Phe in 50 mM TRIS-HCl buffer, pH 8.8, was prepared. 1450 µl substrate solution were filled into 1.5 ml QS-cuvettes with caps, and incubated for 6 min at 30 °C. The reaction was started by adding 50 µl of the enzyme solution (≤ 2.6 mg/ml total protein) and inverting the cuvette 3 times. Production of *trans*-cinnamic acid was followed at 275 nm for 2 min. All measurements were done in duplicate with buffer as a blank. The activity was calculated using the slope of the first 80 s and following Equation 4:

Equation 4

$$specific\ activity\ [\frac{U}{mg}] = \frac{\frac{\Delta A_{275\ nm}}{min} * V * f}{\varepsilon_{275\ nm} * d * c * v}$$

$\Delta A_{275\ nm}$/min = increase of absorbance at 275 nm per minute [min^{-1}]
V = total assay volume [1500 µl]
f = dilution factor of the enzyme solution
$\varepsilon_{275\ nm}$ = extinction coefficient of *trans*-cinnamic acid [17.218 mM^{-1} cm^{-1}]
d = path length cuvette [1 cm]
c = enzyme concentration [mg/ml]
v = volume enzyme sample [50 µl]

3.4.3.2 pH optima wt PALs (deamination)

The measurement was conducted as described above (3.4.3.1) with following modification: 30 mM L-Phe was dissolved in 100 mM buffers with different pH values (TRIS-HCl: pH 7.5-9.0; CAPSO-NaOH: pH 9.5-10.0). Buffers were prepared at RT for measurement at 30 °C according to the buffer calculator tool: (http://www.liv.ac.uk/buffers/buffercalc.html).

3.4.3.3 Temperature optima wt PALs (deamination)

The assay was performed as described above (3.4.3.1) but at different temperatures (30-60 °C). The temperature in the cuvette was controlled with an external thermometer. The TRIS-HCl buffers were prepared at RT according to the calculations with a buffer calculator tool (http://www.liv.ac.uk/buffers/buffercalc.html). The pH at each measuring temperature was pH 8.5

3.4.3.4 Amination of *trans*-cinnamic acid with PALs

Amination reactions were performed in 5 M NH_3 adjusted with sulfuric acid to the respective pH or in 2.5 M $(NH_4)_2CO_3$ (pH 8.9) with 4 mM t-CA as substrate. 480 µl of the substrate solution was warmed to 30 °C in a reaction tube in a thermo shaker. Afterwards 20 µl enzyme solution (5-17 mg/ml enzyme content) was added. After short mixing 180 µl were transferred to a 0.02 cm quartz glas cuvette and measured for 2 min in the photometer at 275 nm. The activity was calculated using the slope of the first 80 s and following Equation 5:

Equation 5

$$\boldsymbol{specific\ activity}\ [\frac{\boldsymbol{U}}{\boldsymbol{mg}}] = \frac{\frac{\Delta \boldsymbol{A}_{\boldsymbol{275\ nm}}}{\boldsymbol{min}} * \boldsymbol{V} * \boldsymbol{f}}{\boldsymbol{\varepsilon}_{\boldsymbol{275\ nm}} * \boldsymbol{d} * \boldsymbol{c} * \boldsymbol{v}}$$

$\Delta A_{275\ nm}$/min = decrease of absorbance at 275 nm per minute [min^{-1}]
V = total assay volume [500 µl]
f = dilution factor of the enzyme solution
$\varepsilon_{275\ nm}$ = extinction coefficient of *trans*-cinnamic acid [17.218 mM^{-1} cm^{-1}]
d = path length cuvette [0.02 cm]
c = enzyme concentration [mg/ml]
v = volume enzyme sample [20 µl]

3.4.3.5 Deamination of L-tyrosine with TAL

A substrate solution containing 5 mM L-tyrosine in 50 mM TRIS-HCl buffer, pH 8.8, was prepared. 1450 µl substrate solution were filled into 1.5 ml QS-cuvettes with caps, and incubated for 6 min at 30 °C. The reaction was started by adding 50 µl of the enzyme solution (~10.5 mg/ml) and inverting the cuvette 3 times. Production of *para*-hydroxy-cinnamic acid was followed at 310 nm for 2 min. All measurements were done in duplicate with buffer as a blank. The activity was calculated using the slope of the first 80 s and following Equation 6 :

Equation 6

$$\boldsymbol{specific\ activity}\ [\frac{\boldsymbol{U}}{\boldsymbol{mg}}] = \frac{\frac{\Delta \boldsymbol{A}_{\boldsymbol{310\ nm}}}{\boldsymbol{min}} * \boldsymbol{V} * \boldsymbol{f}}{\boldsymbol{\varepsilon}_{\boldsymbol{310\ nm}} * \boldsymbol{d} * \boldsymbol{c} * \boldsymbol{v}}$$

$\Delta A_{310\ nm}$/min = increase of absorbance at 310 nm per minute [min^{-1}]
V = total assay volume [1500 µl]
f = dilution factor of the enzyme solution
$\varepsilon_{310\ nm}$ = extinction coefficient of *para*-hydroxy-cinnamic acid [12.647 mM^{-1} cm^{-1}]
d = path length cuvette [1 cm]
c = enzyme concentration [mg/ml]
v = volume enzyme sample [50 µl]

3.4.3.6 Kinetic measurements for the deamination

The specific activity of PAL at different substrate concentrations (0-40 mM L-Phe, 0-5 mM L-Tyr) was measured with the respective assay (3.4.3.1 and 3.4.3.5). The kinetic parameters K_M and V_{max} were obtained by hyperbolic fit using origin 7G. Using V_{max} and the molecular weight of one subunit (with one active site each), k_{cat} was calculated with following Equation 7:

Equation 7

$$\boldsymbol{k_{cat}}\ \left[\frac{\boldsymbol{1}}{\boldsymbol{s}}\right] = \boldsymbol{V_{max}} * \boldsymbol{M_{enzyme}}$$

V_{max} = specific activity [U/mg] = [µmol/min*mg]
M_{enzyme} = molecular weight of one enzyme subunit [Da] = [g/mol]

3.4.4 Chiral HPLC methods

To measure conversion and *ee* in biotransformation samples (3.5) a HPLC analysis system Series 1100 was used, equipped with a G1315A diode array detector (Agilent/Hewlett Packard) and two different chiral HPLC columns.

3.4.4.1 Quantification of α-amino acids

A 20-25 µl sample was taken and heated up for 5 min at 80 °C to remove excess ammonia and to inactivate the biocatalyst. Afterwards the sample was mixed with an appropriate amount of the mobile phase (280-800 µl) and centrifuged (3 min, RT, 13000 rpm). 150 µl of the supernatant was transferred to glass vials with inlet. 10 µl of the sample was injected and analyzed on an ASTEC Chirobiotic T column (25 cm x 4.6 mm; 5 µm, Supelco) with a mobile phase consisting of 60 % methanol (MeOH) and 40 % ddH_2O, at 1 ml/min flow rate, 25 °C, and five different wavelengths: 210, 230, 270, 275, and 310 nm. Calibration samples were prepared from stock solutions as described above. The most appropriate wavelength for each analyte was choosen and the peak areas were used to calculate the analyte concentration using the respective calibration curve at the same wavelength. The enantiomeric excess (*ee*) of the product was calculated using the following Equation 8:

Equation 8

$$\boldsymbol{ee}\ [\%] = \frac{[\boldsymbol{m1} - \boldsymbol{m2}]}{[\boldsymbol{m1} + \boldsymbol{m2}]} * \mathbf{100}$$

m1= mass enantiomer 1
m2= mass enantiomer 2; (with m1 > m2)

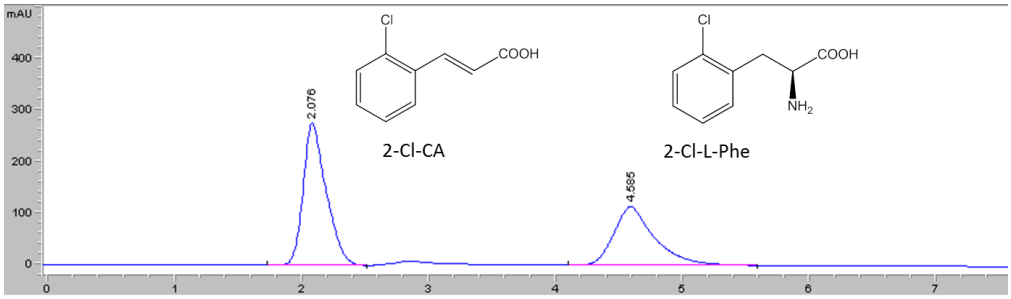

Figure 15: HPLC chromatogram of a reaction sample from the conversion of 2-Cl-CA to 2-Cl-L-Phe using *At*PAL whole cells. HPLC conditions: 10 µl injection, ASTEC Chirobiotic T column (25 cm x 4.6 mm; 5 µm,) with a mobile phase consisting of 60 % methanol (MeOH) and 40 % ddH2O, at 1 ml/min flow rate, 25 °C and 210 nm.

Table 9: Retention times of CAs and α-amino acids on Chirobiotic T in 60%/40% MeOH/H_2O at 25 °C and 1 ml/min flow. / = no standard available, *: no standard available, but appearing peak may be the D-amino acid isomer.

substituent	cinnamic acid derivative retention time [min]	L-α-amino acid retention time [min]	D-α-amino acid retention time [min]
H	2.2	6.0	7.2
2-F	2.1	5.5	6.6
3-F	2.3	6.5	6.9
4-F	2.3	6.5	6.9
2-Cl	2.1	4.6	5.3*
3-Cl	2.4	6.7	7.1*
4-Cl	2.3	6.0	7.0
2-OH	2.3	5.5	6.4
3-OH	2.5	5.3	8.1
4-OH	2.5	5.2	6.2
2-MeO	2.2	6.1	/
3-MeO	2.2	5.6	6.9
4-MeO	2.7	6.0	/
2,3-diMeO	2.1	/	/
2,4-diMeO	2.2	/	/
3,4-diMeO	2.2	5.5	/
3-MeO-4-OH	2.2	5.1	/

3.4.4.2 Quantification of α- and β-amino acids

The reaction tube was centrifuged for 30 s at 8000 rpm and RT to separate the cells from the reaction solution for sampling. A 10 µl sample was transferred to a 1.5 ml reaction tube and heated at 80 °C for 5 min with open lid to remove excess ammonia. Afterwards the sample was mixed with 180-800 µl of 60 % MeOH, depending on the substrate concentration used, and centrifuged (3 min, RT, 13000 rpm). 150 µl of the supernatant was transferred to a 2 ml glass vial with inlet. 10 µl of the sample was injected and analyzed on an CHIRALPAK® ZWIX (+) column (150 x 4.0 mm, 3 µm, Daicel) with a mobile phase consisting of 59/39/2 MeOH/ACN/H_2O with 5 mM formic acid and 2.5 mM diethylamine, 1 ml/min flow rate, 25 °C and four different wavelengths: 210, 230, 270 and 310 nm. The most appropriate wavelength for each analyte was choosen and the peak areas were used to calculate the analyte concentration using the respective calibration curve at the same wavelength. The enantiomeric excess (*ee*) of the product was calculated using the equation above (Equation 8).

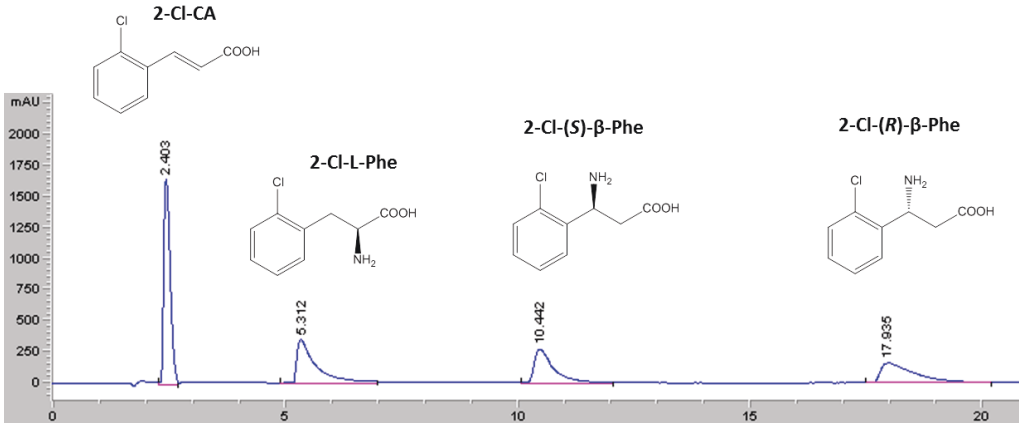

Figure 16: Separation of 2-Cl-CA and 3 isomers of 2-Cl-amino acids (2 mM each). HPLC conditions: 10 µl injected and analyzed on a CHIRALPAK® ZWIX (+) column (150 x 4.0 mm, 3 µm), mobile phase consisting of 59/39/2 MeOH/ACN/H_2O with 5 mM formic acid and 2.5 mM diethylamine, 1 ml/min flow rate, 25 °C and 210 nm.

Table 10: Retention times of CAs and α- and β-amino acids on a CHIRALPAK® ZWIX(+) HPLC column with a mobile phase of MeOH/ACN/H_2O 59/39/2 with 5 mM HCOOH and 2.5 mM DEA at 25 °C and 1 ml/min flow rate. / = no standard available

substituent	CA RT [min]	D-α-aa RT [min]	L-α-aa RT [min]	(*S*)-β-aa RT [min]	(*R*)-β-aa RT [min]
H	2.0	4.7	5.2	11.1	13.1
2-F	2.3	4.9	5.4	9.8	12.9
3-F	2.2	4.9	5.4	11.9	14.1
4-F	2.2	5.1	5.6	12.6	15.0
2-Cl	2.4	/	5.3	10.4	17.9
3-Cl	2.3	/	5.6	12.9	15.3
4-Cl	2.3	5.6	6.2	13.8	16.2
2-OH	2.2	6.9	7.3	10.7	12.8
3-OH	2.4	6.3	6.7	15.4	21.1
4-OH	2.0	4.5	5.2	14.5	17.5
2-MeO	2.5	/	5.2	9.9	10.9
3-MeO	2.1	/	5.1	/	/
4-MeO	2.1	/	5.1	12.0	13.9
2,3-diMeO	2.3	/	/	/	/
2,4-diMeO	2.0	/	/	/	/
3,4-diMeO	2.2	/	7.9	14.8	16.2
3-MeO-4-OH	2.0	/	9.8	/	/

3.4.5 **NMR**

For the measurement of the NMR spectra the isolated product (see 3.5.3) was dissolved in deuterated water until saturation. Nuclear magnetic resonance (NMR) spectra were measured on a DRX 600 spectrometer (Bruker) operating at 600 MHz.

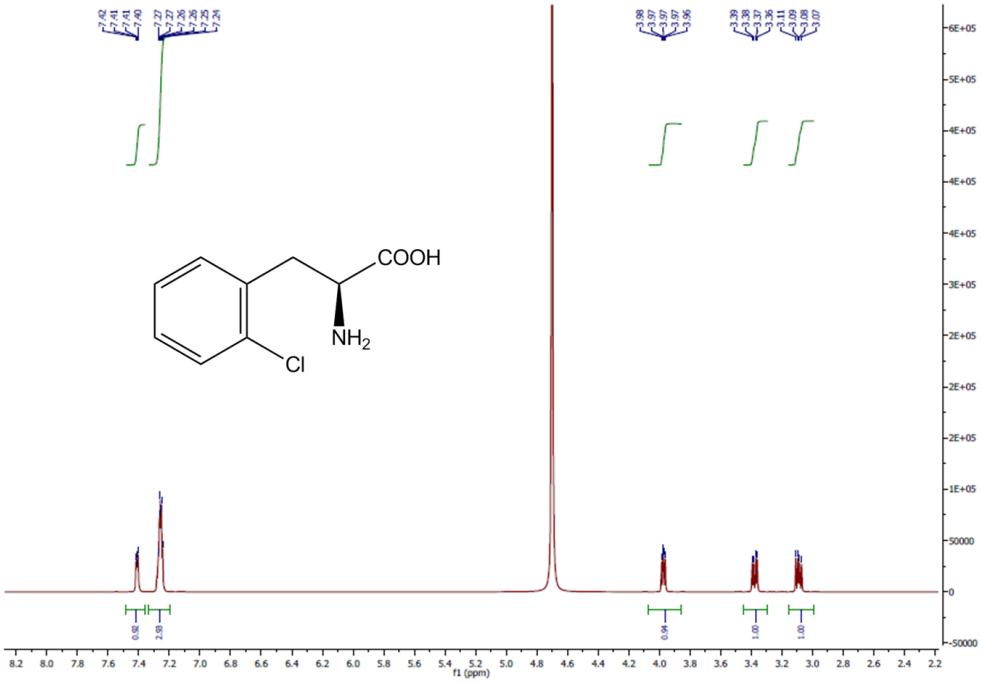

Figure 17: ^{1}H-NMR (600 MHz, D_2O) of 2-Cl-L-Phe: δ = 3.08 (dd, *J* = 14.4, 8.71, 1 H, CH_2), 3.37 (dd, *J* = 14.4, 6.1, 1 H, CH_2), 3.97 (m, 1 H, CH), 7.24-7.27 (m, 3 H, CH), 7.40-7.42 (m, 1 H, CH).

3.5 Biotransformations

3.5.1 Substrate range AL whole cells

To compare wet and lyophilized whole cells 1 ml 50 mM t-CA in 2.5 M $(NH_4)_2CO_3$, pH 8.9, was mixed with 50 mg/ml lyophilized cells or 250 mg/ml wet whole cells in 2 ml reaction tubes and incubated for 24 h at 30 °C, 1200 rpm. To compare free enzyme and lyophilized whole cells 50 mM 3-F-CA and 1 mg/ml lyophilized cells or 0.1 mg/ml purified enzyme was used.

To investigate the substrate range of ALs, 2.5 - 50 mM CA derivative in 2.5 M ammonium carbonate buffer, pH 8.9, using the respective maximal soluble concentration in this buffer, was mixed with 1 mg/ml (*Pc*PAL1, *At*PAL2) or 5 mg/ml (*Rt*PAL) lyophilized whole cells and incubated at 30 °C in 1.5 ml reaction tubes at 1200 rpm. For amination of methoxy-CAs generally 10 mg/ml lyophilized cells were used.

3.5.2 Reaction engineering *At*PAL2

Batch reactor

A 250 ml round bottom flasks was filled with 140 ml substrate solution (27 mM 2-Cl-CA in 2.5 M ammonium carbonate buffer, pH 8.9) and tempered with a water bath to 30 °C before 0.5 mg/ml whole cells containing *At*PAL2 were added. The reaction was performed for 24 h. Several samples were taken at different time points and analyzed with chiral HPLC (3.4.4.1)

Fed-batch reactor

The reaction was performed in 130 ml scale (end volume) in a 150 ml round bottom flasks tempered to 30 °C with a water bath. A 2-Cl-CA feed solution (65 mM) was prepared. 70 mg whole cells were resuspended in 2 ml 2.5 M ammonium carbonate buffer, pH 8.9, without substrate. Afterwards the feed was started with a flow rate of 5 ml/h and adjusted over time to keep the substrate conversion at 90 %. After 48 h the maxium volume of the reactor was reached and the reaction was stopped. Several samples were taken at different time points and analyzed with chiral HPLC (3.4.4.1)

EMR

The EMR with a volume of 20 ml was built by the mechanical workshop (IBG-1, Forschungszentrum Jülich) and equipped with a YM-30 membrane consisting of regenerated cellulose (44.5 mm diameter, 30 kDa cut off, Millipore). A feed solution was prepared with 60 mM 2-Cl-CA in 2.5 M ammonium carbonate buffer, pH 8.9. The reactor was filled with 700 mg lyophilized *E. coli* BL21 whole cells containing *At*PAL2 wt dissolved in 20 ml buffer. The

reaction was performed at 30 °C with a substrate feed rate of 5-10 ml/h for 72 h. Samples were analyzed with chiral HPLC (3.4.4.1)

For the second reaction with lower feed concentration a 25 mM 2-Cl-CA solution was used with 225 mg lyophilized *E. coli* BL21 whole cells containing *At*PAL2 wt and a substrate feed rate of 10-15 ml/h for 187 h.

3.5.3 **Product isolation: 2-Cl-L-Phe**

The reaction solutions of two 130 ml scale fed-batch reactions were pooled after the cells were removed by centrifugation (260 ml with 60 mM 2-Cl-L-Phe, 3.11 g 2-Cl-L-Phe). The volume of the solution was reduced under vacuum (500 mbar) at 60 °C in a Rotavapor R114 rotary evaporator (Büchi) until first crystals appeared. The concentrated solution was stored at 4 °C overnight. Afterwards the crystals were collected by filtration, washed and dried at 60 °C. The purity of the product was checked via chiral HPLC (3.4.4.1) and NMR (3.4.5).

3.5.4 **Reaction engineering *At*PAL2-CBM**

Batch reactor

A crude cell extract (3.3.3) was prepared from 0.35 g *E. coli* BL21 containing *At*PAL2-CBM. The crude cell extract (15.8 U/ml, protein content 21.1 mg/ml) was incubated with 0.5 g Avicel powder (1 g Avicel per 0.8 g wet cells) for 1 h at 30 °C in a 15 ml reaction tube. Afterwards the Avicel was pelleted, washed with ammonium carbonate buffer, pelleted again, before the supernatant was removed with a pipette. The activity of the CCE after immobilization and Avicel removal was 0.01 U/ml and the activity of the wash fraction 0.05 U/ml. The washed Avicel with immobilized *At*PAL-CBM was mixed in a 15 ml reaction tube with 10 ml 22 mM 2-Cl-CA in ammonium carbonate buffer, pH 8.8, to start the amination reaction. The reaction was conducted for 24 h at 30 °C in a thermo shaker. For sampling 100 µl of the solution was removed from the reaction and centrifuged for 1 min at 13000 rpm to pellet the Avicel. 10 µl supernatant were taken for HPLC analysis (3.4.4.1). The Avicel with immobilized enzyme was returned to the reactor.

Repetitive batch reactor

After 1 h batch reaction (see above) the Avicel was separated from the reaction solution by centrifugation, washed with 5 ml ammonium carbonate buffer and mixed with 10 ml fresh substrate solution for a new batch reaction. Eleven repetitive batch reactions (each for 1 h) were performed. After the 7^{th} cycle, the Avicel was removed from the reaction solution,

washed with TRIS-HCl buffer, removed from the wash buffer and stored at 4 °C for 67 h. Afterwards the immobilized enzyme was mixed with fresh substrate solution for the 8th batch reaction.

Fed-Batch reactor

A feed solution was prepared with 60 mM 2-Cl-CA in 2.5 M $(NH_4)_2CO_3$, pH 8.9. 2 g Avicel were incubated for 50 min with the CCE (3.3.3) prepared from 1.37 g cells (activity CCE before Avicel: 9.2 U/ml; activity after Avicel: 0.2 U/ml). Afterwards the CCE with Avicel was centrifuged for 2 min, the supernatant was removed, and the Avicel pellet was washed first with 5 ml TRIS-HCl and after a second centrifugation with 5 ml ammonium carbonat. Washed Avicel with immobilized enzyme was poured into a 250 ml round bottom flask filled with 15 ml 2.5 M ammonium carbonate buffer. The reaction was kept at 30 °C with a water bath. By adjusting the start feed rate of 10 ml/h the enzyme inhibition was balanced. After 21.6 h and 45.4 h the reactor was drained except for 15-24 ml to avoid the decrease in product *ee*. After 117 h the feed was stopped and the conversion of the remaining substrate was awaited before the enzyme was removed from the reaction. For sampling 100 µl of the solution was removed from the reaction and centrifuged for 1 min at 13000 rpm to pellet the Avicel. 10 µl supernatant were taken for HPLC analysis (3.4.4.1). The immobilizate was returned to the reactor.

Plug-flow reactor

1 g Avicel was resuspended in buffer and poured into a XK 16/20 chromatography column (GE Healthcare). The bed volume of the reactor was 4 ml. A crude cell extract (3.3.3) was prepared from 0.79 g whole cells containing *At*PAL2-CBM. The clarified CCE (2.45 ml, 8.8 U/ml, protein content 25.3 mg/ml) was pumped through the column with a flow of 0.2 ml/min. The flow through was collected (7.5 ml, 1.6 U/ml, 6.9 mg/ml). After binding, the column was washed and equilibrated with 2-3 column volumes 2.5 M ammonium carbonate buffer, pH 8.9. The reaction was started by pumping the 25 mM 2-Cl-CA substrate solution through the column, flow rate 15-5 ml/h. Product formation was tracked with chiral HPLC (3.4.4.1). The reactor was heated to 30 °C with a water bath. After 69 h the reaction was stopped.

3.5.5 Specific activity of immobilized *At*PAL2 vs whole cells

The 2-Cl-L-Phe product concentrations (µmol/L) from batch reactions (3.5.1 and 3.5.4) were plotted against the reaction time (min). From the data points (≤ 46 % conversion) the slope was calculated and divided by the enzyme concentration (mg/ml). From one mg lyophilized whole cells containing *At*PAL2, 0.15 mg enzyme can be isolated via NiNTA, therefore 0.15 mg/ml was used for the calculation of the initial activity of whole cells.

3.5.6 **Substrate range of aminomutases in whole cells**

Solutions containing the respective CA derivative in 2.5 M ammonium carbonate buffer, pH 8.9 (Table 11) were incubated with 100 mg/ml lyophilized whole cells containing AM for 71 h at 30 °C and 1200 rpm in 1.5 ml reaction tubes. The product distribution was monitored with HPLC (3.4.4.2).

Table 11: Prepared substrate solutions of CA derivatives in 2.5 M $(NH_4)_2CO_3$.

a) t-CA, 50 mM	h) 2-OH-CA, 50 mM	n) 2,3-diOCH_3-CA, 15 mM
b) 2-F-CA, 50 mM	i) 3-OH-CA, 50 mM	o) 2,4-diOCH_3-CA, 14.5 mM
c) 3-F-CA, 50 mM	j) 4-OH-CA, 50 mM	p) 3,4-diOCH_3-CA, 15 mM
d) 4-F-CA, 40 mM	k) 2-OCH_3-CA, 15 mM	q) 3-OCH_3-4-OH-CA, 14.9 mM
e) 2-Cl-CA, 25 mM	l) 3-OCH_3-CA, 15 mM	
f) 3-Cl-CA, 5 mM	m) 4-OCH_3-CA, 15 mM	
g) 4-Cl-CA, 2.5 mM		

3.5.7 **Immobilization of *Cc*TAM K2E-CBM to Avicel**

A CCE was prepared from 1.5 g wet cells containing *Cc*TAM-K2E-CBM in 5 ml 50 mM TRIS-HCl buffer and incubated with 1 g Avicel for 1 h at 30 °C. Another 1.5 g wet cells were directly used for the reaction. Wet cells and immobilizate were washed twice with 5 ml ammonium carbonate buffer before the reaction. The amination was started by adding 4 ml substrate solution, containing 20 mM 2-Cl-CA in ammonium carbonate buffer, to the Avicel or cell pellet with subsequent mixing. Reactions were incubated in 15 ml reaction tubes for 45 h at 20 rpm and 30 °C in an overhead shaker. Product formation was tracked with chiral HPLC (3.4.4.2).

4 Results and Discussion

4.1 Toolbox creation of MIO-enzymes

To establish a MIO-enzyme toolbox for the production of unnatural amino acids, enzymes were selected from literature data according to the following criteria: the active production in *E. coli* should be possible and a crystal structure should be available [78,94,109–111]. Five ammonia lyases: PAL1 from *P. crispum*, PAL2 from *A. thaliana*, PAL/TAL from *R. toruloides*, TAL from *R. sphaeroides*, and TAL from *R. capsulatus*. Further, four aminomutases: two PAMs from *T. chinensis* and *T. canadensis*, and two TAMs from *C. crocatus* and *S. globisporus* were selected (Figure 18). The crystal structures of *Pc*PAL [71], *Rt*PAL [112], *Rs*TAL [79], *Tca*PAM [88], *Tch*PAM [113] and *Sg*TAM [89] are available. For *At*PAL2 a homology model was created.

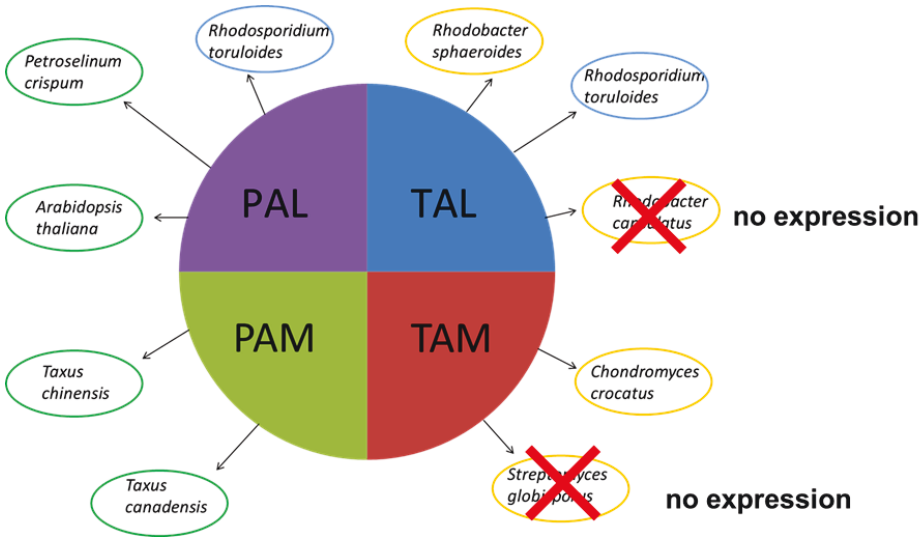

Figure 18: Created toolbox of active MIO-enzymes. The enzymes, originating from plants (green), yeast (blue), and bacteria (yellow), were functionally produced in *E.* coli. The red-crossed enzymes could not be solubly produced in *E. coli*.

The respective coding sequences (see appendix) were extracted from NCBI and synthetic genes were ordered, codon optimized for *E. coli* expression (3.1.4). All genes were subcloned in pET22b or pET28a expression vectors (Table 5) such that expression resulted in fusion enzymes with a C-terminal His_6tag. The soluble expression of the nine enzymes was investigated in two different media, LB- and AI medium (3.3.1). *Pc*PAL, *At*PAL, *Rt*PAL, *Rs*TAL and *Cc*TAM exhibited the highest soluble expression in AI medium at 20 °C. The strong expression of the genes encoding *Tca*PAM and *Tch*PAM in LB and AI medium resulted in the formation of inclusion bodies. Therefore PAM genes were coexpressed in LB medium with

different chaperone genes (3.3.2), to assist in protein folding and increase the soluble fraction of the target enzyme. The presence of a trigger factor (plasmid 5) was most effective in case of both PAMs (Figure 19; *Tca*PAM: 77.6 kDa, *Tch*PAM: 76.4 kDa per subunit).

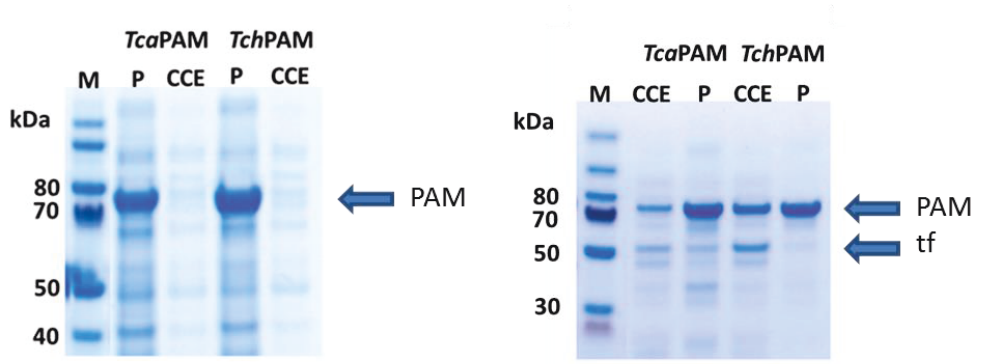

Figure 19: SDS-PAGE analysis of soluble and insoluble fractions after PAM gene expression without chaperones (left) and after coexpression with chaperone 5 containing the trigger factor (tf) (right). Analysis conditions see 3.3.3 and 3.4.1, Marker: PAGE PageRuler™ (Plus) Prestained Protein Ladder. CCE: crude cell extract; P: pellet after disruption. *Tca*PAM: 77.6 kDa, *Tch*PAM: 76.4 kDa, trigger factor: around 56 kDa.

All enzymes, except *Rc*TAL and *Sg*TAM, were active in the deamination of phenylalanine and tyrosine, respectively, as well as in the reverse amination reactions. The genes encoding *Rc*TAL and *Sg*TAM, respectively, could not be expressed at all in both media, neither in *E. coli* BL21 (DE) nor in *E. coli* BL21 Gold (DE3).

The ammonia lyases *Pc*PAL1, *At*PAL2, *Rt*PAL, and *Rs*TAL were purified with IMAC using the same protocol (3.3.4). As an example the purification of *At*PAL2 is shown (Figure 20). Crude cell extract was prepared in TRIS-HCl buffer (3.3.3) and applied to the NiNTA column. The flow through contained a small amount of the target enzyme, due to overloading of the column. By washing with buffer, containing 30 mM imidazole, weakly bound proteins were flushed. Afterwards the target enzyme was eluted with 300 mM imidazole in good purity. The purified enzymes were desalted (3.3.5), lyophilized (3.3.6), and stored at -20 °C. Additionally wet and lyophilized whole cells containing AL or AM were stored for biotransformations with whole cell.

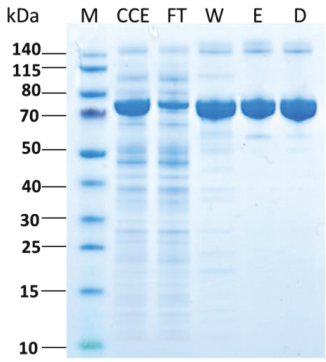

Figure 20: IMAC purification of *At*PAL2. M: marker, PAGE Ruler prestained; CCE: crude cell extract 1:35; FT: flow through 1:10; W: wash fraction 1:1; E: elution 1:10; D: desalting 1:3. 13 µl sample, 5 µl NuPage LDS Sample Buffer 4x, 2 µl NuPage Reducing Agent 10x; 2 min 99°C, 10 µl loaded onto gel; 200 V, 100 mA, 15 W, 60 min; 1 h Coomassie staining, destaining in water.

Four wild-type ammonia lyases (PAL/TAL), one variant with altered substrate specificity, and three wild-type aminomutases (PAM/TAM) from plants, yeast, and bacteria were actively produced in *E. coli* and different enzyme preparations (wet and lyophilized whole cells, free enzyme) were stored for further experiments.

4.2 Characterization of ammonia lyases

In literature a broad range of data is already available for several of the enzymes tested also in this thesis. However, the different experimental conditions make a comparison difficult. Therefore, the enzymes were characterized under identical assay conditions to identify optimal reaction conditions for the production of amino acids. Furthermore, temperature optima were recorded to elucidate the extent of possible activity increase by increasing the reaction temperature (4.2.1). Stability under reaction conditions is also an important issue (see 4.2.5).

4.2.1 pH- and temperature optima wt PALs (deamination)

Since the focus of this thesis is on the amination reaction the activity in the alkaline pH-range was studied. For the purified PAL enzymes the specific activity at different pH values was determined with a photometric assay (3.4.3.1). As demonstrated in Figure 21, the optimal pH-range of *Rt*PAL is between pH 7.5 and pH 9.0 and decreases strongly when the pH exceeds pH 9.0. By changing the pH from 9.0 (2.03 U/mg) to 10.0 (0.76 U/mg) the activity decreased by more than 62 %. A similar pH-dependent initial activity range was found for for *Pc*PAL1 between pH 8.0 and 9.5. *At*PAL2 shows maximal activity at pH 8.5. The data are in agreement with the pH-optima measured by Cochrane *et al.* for *At*PAL2 (pH 8.4 - 8.9) [78] and by Appert *et al.* for *Pc*PAL1 (pH 8.5) [114]. All enzymes show a low specific activity in the physiological reaction, which is not unusual for enzymes of the secondary metabolism.

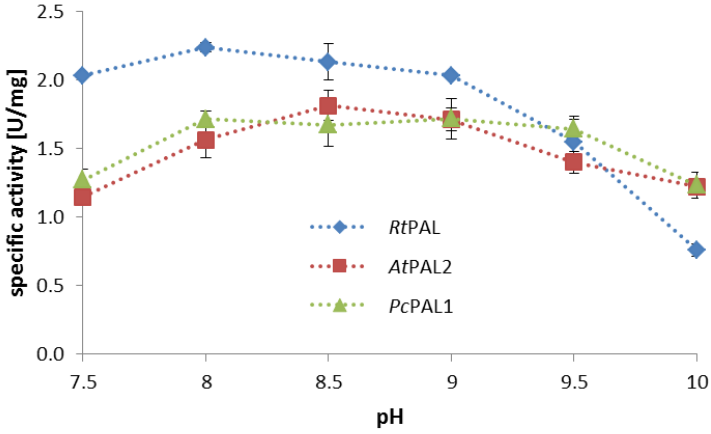

Figure 21: Specific activity of wt PALs at 30 °C and varying pH values. The deamination of 30 mM L-Phe was monitored at 275 nm for 2 min in 100 mM Tris-HCl (pH 7.5-9.0) or CAPSO-NaOH (pH 9.5-10.0). Enzymes were stored in TRIS-HCl, pH 8.8 until measurement. Initial rate activities were used to calculate the specific activity. Measurements were conducted in duplicate.

Afterwards the temperature optimum was determined by following the deamination L-Phe at different temperatures ranging from 30 – 60 °C (3.4.3.1). The pH of the substrate solutions was fixed to 8.0 for *Rt*PAL and *Pc*PAL1 and to pH 8.5 for *At*PAL2. As demonstrated in Figure 22 the activity of all three enzymes increased with increasing temperature up to 55 °C. At 55 °C the maximum was reached for *At*PAL2 and at higher temperature the activity started to decrease slightly. Therewith the temperature optimum for *At*PAL2 observed in this thesis is 7 °C higher compared to ealier studies, which can most probably be explained by the different assay conditions used by Cochrane *et al.* (Bis–TRIS propane buffer, pH 8.2) [78]. *Rt*PAL (7.1 U/mg) and *Pc*PAL1 (7.7 U/mg) reached the maximum activity at 60 °C which is in agreement to the results of Appert *et al*. for *Pc*PAL1 (58 °C), although a different assay was used in their work (0.2 M sodium borate/NaOH, pH 8.8) [114]. The weak specific activity of PALs was only slightly increased by increasing the temperature therefore all further measurements were performed at 30 °C.

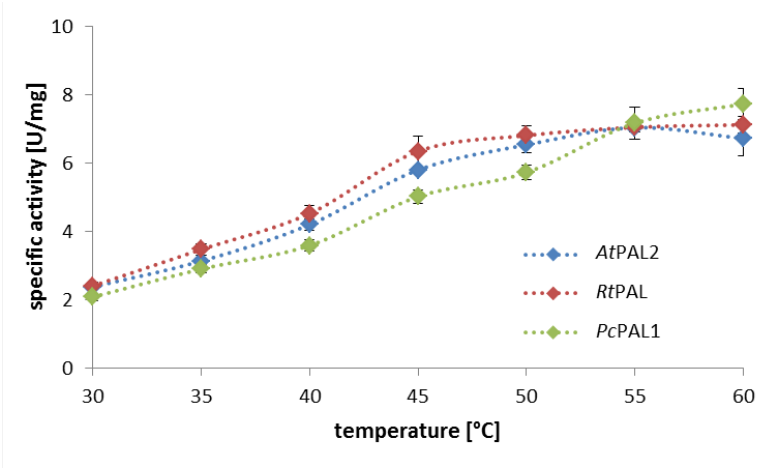

Figure 22: Temperature optimum of wt PALs. The deamination of 30 mM L-Phe was monitored at 275 nm for 2 min in 100 mM TRIS-HCl (*Pc*PAL and *Rt*PAL: pH 8.0; *At*PAL2: pH 8.5) at different temperatures ranging from 30 – 60 °C. The reaction solutions were heated until the respective temperature inside the cuvette was reached. The temperature in the cuvette was controlled with an external thermometer. Measurements were started by adding the enzyme. Initial rate activities were used to calculate the specific activity. Measurements were conducted in duplicate.

The Temperature- and pH-optimum of *Rs*TAL was not measured, because of its low activity (0.06 U/mg) and the required high enzyme amounts, according to Xue *et al*. a pH of 8.5 was used for further experiments using *Rs*TAL [115]. Regarding the temperature, all further measurements were conducted at 30 °C to keep a good balance between activity and stability of the enzymes, because the shown measurements are initial rate measurements over 2 min and stability is expected to decrease with prolonged incubation at higher temperature.

Following the deamination of L-Phe, pH and T optima of *Pc*PAL1 (pH 8.0-9.5; 60 °C), *Rt*PAL (7.5 -9.0; 60 °C) and *At*PAL2 (pH 8.5; 55 °C) were measured. All further measurements were performed at 30 °C.

4.2.2 **Kinetic measurements of the deamination reaction**

The kinetic parameters of purified ALs for the natural substrates L-Phe and L-Tyr were investigated in photometric assays (3.4.3). Kinetic data for the *At*PAL2 F136H variant, created by T. Hilberath [108] during the course of this thesis, with the aim to generate an enzyme with higher TAL activity in reference to *Rs*TAL, were included for comparison (Table 12).

Table 12: Kinetic parameters for the deamination of L-Phe and L-Tyr, respectively, catalyzed by wt PALs and the variant *At*PAL2 F136H [108]**.** Assay conditions: 30 °C, 1 cm cuvette, 50 mM Tris-HCl buffer, pH 8.8, 50 µl enzyme solution, 1.5 ml assay volume, 2 min measuring time; a) 0-40 mM L-Phe, 275 nm, b) 0-5 mM L-Tyr, 310 nm. The kinetic parameters were obtained by hyperbolic fit using origin 7G.

substrate	enzyme	K_M [mM]	k_{cat} [s^{-1}]	k_{cat}/K_M [mM s^{-1}]	V_{max} [U/mg]
L-Phe	*At*PAL2 wt	0.05 ± 0.00	2.60 ± 0.02	56.62	1.98 ± 0.02
	*At*PAL2 F136H	0.88 ± 0.03	1.86 ± 0.01	2.13	1.42 ± 0.01
	*Pc*PAL1 wt	0.05 ± 0.01	2.64 ± 0.04	55.06	2.01 ± 0.04
	*Rt*PAL/TAL wt	0.54 ± 0.04	5.99 ± 0.06	11.03	4.61 ± 0.06
L-Tyr	*At*PAL2 wt	1.68 ± 0.19	0.05 ± 0.00	0.03	0.04 ± 0.00
	*At*PAL2 F136H	0.25 ± 0.01	0.06 ± 0.00	0.24	0.05 ± 0.00
	*Rs*TAL wt	0.21 ± 0.02	0.06 ± 0.00	0.28	0.06 ± 0.00
	*Rt*PAL/TAL wt	0.21 ± 0.01	1.02 ± 0.01	4.92	0.78 ± 0.01

The measured data are in good agreement with the already available literature data for the enzymes, even if the values cannot be compared exactly, because the different assay conditions assay pH and temperature may have a major influence. For both plant enzymes, *At*PAL2 and *Pc*PAL1, the pysiological substrate is L-Phe, which is reflected in the low K_M values of about 0.05 mM resulting in catalytic efficiencies of 55-56 mM^{-1} s^{-1}. With L-Tyr the K_M value for *At*PAL2 wt increases to 1.68 mM and the k_{cat} decreases 55-fold to 0.05 s^{-1}, the same behavior was observed with *Pc*PAL by Bartsch *et al*. [116]. The values determined by Crochane *et al* for *At*PAL2 wt with L-Phe are K_M: 0.064 mM, k_{cat}: 3.2 s^{-1} and k_{cat}/K_M: 51.2 mM^{-1}

s^{-1} and for L-Tyr k_{cat}/K_M: 0.04 mM^{-1} s^{-1} [78]. By a single mutation in the active site of *At*PAL2, the preference for L-Phe could be switched to L-Tyr [108]. The yeast enzyme *Rt*PAL converts L-Phe (k_{cat}/K_M: 11.03 mM^{-1} s^{-1}) and L-Tyr (k_{cat}/K_M: 4.92 mM^{-1} s^{-1}) with similar catalytic efficiency. And is therefore a "better" TAL enzyme as the wt enzyme *Rs*TAL, with a comparable K_M of about 0.21 mM, but a much lower k_{cat} of 0.06 s^{-1} (*Rt*PAL: 1.02 s^{-1}).

*At*PAL2 and *Pc*PAL1 show the highest affinity and catalytic activity for L-Phe. In comparison the K_M values for the tested TALs are by a factor of 4 higher which goes in line with a 40-50-fold lower catalytic activity.

4.2.3 Kinetics and pH optima of wt PALs for the amination of trans-cinnamic acid

To obtain relevant data for the subsequent production of non-natural amino acids, the amination of t-CA with wt PALs was tested in more detail. As already stated, the equilibrium of the amination reaction is on the educt (t-CA) site (equilibrium constant: 4.7 mol/L [82]). The enzyme activity is strongly depending on the ammonia concentration and increases with increasing NH_3 concentration. Using five different solutions with concentrations ranging from 1 M to 5 M NH_3, the initial activity increased linearly from 1 M to 5 M NH_3 (data not shown). Higher ammonia concentrations were not tested due to an expected negative impact on the enzyme stability and because of the difficult handling of highly concentrated ammonia solutions at larger scale.

The initial kinetic studies were performed in continuous photometric assays (3.4.3) following the depletion of the substrate t-CA. Due to the high extinction coefficient of t-CA at 275 nm, the substrate concentration was limited to 4 mM, even in cuvettes with a light path of 0.2 mm. All three enzymes showed typical hyperbolic Michaelis Menten curves. The kinetic parameters are listed below (Table 13). In case of *Rt*PAL V_{max} was not reached, when the detection limit of the photometer was reached (see Appendix).

Table 13: Kinetic parameters for the amination of trans-cinnamic acid (t-CA) catalyzed by wt PALs. Assay conditions: 0-4 mM t-CA, 275 nm, 5 M NH_3-solution, pH 10, assay was started with 5-20 µl enzyme solution, in 0.2-10 mm cuvette, 0.5 - 1 ml assay volume, 1- 2 min measuring time; 275 nm, 30 °C.

enzyme	K_M [mM]	k_{cat} [s^{-1}]	k_{cat}/K_M [mM s^{-1}]	V_{max} [U/mg]
*At*PAL2 wt	0.05 ± 0.01	0.39 ± 0.01	8.19	0.30 ± 0.01
*Pc*PAL1 wt	0.05 ± 0.02	0.46 ± 0.02	9.13	0.35 ± 0.02
*Rt*PAL/TAL wt	0.93 ± 0.23	1.04 ± 0.07	1.11	0.80 ± 0.07

The K_M values in the amination of t-CA are similar to the values measured for the deamination of L-Phe before, but the k_{cat} is 6-fold lower for all three enzymes. The specific activity of *Pc*PAL1 measured in this thesis (0.35 U/mg) is comparable to the specific activity determined by Bartsch *et al.* for the enzyme with t-CA (0.3 U/mg) [80]. To increase the activity the influence of the pH was tested by measuring the pH-optima of the wt PALs (Figure 23).

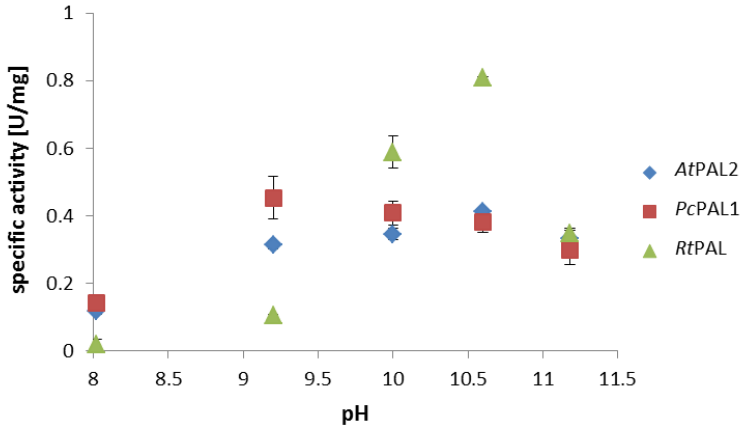

Figure 23: pH-optima of wt PALs for the amination of t-CA. Conditions: The amination of 4 mM t-CA was monitored at 275 nm for 2 min in 5 M NH_3 at 30 °C; pH was adjusted with sulfuric acid. The reaction was started by adding the enzyme. Initial rate activities were used to calculate the specific activity. Measurements were conducted in duplicate.

As demonstrated in Figure 23 resonable activity for all enzymes was only found at pH > 9. *Pc*PAL1 and *At*PAL2 show very smiliar pH-optima with maximal activities of about 0.3 to 0.45 U/mg in the pH-range between 9.2 and 11.2. Besides, the pH-dependent inital rate activity of *Rt*PAL looks different, showing reasonable activities only at pH > 10 with a clear maximum (0.81 U/mg) at pH 10.6.

The kinetic parameters and pH-optima for the amination of t-CA were measured for *Pc*PAL1 (pH 9.2), *At*PAL2 (pH 10.6) and *Rt*PAL (pH 10.6). *Pc*PAL1 and *At*PAL2 show identical K_M-values for t-CA and L-Phe but the reaction velocity of the amination reaction is by a factor of six lower relative to the deamination reaction.

4.2.4 Ammonium carbonate as alternative ammonia source

In larger scale the preparation of a 5 M NH_3 solution carries a high risk of accidents at work, because it is prepared by dilution of a higher concentrated ammonia solution (32 %). The risk is even higher, when strong acids (HCl, H_2SO_4) are used to adjust the pH from above pH 12 to pH 9-10 used in the enzyme reaction. Therefore, aqueous ammonia was replaced by ammonium carbonate buffer. Ammonium carbonate is less aggressive and the pH of a 2.5 M solution is at around pH 8.9 and thus must not be adjusted, since this value is close to pH-optima at least of *Pc*PAL1 and *At*PAL2 (see Figure 23) and it could be expected that the stability optimum is at lower pH (see 4.2.5). Furthermore chiral HPLC columns are used to monitor the reaction, which are sensitive to high pH values, therefore the excess of ammonia should be removed before analysis. By heating the samples to > 60 °C, the volatile ammonium carbonate buffer disintegrates into 2 NH_3, H_2O and CO_2. Thus, buffer removal and heat inactivation of the enzyme can be done in one step. Lovelock and Turner [117] have already demonstrated the applicability of this buffer in the amination of 2-Cl-CA and 4-CF_3-CA using a PAL from *A. variabilis*. Hence 2.5 M ammonium carbonate buffer (pH 8.9) was used without adjusting the pH, to avoid the presence of non volatile salts. The activity of the wt PALs in ammonium carbonate buffer was compared to the previous results in ammonium sulfate buffer at pH 9.2 (Figure 24).

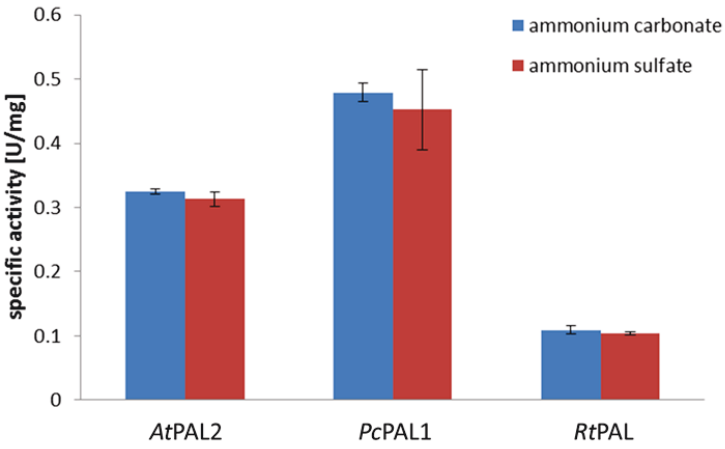

Figure 24: Specific amination activity of wt PALs in 2.5 M ammonium carbonate buffer (pH 8.9) and 5 M NH_3 (adjusted with sulfuric acid to pH 9.2) for the amination of t-CA. Assay conditions: 4 mM t-CA, 30 °C, 275 nm, 20 µl enzyme solution, 2 min measuring time, 0.5 ml assay volume, 0.2 cm quartz cuvette. Initial rate measurements were conducted in duplicate.

As demonstrated in Figure 24, the specific activity of all three purified PAL enzymes in ammonium carbonate buffer is comparable to the previous results in ammonium sulfate buffer, even when the pH differs slightly.

4.2.5 Enzyme stability in ammonium carbonate buffer

As initial rate measurements are not informative concerning the stability of the enzymes under reaction conditions, stability studies were conducted to identify an appropriate reaction buffer for the further studies. Therefore the residual activity of the three PALs was studied in ammonium carbonate buffer, pH 8.9, and ammonium sulfate buffer, pH 9.2 and pH 10.6, respectively. Exemplary the stability of *At*PAL2 in the three different buffers is shown (Figure 25).

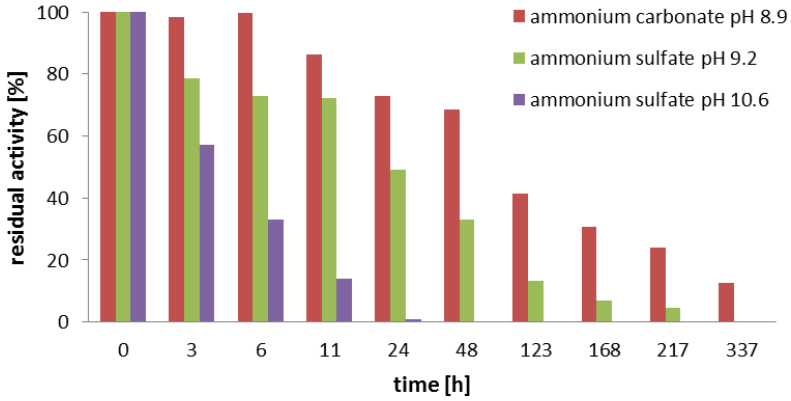

Figure 25: Residual volumetric activity after incubation of *At*PAL2 in ammonium carbonate (pH 8.9) and ammonium sulfate (pH 9.2 or pH 10.6). Incubation conditions: 8-9 mg lyophilized enzyme in 1.5 ml of the respective buffer at 30 °C and 300 rpm. At each time point samples were taken and transferred to a 1 cm cuvette to follow the deamination of L-Phe (3.4.3.1). The volumetric activity at the beginning was set to 100 %.

As expected, the stability at pH 10.6 (pH optimum of *At*PAL2 in initial rate measurements) is the lowest. After 24 h only 1 % initial activity was left in ammonium sulfate buffer, pH 10.6. In the same buffer with pH 9.2, the enzyme is more stable, with 4.5 % residual activity even after 217 h (9 days) incubation. Besides, in ammonium carbonate buffer with pH 8.9, 23.8 % of the activity was detectable at that time point. After 337 h (14 days) the experiment was stopped, although the enzyme in ammonium carbonate buffer still showed 12.5 % residual activity. The same experiments were conducted for *Rt*PAL and *Pc*PAL1 (see Appendix). All wt PALs are still active after 14 days in ammonium carbonate buffer, pH 8.9, with 5.6 % (*Pc*PAL1), 12.5 % (*At*PAL2) and 33.7 % (*Rt*PAL) residual activity (Figure 26).

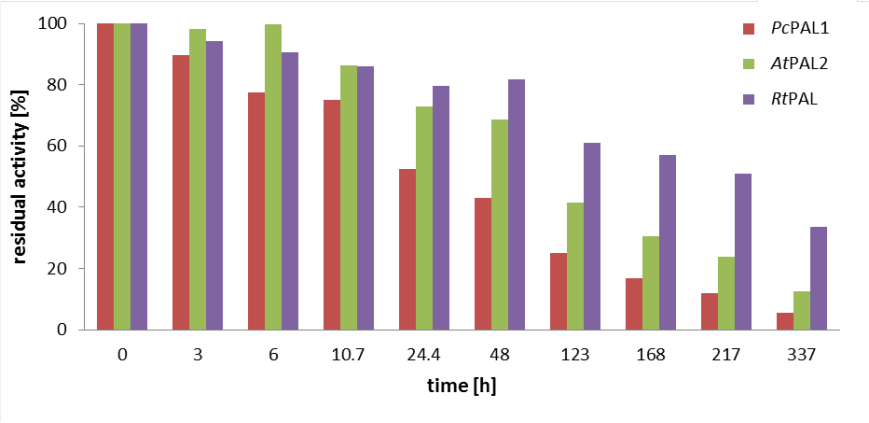

Figure 26: Residual activity of wt PALs after incubation in 2.5 M ammonium carbonate buffer, pH 8.9, at 30 °C and 300 rpm for 14 days.

The reaction rates for the amination of t-CA catalyzed by wt PALs in ammonium carbonate buffer are comparable to those in ammonium sulfate buffer with a similar pH. wt PALs are most stable in ammonium carbonate buffer at pH 8.9, compared to ammonium sulfate buffer at pH 9.2 and 10.6.

Therefore all further experiments are conducted in 2.5 M ammonium carbonate buffer, pH 8.9.

4.2.6 **Selection of the enzyme preparation**

Before starting the substrate screening, the best AL enzyme preparation should be selected. Therefore the amination properties of wet whole cells, lyophilized whole cells, and purified lyophilized enzyme were investigated. As an example the amination with three *At*PAL2 enzyme preparations is described here in more detail (3.5.1). First wet whole cells containing *At*PAL2 were compared with lyophilized cells for the amination of t-CA (Figure 27). To keep the catalyst load comparable, the ratio between the used cell loads is 1:5, because wet cells loose 80 % of their weight (water) during the freeze drying process. Both cell preparations catalyze the reaction very fast with 91.2 % (lyophilized cells) and 87.9 % conversion (wet cells) after only 54 min. The *ee* of L-Phe was in both reactions ≥ 99 % at that time point. With prolonged incubation the *ee* dropped continuously to 94.1 % (lyophilized cells) and 91.4 % (wet cells) after 9.3 h. Due to the slightly better results with lyophilized cells and their easier handling, dry cells were compared with purified enzyme in the next step.

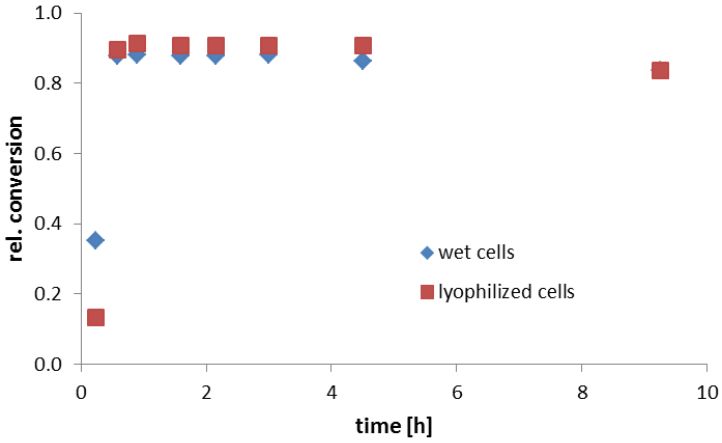

Figure 27: Amination of t-CA with wet or lyophilized *E. coli* BL21 (DE) whole cells containing *At*PAL2. Reaction conditions: 50 mM t-CA, 30 °C, 2.5 M $(NH_4)_2CO_3$, pH 8.9, 1200 rpm, 1.5 ml, 50 mg/ml lyophilized cells or 250 mg/ml wet whole cells.

The ratio between free enzyme and lyophilized whole cells is 1:10, because 0.12-0.18 mg free enzyme can be isolated via NiNTA chromatography from 5 mg wet cells, which corresponds to 1 mg cells after lyophilization. Exemplarily the amination of 3-F-CA was examined to compare the catalytic activity of lyophilized purified *At*PAL2 and the respective amount of lyophilized whole cells. The results are shown in Figure 28.

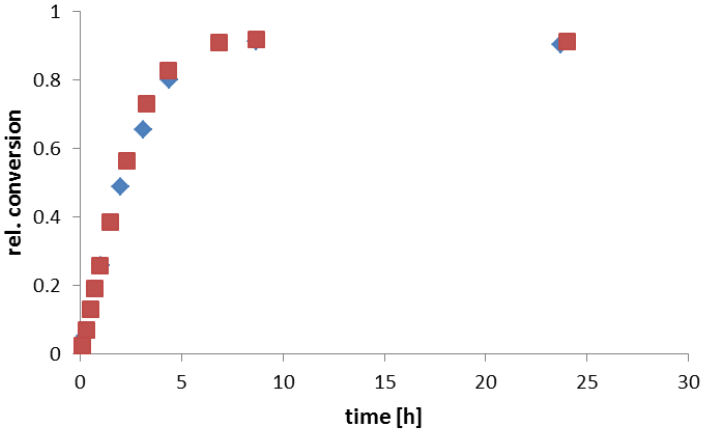

Figure 28: Amination of 3-fluoro-CA with lyophilized whole cells (blue) containing *At*PAL2 or lyophilized purified *At*PAL2 (red). Reaction conditions: 50 mM 3-F-CA, 30 °C, 2.5 M $(NH_4)_2CO_3$, pH 8.9, 1.5 ml, 1 mg/ml lyophilized cells or 0.1 mg/ml purified enzyme.

With both enzyme preparations very similar conversion curves were obtained, reaching a maximum > 91% after 8.7 h. The *ee* of L-Phe remained > 99 % for both reactions over 24 h. Most probably the decrease of the *ee* of L-Phe observed in the previous experiments (Figure 27) is catalyzed by other cellular enzymes. In the present case the cell load was only 1 mg/mL compared to 50 mg/mL in the previous studies. Because the results with all tested enzyme preparations were very similar, lyophilized whole cells were used for further experiments, because they are easier to handle than sticky wet cells and they are cheaper, because chromatographic enzyme purification would last two days. No side-products could be detected by HPLC analysis (3.4.4.1), which is often a disadvantage of using whole cell biocatalysts. Further, the cell load was with 1 mg/ml very low, due to the high concentration of the enzyme in the cell.

Lyophilized whole cells containing *At*PAL2 convert cinnamic acids with high conversions and *ee* values similar to the free enzyme, without detectable formation of side-products.

Therefore all further substrate screening experiments are conducted with lyophilized whole cells. The results suggest an L-Phe racemizing activity in *E. coli*, which leads to a continuous decrease of the *ee* in presence of higher concentrations of the whole cell catalyst.

4.2.7 **Substrate range of ammonia lyases for the amination of t-CA derivatives**

Trans-cinnamic acid and 17 derivatives (see Table 14) were selected to investigate the substrate range of *Pc*PAL1, *At*PAL2, *Rt*PAL, and *Rs*TAL as respective lyophilized recombinant *E. coli* whole cells (see 3.5.1).

Exemplary the conversion of chloro-CAs with wt PALs is shown in Figure 29. The three enzymes differ in conversion rates depending on the position of the substituent. 3-Cl-CA was converted by all three enzymes with similar velocity. About 90 % were aminated in less than 5 h to the corresponding amino acid. The same tendency could be observed for 4-Cl-CA with *Pc*PAL1 (89.1 %) and *At*PAL2 (91.7 %). But with *Rt*PAL no product formation was detected, probably due to unfavourable interactions of the chloro substituent in *para*-position of the substrate with His137 in the binding pocket (see 2.3.1), which is replaced by phenylalanine in *Pc*PAL1 and *At*PAL2 [81]. Only *At*PAL2 converted all Cl-CA-derivatives with equal velocity. In case of 2-Cl-CA, an important precursor of hypertension drugs (Figure 13), only the PAL from *A. thaliana* exhibits high product formation (96.4 % conversion, *ee* ≥ 99 %) after only 8.7 h with a cell load of only 1 mg/ml (*Rt*PAL: 21.6 h, 51.4 % conversion, 5 mg/ml cell load; *Pc*PAL: 23.8 h, 50.5 % conversion, 1 mg/ml cell load).

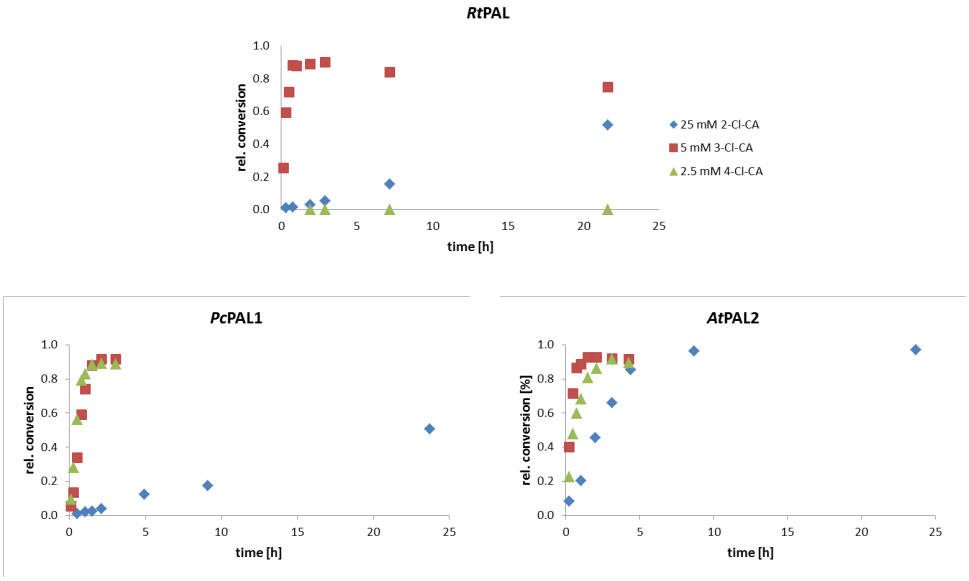

Figure 29: Relative conversion of mono-substituted chloro-cinnamic acids over time using wt PALs. Reaction conditions: 2.5-25 mM substrate in 2.5 M $(NH_4)_2CO_3$, pH 8.9, 30 °C, 1 ml volume, 1200 rpm, cell load: 1 mg/ml (*Pc*PAL1, *At*PAL2) or 5 mg/ml (*Rt*PAL).

The amination of hydroxy-CAs (**h-j**) (see Table 14) was examined with *Rs*TAL. With **h** and **i** no product formation was observed. Due to the low activity of *Rs*TAL, even with the natural substrate 4-OH-CA (**j**) (35.5 % conversion after 24 h with 20 mg/ml cells, *ee* 99 %) and a 20-fold higher cell load compared to *Pc*PAL1 and *At*PAL2. Therefore the substrate range of this enzyme was not further investigated.

Dimethoxy-CAs (**n-p**) are no substrates for all three PAL enzymes, probably due to steric hindrance caused by these bulky substrates. 3,4-dihydroxy-CA (**r**), a precursor of L-Dopa, oxidized immediately after dissolving in ammonium carbonate buffer, probably due to the high pH of the solution and the pka value of the 3-OH-group. Alkaline oxidation of L-Dopa (pKa 3-OH: 8.7-9.1) was already described by Lippolt and Jaeger [118]. Therefore the amination of this substrate was not further investigated. Instead the oxidation sensitive 3-hydroxy-group was protected against oxidation with a methoxy-group in substrate (**q**)**.** 3-Methoxy-4-hydroxy-CA (**q**) was stable in ammonium carbonate and a good substrate for *Rt*PAL. By deprotection of the aminated product under acidic conditions L-Dopa may be obtained (not tested)[119]. As described previously for *Pc*PAL, [80,120] mono-substituted CAs (**b-m**) were good substrates for all tested PALs. The respective L-amino acids were produced with excellent optical purity. Only for a few compounds [*Pc*PAL1/*At*PAL2: **h** and **i**; *Rt*PAL: **c, f, i**] a slight decrease in *ee* after prolonged incubation was observed (see Appendix).

Table 14: Investigated substrates and conversion at time point of maximum *ee* for the amination of CAs with wt PALs. Conditions: The concentration of each CA was 50 mM or less, depending on their solubility in 2.5 M ammonium carbonate buffer, pH 8.9. Some CAs were only poorly soluble in this buffer for example 3-Cl-CA (5 mM) or 4-Cl-CA (2.5 mM). Each substrate solution was incubated with 1-10 mg/ml lyophilized whole cells containing the respective AL at 30 °C. Samples were taken at different time points and analyzed with HPLC for conversion and *ee* (3.4.4.1; single measurements). The retention times of the products are in agreement with the references ordered from Peptech. / = no conversion.

a) t-CA, 50 mM
b) 2-F-CA, 50 mM
c) 3-F-CA, 50 mM
d) 4-F-CA, 40 mM
e) 2-Cl-CA, 25 mM
f) 3-Cl-CA, 5 mM
g) 4-Cl-CA, 2.5 mM
h) 2-OH-CA, 5 mM
i) 3-OH-CA, 5 mM
j) 4-OH-CA, 5 mM
k) 2-OCH_3-CA, 15 mM
l) 3-OCH_3-CA, 15 mM
m) 4-OCH_3-CA, 15 mM
n) 2,3-diOCH_3-CA, 15 mM
o) 2,4-diOCH_3-CA, 14.5 mM
p) 3,4-diOCH_3-CA, 15 mM
q) 3-OCH_3-4-OH-CA, 14.9 mM
r) 3,4-diOH-CA, oxidation

	***Pc*PAL1**			***At*PAL2**			***Rt*PAL/TAL**		
	conv.	time [h]	*ee***	conv.	time [h]	*ee***	conv.	time [h]	*ee***
a	85.2	23.8	>99	89.6*	24.5	>99	83.3	21.6	>99
b	95.8	23.8	>99	96.1	23.7	>99	94.3	21.6	>99
c	52.1	23.8	>99	91.2	8.7	>99	61.5	7.6	>99
d	65.9	23.8	>99	84.7	23.7	>99	57.5	21.6	>99
e	50.5	23.8	>99	96.4	8.7	>99	51.4	21.6	>99
f	91.7	3.1	>99	92.6	2.1	>99	71.6	0.5	>99
g	89.1	2.1	>99	91.7	3.1	>99	0	21.6	n.d.
h	15.5	5	>99	22.0	5	>99	15.7	23.9	>99
i	85.7	5	>99	70.6	5	>99	30.3	5	>99
j	0.8	23.9	n.d.	0.9	23.9	n.d.	61.1	23.9	>99
k	54.6	31.1	n.d.	52.7	31.1	n.d.	64.9	31.1	n.d.
l	85.7	26.4	>99	85.0	26.4	>99	77.8	48.1	>99
m	6.4	26.8	n.d.	2.5	26.8	n.d.	0.7	26.8	n.d.
n	/	26.2	n.d.	/	26.2	n.d.	/	26.2	n.d.
o	/	26.2	n.d.	/	26.2	n.d.	/	26.2	n.d.
p	/	26.2	n.d.	/	26.2	n.d.	/	26.2	n.d.
q	/	26.3	n.d.	/	26.3	n.d.	60.3	26.3	n.d.

Reaction conditions: x mM x-CA in 2.5 M $(NH_4)_2CO_3$, pH 8.9, 30 °C, 1 ml volume, 1200 rpm, cell load: **a-j:** 1 mg/ml (*Pc*PAL1, *At*PAL2) or 5 mg/ml (*Rt*PAL); **k-m:** each reaction with 10 mg/ml cells; n.d. = not determined; *= here 5 mg/ml cell load; ** *ee* of the L-enantiomer.

Although the cell load of *Rt*PAL was 5-fold higher compared to both plant PALs (to compensate the 5-fold lower expression level of *Rt*PAL), conversions were in general lower. Only with the natural substrate (**a**) and with 2-fluoro-CA (**b**) high *ee* and conversions > 83 % could be reached. As expected tyrosine (**j**) was converted with 61.1 % yield by *Rt*PAL, due to the PAL/TAL bifunctionality of this enzyme in yeast, in contrast to the plant PALs, which are highly selective for L-Phe. The replacement of the *para*-hydroxy group through a fluoro substituent (**d**) has almost no influence on the conversion of *Rt*PAL (57.5 %). Besides, CA-derivatives with larger groups in this position of the phenyl ring, for example chloro- (**g**) or methoxy-groups (**m**), were no substrates for this enzyme.

To our knowledge the substrate range of *At*PAL2 for the production of enantiopure L-amino acids was not investigated in detail yet. Due to their plant origin, a similar substrate range for *Pc*PAL1 and *At*PAL2 was expected, which was confirmed, except for some interesting differences. *At*PAL2 is in general a very good catalyst for fluoro- and chloro-CAs (**b-g**) with conversions ≥ 84.7 % and excellent *ee* values > 99 %. But significant differences to the other PALs can be seen in the conversion of **c-e**, which is highlighted in Table 14. With 50 mM 3-F-CA (**c**) a conversion of 91.2 % was reached after only 8.7 h, which is 29 % higher than with *Rt*PAL after 7.6 h using the 5-fold amount whole cells and 39 % higher than the yield reached with *Pc*PAL after 23.8 h using the same amount of whole cells. With 40 mM 4 F-CA (**d**) *At*PAL2 yields a 18 % (compared to *Pc*PAL1) and 27 % (compared to *Rt*PAL) higher product concentration than with the other PALs after a similar reaction time. But the biggest difference could be observed for *At*PAL2 with 2-Cl-CA (**e**) as already shown in Figure 29 with 96.4 % conversion after 8.7 h, in contrast to around 51 % with *Pc*PAL1 and *Rt*PAL after almost one day. The fact that this reaction leads to the formation of enantiopure 2-Cl-L-Phe, a key intermediate for the production of hypertension therapeutics [61] motivated further investigation of this reaction in the following (4.2.8).

*At*PAL2 shows superior conversions of 3-F-CA, 4-F-CA and 2-Cl-CA to the respective α-amino acid compared to *Pc*PAL wt and *Rt*PAL wt with excellent *ee* > 99 %.

Therefore the amination of 2-Cl-CA to 2-Cl-L-Phe, a precursor of hypertension drugs, was further investigated.

4.2.8 Reaction engineering *At*PAL2 for 2-Cl-L-Phe production

In 2011 de Lange *et al*. [61] investigated the application of PAL from *R. glutinis* for the direct amination of 2-Cl-CA in a chemoenzymatic reaction to yield (*S*)-2-indolinecarboxylic acid (Figure 13). These authors observed a strong substrate surplus inhibition by 2-Cl-CA, which made a substrate feeding strategy necessary (reaction time 8.5 h, 1 L volume). With 130 g/L *E. coli* whole cells carying *Rg*PAL a conversion of 91 % was reached.

In this thesis *At*PAL2 showed up to 96.4 % conversion of 2-Cl-CA after 8.7 h (Table 14) with very low cell loads, therefore the production of 2-Cl-L-Phe with *At*PAL2 was investigated in detail. First the maximal substrate concentration was estimated in small scale batch reactions (Figure 30), afterwards 2-Cl-L-Phe was produced in 140 ml scale in a batch reactor. To overcome the substrate surplus inhibition but without laborious substrate addition every 5-25 minutes, the reaction was conducted in fed-batch and continuous mode with a continuous substrate feed. STYs and catalyst productivity were compared for the different reaction modes.

4.2.8.1 Batch reactor

First the amination of 2-Cl-CA to 2-Cl-L-Phe was investigated in small scale (1 ml volume) to receive first information about the reaction system and the appropriate substrate concentration. Therefore *At*PAL2 whole cells were incubated with substrate concentrations ranging from 25 mM to 80 mM 2-Cl-CA for 24 h, respectively. The initial activity (see 3.5.5) of lyophilized whole cells for the amination of 25 mM 2-Cl-CA was 0.6 U/mg cells. As demonstrated in Figure 30 a strong substrate surplus inhibition was observed above 25 mM 2-Cl-CA, even when the cell amount was doubled to 2 mg/ml for the transformation of concentrations > 25 mM.

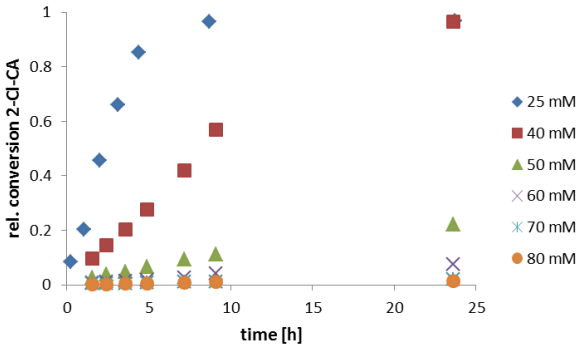

Figure 30: Relative conversion in the amination of 2-Cl-CA with whole cells containing *At*PAL2 wt, starting from different substrate concentrations. Reaction conditions: 25-80 mM 2-Cl-CA in 2.5 M $(NH_4)_2CO_3$, pH 8.9, 30 °C, 1200 rpm, 1 ml reaction volume, 1-2 mg/ml lyophilized *E. coli* BL21 whole cells containing *At*PAL2 wt.

It is important to note that 2-Cl-CA causes an irreversible inactivation of the enzyme. Therefore it was crucial not to exceed the maximum substrate concentration to retain the enzyme activity in the following preparative scale experiment. First the reaction was tested in a 140 mL scale (3.5.2, Figure 31).

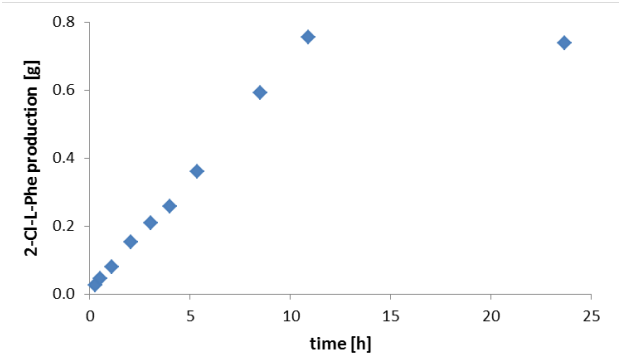

Figure 31: 2-Cl-L-Phe formation over time in a 140 ml batch reaction. Reaction conditions: 140 ml substrate solution (27 mM 2-Cl-CA in 2.5 M ammonium carbonate) was incubated with 0.5 mg/ml *At*PAL2 containing whole cells for 24 h at 30 °C. Several samples were taken at different time points and analyzed with chiral HPLC (3.4.4.1) for product formation and *ee*.

After 24 h a conversion of 97 % was reached, which corresponds to 0.74 g 2-Cl-L-Phe (*ee* > 99 %). Because there was no further increase in product formation after 10.9 h, the space-time-yield (11.8 $g_{product}/L*d$) and the catalyst productivity (10.8 $g_{product}/g_{catalyst}$) were calculated at that time point. The calculated space-time-yield (STY) is within the industrial benchmark of 2.4 - 3120 g/L*d [47], the catalyst productivity of this process is lower than the benchmark of 15 g/g for whole cells processes [6], although the cell load is very low (0.5 mg/ml), but the limited substrate concentration in batch mode limits also the product concentration. To overcome this limitation the reaction was subsequently performed in a fed-batch mode.

4.2.8.2 Fed-batch reactor

To increase the product concentration, the reaction was performed in fed-batch mode (final volume 130 ml), which enabled a concentration of 65 mM (solubility limit) of 2-Cl-CA in the feed solution (3.5.2). The conversion curve is shown in Figure 32. Besides the previous batch studies, which delivered stable conversions over 10 hours, the fed batch was performed for 50 h.

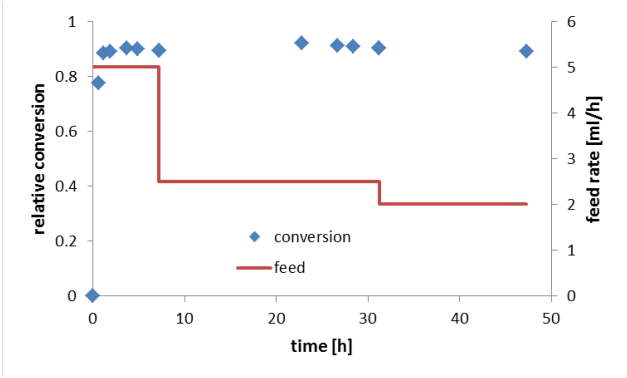

Figure 32: Amination of 2-Cl-CA with *At*PAL2 whole cells in a fed-batch reactor. Relative conversion over time and feeding rate of 2-Cl-CA are shown. Reaction conditions: feed 65 mM 2-Cl-CA in 2.5 M $(NH_4)_2CO_3$, pH 8.9, 30 °C, 500 rpm, 0.5 mg/ml lyophilized *E. coli* BL21 whole cells containing *At*PAL2 wt. 70 mg whole cells were resuspended in 2 ml 2.5 M ammonium carbonate buffer without substrate. Afterwards the feed was started with a flow rate of 5 ml/h.

To compensate the catalyst inactivation over time, the substrate feed was adjusted to 2.5 ml/h after 7.2 h and further reduced to 2.0 ml/h after 31.2 h. This strategy kept the conversion constant at around 90 %. After 48 h the maximum reactor volume of 130 ml was reached and the process was stopped resulting in 1.6 g 2-Cl-L-Phe after 48 h (*ee* > 99 %). The STY of this process is 6.1 g/L*d and the catalyst productivity 22.2 g/g. The lower STY compared to the batch reaction (4.2.8.1) is due to the 4-times longer reaction time of the fed-batch process, leading to only a 2-times higher product amount, since the reaction velocity decreased over time. But because of the higher product formation with a comparable cell load, the catalyst productivity was enhanced in fed-batch. For a better visualization the continuous increase of the product 2-Cl-L-Phe in the fed batch reactor is shown in Figure 33.

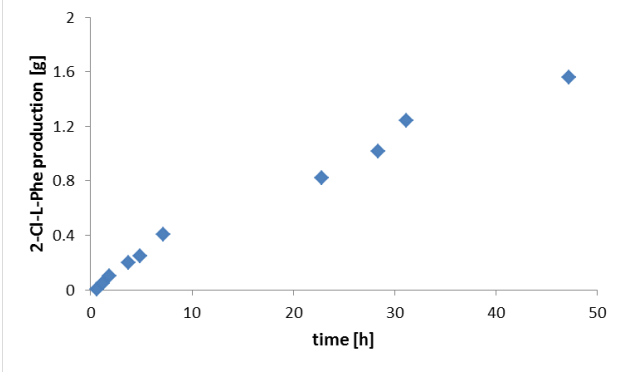

Figure 33: Continuous increase of 2-Cl-L-Phe over time in the fed batch reaction. For further details see Figure 32.

4.2.8.3 Continuous enzyme membrane reactor (EMR)

To further increase the productivity, a continuous enzyme membrane reactor (EMR) was tested. Due to the continuous mode, operating under efflux conditions (see 2.1.3), the reaction is neither limited by the substrate concentration as in the batch reactor nor by the reactor volume as in fed-batch mode. First experiments were performed in a 20 mL reactor using 700 mg *At*PAL2 in whole cells (3.5.2). The conversion curve is shown in Figure 34.

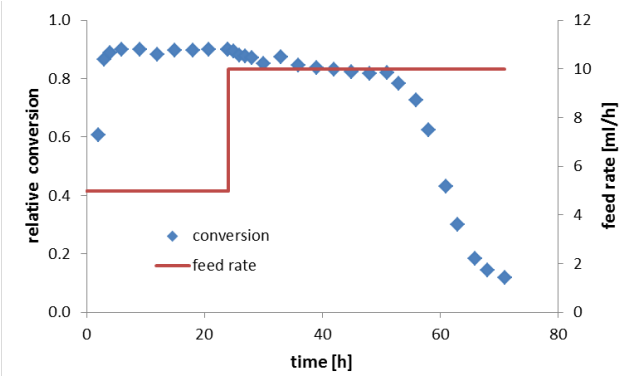

Figure 34: Amination of 2-Cl-CA with *At*PAL2 whole cells using a continuous EMR with high cell load (700 mg). Feed rate and relative conversion are shown. Reaction conditions: feed 60 mM 2-Cl-CA in 2.5 M $(NH_4)_2CO_3$, pH 8.9, 30 °C, 20 ml reactor, 700 mg lyophilized *E. coli* BL21 whole cells containing *At*PAL2 wt. The reactor was filled with 700 mg whole cells, since a longer reation time was expected. The feed was started with 5 ml/h, conversion was tracked with HPLC (3.4.4.1).

During the first 24 h the conversion was at around 90 %, but the *ee* was only > 89 %. Although the residence time of the substrate in the reactor was too short to reach conversions as high as in batch mode (97.1 %, see 4.2.8.1) racemization of the product was observed, probably due to the high cell load of 700 mg in the 20 ml reaction chamber (see 4.2.6). This racemization may be caused by other enzymes, which are still present in whole cells. Therefore after 24 h the feed rate was doubled to 10 ml/h. Due to the shorter residence time and the higher substrate concentration, the conversion declined slowy from 90 % to 82 % after 51 h, but the *ee* increased to > 99 %. Because of catalyst inactivation, the substrate concentration in the reactor increased continuously over time, after 51 h a critical concentration (14.4 mM 2-Cl-CA) was reached which accelerated the inactivation. The STY of this process (61.0 g/L*d after 72 h) was 10-times higher than in fed-batch, due to the small reaction chamber (20 ml), but the catalyst productivity was only 5.2 g/g, because of the 10-fold higher catalyst amount used in this process.

To enhance the catalyst productivity of this process, the reaction was repeated, but with a feed concentration of only 25 mM 2-Cl-CA (3.5.2), which had no negative influence on the catalyst in the batch reaction (4.2.8.1). Therefore the catalyst amount was reduced to 100 mg whole cells. The results are shown in Figure 35.

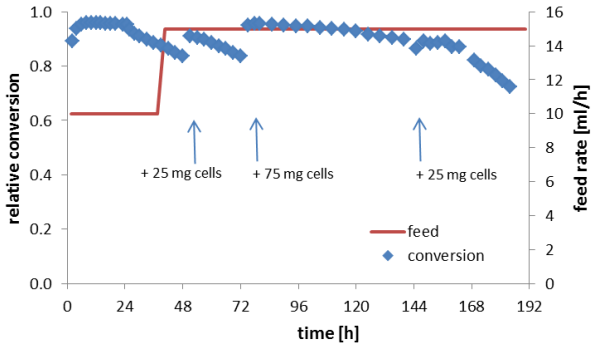

Figure 35: Amination of 2-Cl-CA with *At*PAL2 whole cells using a continuous EMR with lower cell load. Feed rate and relative conversion are shown. Reaction conditions: feed 25 mM 2-Cl-CA in 2.5 M $(NH_4)_2CO_3$, pH 8.9, 30 °C, 20 ml reactor, 225 mg lyophilized *E. coli* BL21 whole cells containing *At*PAL2 wt (initial cell load 100 mg).

During the first 25 h the conversion was stable at around 95 % (Figure 35), as in the batch reaction (4.2.8.1), but after that time point the conversion decreased, therefore three further portions of the whole cell biocatalyst were added as indicated in Figure 35 after 48 h, 72 h and 145 h to run the process with maximal conversion for 187 h. However, the increased cell load (225 mg in total) in the reactor did not impair the *ee* of the product, which was > 99 % over the whole reaction time. After 187 h the process was stopped and STY and productivity were calculated. The STY of this process (67.8 g/L*d) is in the same range as the first EMR (see Figure 34). But due to the longer production phase (Figure 36, overall 10.53 g product) and a lower catalyst load of only 225 mg, the catalyst productivity increased 9-fold to 46.8 g/g.

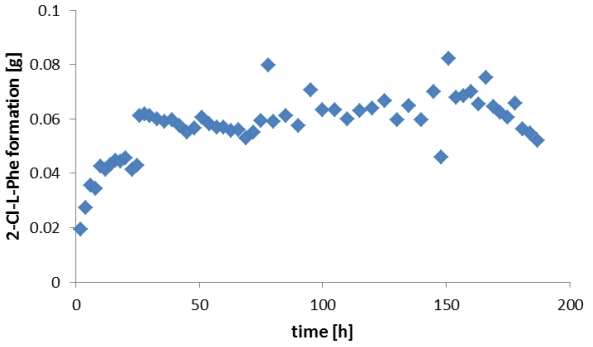

Figure 36: Product formation over time in a continuous EMR with 225 mg *At*PAL2 whole cells and a 25 mM 2-Cl-CA feed solution. In total 10.53 g 2-Cl-L-Phe were formed.

All calculated STYs and productivities are summarized in Table 15. The STYs of all four processes are in the range of the industrial benchmark from 2.4 – 3120 g/L*d calculated by

Straathof *et al.* [47]. The minimum catalyst productivity of > 15 g/g was only reached with fed-batch and the second EMR with lower substrate concentration. The most efficient process is the continuous EMR with a feed solution of 25 mM 2-Cl-CA, leading to the highest STY and productivity. De Lange *et al*. [61] produced 18.1 g 2-Cl-L-Phe with 130 g wet *E. coli* cells containing *Rg*PAL in a repetitive batch process, which corresponds to a catalyst productivity of 0.14 g/g (note that here wet cells are compared with lyophilized cells and that the cell weight is reduced by 80 % during the freeze drying process). A catalyst productivity of 0.14 g/g with wet cells corresponds to a catalyst productivity of around 0.7 g/g, if the weight of lyophilized cells is used for calculation, which is still 66-fold lower than the productivity (46.8 g/g) reached in this thesis with the second EMR.

Table 15: STY and catalyst productivity for the amination of 2-Cl-CA using *At*PAL2 whole cells and different reactor setups, DCW: dry cell weight, EMR: enzyme membrane reactor.

reactor	substrate concentration	amount of whole cell catalyst (mg_{DCW})	space-time-yield ($g_{product}/L*d$)	productivity cell ($g_{product}/g_{DCW}$) [final volume]
Batch	25 mM	70	11.8	10.8 [140 ml]
Fed-batch	65 mM feed	70	6.1	22.2 [130 ml]
Continuous EMR	60 mM feed	700	61.0	5.2 [600 ml]
Continuous EMR	25 mM feed	225	67.8	46.8 [2680 ml]

4.2.8.4 Product isolation

To prove the applicability of these reactions for the production of enantiopure 2-Cl-L-Phe, the product should be isolated. As an example the reaction solutions of two 130 ml scale fed-batch reactions were pooled after the cells were removed by centrifugation (260 ml with 60 mM 2-Cl-L-Phe, 3.11 g 2-Cl-L-Phe). The volume of the solution was reduced under vacuum at 60 °C by removing the volatile ammonium carbonate buffer (3.5.3). The concentrated solution was cooled to 4 °C and the crystals were collected by filtration, washed and dried. The purity of the product was checked via chiral HPLC (3.4.4.1) and NMR (3.4.5). From the 3.11 g 2-Cl-L-Phe in the reaction solution, 1.78 g product could be isolated (57.2 %). Neither with HPLC (> 99 % purity, > 99 % *ee*) nor with NMR impurities could be detected.

Figure 37: Isolated product 2-Cl-L-Phe.

This simple product downstream processing works best with low cell loads. In case of higher cell concentrations (100 mg/mL) the removal of the volatile ammonium carbonate buffer *in vaccuo* is hampered, probably due to increased cell lysis (caused by the stir bar) with increasing cell concentration and the consequent release of cellular components into the reaction solution. In this case the usage of purified enzyme would be benefical. If the catalyst is immobilized this would be an easy method to separate the biocatalyst from the reaction. Therefore further trials to scale the process for the production of 2-Cl-Phe were started with immobilized *At*PAL2.

Different reactor setups were tested for the production of 2-Cl-L-Phe using whole cells containing *At*PAL2. Best results were obtained with a continuous EMR, which could be operated for more than 7 days (187 h) with a productivity of 46.8 g 2-Cl-L-Phe per g catalyst.

The product 2-Cl-L-Phe was isolated from the reaction solution with a simple downstream process with 57 % yield and high purity > 99 %.

4.2.9 **Immobilization of an *At*PAL2-CBM fusion and reaction engineering**

As an alternative to whole cell biocatalysis the application of *At*PAL2 immobilized on cellulose carrier was tested. Therefore fusion enzymes with the N-terminal CBM of the endoglucanase CenA from *C. fimi* or the C-terminal CBM of the exoglucanase/xylanase Cex from *C. fimi* were used, which were prepared by Thomas Hilberath in his Master thesis in the course of this doctoral thesis [108]. The immobilization is fast and easy by simply adding the cellulose carrier to the crude cell extract, incubate ≥ 20 min, and remove impurities by washing. In these studies three *At*PAL2 fusion proteins with CBMs were created, immobilized on cellulose acetate carrier directly from crude extract, and successfully used for biotransformations. Due to the highest activity and expression level the variant with C-terminal CBM (*At*PAL2-CBM) was used in this thesis for further investigations in different reaction modes using Avicel (cellulose powder) as a carrier.

4.2.9.1 Batch reactor

*At*PAL2-CBM was immobilized directly from crude extract to the cellulose carrier without purification of the target enzyme (see 3.5.4). The binding to the carrier is mainly mediated by hydrophobic interactions of the aromatic amino acid residues at the cellulose binding site of the CBM tag and the glucose units of the cellulose carrier. The reaction was first tested in a 10 ml batch reaction (see Figure 38, 3.5.4). Conversion and *ee* were tracked with chiral HPLC (3.4.4.1). The initial amination activity (see 3.5.5) of immobilized *At*PAL2-CBM starting from an initial substrate concentration of 22 mM 2-Cl-CA was calculated from Figure 38 (0.71 U/mg_{enzyme}).

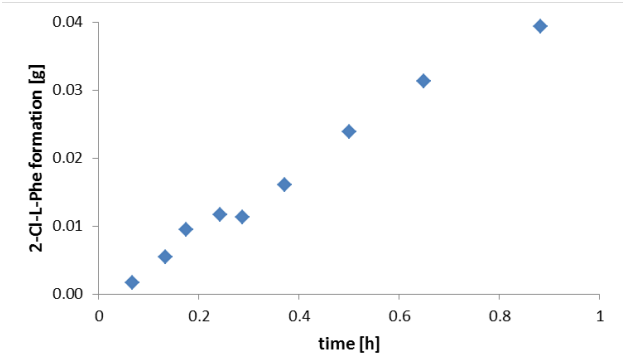

Figure 38: Formation of 2-Cl-L-Phe over time in a 10 ml batch reaction, containing 22 mM 2-Cl-CA and 0.5 g Avicel with about 5.1 mg immobilized *At*PAL2-CBM. Reaction conditions: 22 mM 2-Cl-CA (0.040 g) in 2.5 M ammonium carbonate buffer, pH 8.9, 30 °C, single measurements. 100 % conversion corresponds to 0.044 g 2-Cl-L-Phe. The initial amination activity (see 3.5.5) of immobilized *At*PAL2-CBM was calculated from the first 23 minutes.

After 1 h a conversion of 93.2 % (20.5 mM 2-Cl-L-Phe) was reached and the reaction was stopped. 0.04 g 2-CL-L-Phe was formed (Figure 38) with an *ee* of > 99 %. This corresponds to a catalyst productivity of 8.0 $g_{product}/g_{enzyme}$.

To investigate the reusability of the immobilized enzyme, the immobilisate was separated from the reaction solution by centrifugation, washed with ammonium carbonate buffer (2.5 M, pH 8.9), and mixed with 10 ml fresh substrate solution to start a new batch reaction (3.5.4). Eleven repetitive batch reactions (1 h each) were performed and the conversions after each batch were compared (Figure 39).

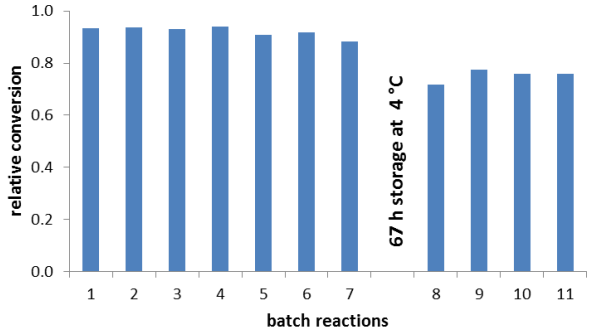

Figure 39: Repetitive batches for the formation of 2-Cl-Phe with *At*PAL2-CBM immobilized on Avicel. Reaction conditions: 22 mM 2-Cl-CA in 2.5 M $(NH_4)_2CO_3$, pH 8.9, 30 °C, 0.5 g Avicel with about 5.1 mg immobilized *At*PAL2-CBM, 10 ml volume, 1 h reaction time, single measurements.

Between the first batch (93.2 % conversion) and the 7th batch reaction (88.3 %) only a slight decrease in activity could be observed. After the 7th cycle, the Avicel was removed from the reaction solution, washed with buffer, removed from the wash buffer by centrifugation and decantation and stored at 4 °C for 67 h. Afterwards the immobilized enzyme was mixed with fresh substrate solution for the 8th batch reaction. The drop in activity in this cycle compared to the following reactions is probably due to a lower temperature at the beginning of the reaction, because the substrate solution was mixed with the cold Avicel from the fridge. In general a loss of activity was observed in all cycles after storage compared to the first seven cycles, probably due to a loss of enzyme during the washing or due to the storage in presence of residual buffer. After the 11th cycle still 76.0 % of the substrate was converted to the product. This is a residual activity of 81.5 % after 11 consecutive cycles in 2.5 M ammonium carbonate and in presence of a substrate, which showed strong substrate inhibition in previous experiments (see Figure 30). Furthermore, the immobilized enzyme could be simply stored at 4 °C until next usage with only little loss of activity. The specific activity of the enzyme during the 11th cycle was 0.55 U/mg (0.28 U per ml of the reaction solution; 0.51 mg/ml). After 11 batch reactions a total amount of 0.42 g 2-Cl-L-Phe was formed, this corresponds to a catalyst productivity of 81.6 $g_{product}/g_{enzyme}$.

The fusion to a CBM and the immobilization on Avicel proved to be a good strategie to stabilize the *At*PAL2, because the remaining activity after eleven batch reactions was with 81.5 % high compared to other immobilization strategies. For example CLEAs prepared from *R. glutinis* PAL, which loose activity after each cycle until only 40 % of the inital activity was left after 10 h (5 cycles)[121].

Analogous to the experiments with whole cells as catalyst, the influence of different reaction modes on the product formation was investigated using the immobilized enzyme.

4.2.9.2 Fed-Batch reactor

First a fed-batch reactor was tested. To start the reaction the immobilizate (see 3.5.4) was added to the reactor filled with 15 ml 2.5 M ammonium carbonate buffer and the reaction was started with a 10 ml/h feed of 60 mM 2-Cl-CA. Product formation and *ee* were measured (3.4.4.1) at different time points (Figure 40).

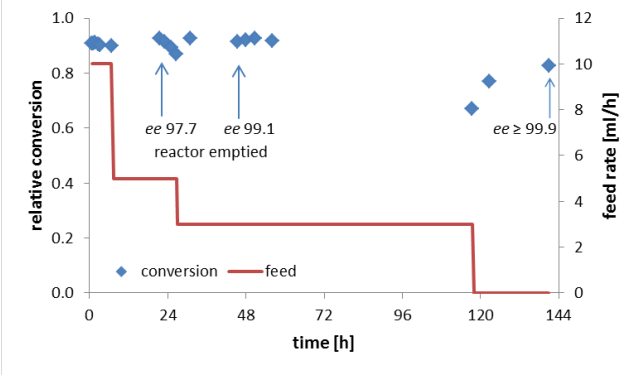

Figure 40: Relative conversion over time and feed rate during the amination of 2-Cl-CA with *At*PAL2-CBM immobilzed on Avicel in a fed-batch reactor. Reaction conditions: feed 60 mM 2-Cl-CA in 2.5 M $(NH_4)_2CO_3$, pH 8.9, 30 °C, 2 g Avicel with 20 mg immobilized *At*PAL2-CBM, single measurements.

By adjusting the feed rate the progressive enzyme inhibition was balanced and conversion was kept constant at around 90 % over 56 h. The *ee* decreased continuously from > 99 % after 48 min to 97.7 % after 21.6 h. Therefore after 21.6 h the reactor was emptied leaving a residual volume of 15 ml to balance the observed decrease in product *ee*. Afterwards the *ee* increased again up to 99.1 % after 45.4 h. To prevent a further decline in *ee* the reactor was emptied at that timepoint leaving a residual volume of 24 ml. These results indicate that the observed decrease in product *ee*, also observed in previous whole cell experiments (4.2.8.3) is probably caused by *At*PAL2 and not by other cellular enzymes. After 117 h the conversion decreased to 67.1 %, probably due to the accumulation of the substrate (18.2 mM), which inhibited the enzyme irreversibly. The feed was stopped and the conversion of the remaining substrate was awaited before the enzyme was removed from the reaction. The reactor was emptied again and the three collected fractions were pooled (452 ml). Although the enzyme was partially inactivated, as indicated by the decreased product formation over time (Figure 41), in total 5.5 g product was formed. This corresponds to a catalyst productivity of 274.0 $g_{product}/g_{enzyme}$.

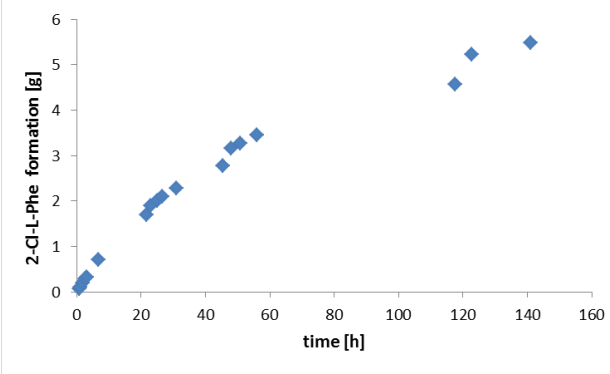

Figure 41: 2-Cl-L-Phe formation over time in a fed-batch reaction containing 2.0 g Avicel with immobilized *At*PAL2-CBM. For reaction conditions see Figure 40.

4.2.9.3 Continuous plug-flow reactor

The fast binding of the CBM to the cellulose carrier enabled enzyme immobilization directly in a plug-flow reactor. In preliminary experiments the appropriate binding conditions for the enzyme to the column under flow (0.2 ml/h) were investigated (Figure 42, left picture). Therefore the flow through after the column was collected and analyzed. The results in Figure 42 show that the binding of the fusion enzyme to the cellulose carrier is fast: a flow of 0.2 ml/min is suitable to bind the target enzyme to the Avicel in the column reactor, indicated by the absence of the enzyme in the flow through (Figure 42 FT). With deionized water the enzyme can be eluted after the reaction, if desired (Figure 42 E).

After immobilization and washing (see 3.5.4) 10 mg protein was bound to the column, which corresponds to a binding capacity of 10 µg protein per mg Avicel. This value, calculated with data obtained using the Bradford assay (3.4.2.2) by following the depletion of protein in the supernatant during immobilization, is in agreement with the protein load on the carrier measured using the BCA assay (3.4.2.2; 10.1 µg/mg Avicel) and with the values reported in literature (8-20 µg protein/mg Avicel) [40]. The reaction was started by pumping the 2-Cl-CA substrate solution (25 mM) through the column. As demonstrated in Figure 42 (right picture) the reaction was performed for 69 h. The amination of 2-Cl-CA started with high conversion up to 96.6 % (*ee* > 99 %). Whereas the conversion was stable for the first 10 h, deactivation of the catalytic bed made the adjustment of the residence time necessary after 24 h and again after 48 h. The observed deactivation was most probably caused by substrate inhibition. Also wash out of the enzyme from the column cannot completely be excluded, although in samples collected behind the column and applied to SDS-PAGE no protein could be detected using Coomassie staining. In total 2.9 g 2-Cl-L-Phe was produced (*ee* > 99%), which corresponds to a catalyst productivity of 288.2 $g_{product}/g_{enzyme}$.

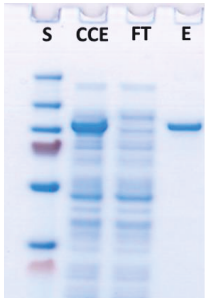

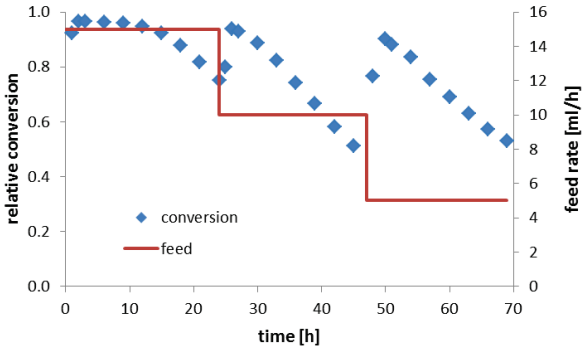

Figure 42: Left: SDS PAGE analysis of *At*PAL2-CBM binding to an Avicel filled column reactor, 6.5 µg of each fraction was applied to the SDS gel, S: PageRuler Prestained Plus Protein Ladder, CCE: crude cell extract, FT: flow through, E: elution fraction with deionized water. Right: Relative conversion and feed rate in the amination of 2-Cl-CA in a plug-flow reactor (XK 16/20 chromatography column, 20 cm x 1.6 cm). Reaction conditions: 25 mM 2-Cl-CA in 2.5 M $(NH_4)_2CO_3$, pH 8.9, 30 °C, 1 g Avicel with 10.1 mg immobilized *At*PAL2-CBM, flow rate 15-5 ml/h (right picture). Product formation was tracked with HPLC (3.4.4.1), single measurements.

The productivity measures for all four reactor modes performed with the immobilized *At*PAL-CBM fusion are summarized in Table 16.

Table 16: STY and catalyst productivity of lyophilized whole cells and purified immobilized enzyme for the amination of 2-Cl-CA. *At*PAL2-CBM immobilized on Avicel was used in different reaction modes, DCW: dry cell weight containing the respective amount of enzyme for immobilisation.

reactor	substrate concentration	amount of immobilized catalyst (mg)	space-time-yield ($g_{product}/L*d$)	productivity cell ($g_{product}/g_{DCW}$) [final volume]	productivity immobilizate ($g_{product}/g_{enzyme}$)
Batch	22 mM	5.1	98.5	0.6 [10 ml]	8.0
Repetitive batch	22 mM	5.1	8.3	5.9 [110 ml]	81.6
Fed-batch	60 mM feed	20.0	2.1	20.0 [452 ml]	274.0
Continuous plug-flow	25 mM feed	10.1	248.6	18.5 [700 ml]	288.2

In order to enable a comparison of the data obtained with whole cells (4.2.8), STY and the productivity were calculated based on the amount of immobilzed enzyme and on the amount of whole cell, which was used to prepare the immobilizate. The respective wet cell weight was divided by five, since 80 % is water. Taking the dry cell weight as a basis for

calculation of the productivity measures, enabled a direct comparison with the data obtained with the whole cell catalyst in Table 15.

As demonstrated in Table 16, the STY of the batch reaction was high, due to the short reaction time of only 1 h, but the low product formation of 0.04 g led to low catalyst productivity of 0.8 $g_{product}/g_{enzyme}$. The highest STY was reached with the plug-flow reactor with a productivity of 288 $g_{product}/g_{enzyme}$ comparable to the fed-batch process, but a 124-fold higher STY due to the small reactor volume of only 4 ml. However, the disadvantage of the plug-flow reactor is that the product formation is limited by the substrate concentration. In the present case 25 mM 2-Cl-CA was shown to be the maximal substrate concentration, because auf the substrate surplus inhibition leading to irreversible enzyme inactivation (see Figure 30). In the plug-flow reactor, where the substrate concentration decreases over the length of the reactor during conversion (see 2.1.3), specifically the enzyme at the column inlet is first prone to inactivation. Therefore the best reactor for this reaction is the fed-batch reactor.

All in all the processes using immobilized *At*PAL2-CBM are less productive than the respective process with whole cells (Table 15). The best whole cell process, the continuous EMR with 25 mM feed, produced 46.8 g product per g catalyst, which is 2.3 fold higher than the best process with immobilized enzyme (fed batch, 20.0 $g_{product}/g_{DCW}$).

It must be taken into account that this comparison is falsified by the calculation of the productivity measures based on the amount of dry cells carying the respective amount of enzyme. In case of the results obtained with the immobilized *At*PAL-CBM fusion the lower productivity may be due to an incomplete cell disruption, because cells which are not disrupted are removed together with the included enzyme before immobilization. Regarding the catalyst productivity based on the amount of immobilized free enzyme gives a different picture. After eleven repetitive batch cycles 81.6 $g_{product}/g_{enzyme}$ was formed, which would have been even higher, if the process had not been stopped. Fed-batch and plug flow reactor reached even higher productivities. Although both processes are under the industrial benchmark of 1000 g/g for purified enzymes (2.1.4), the process may be still economical, because CBM fusion tags allow the direct immobilization from crude cell extracts in one step directly in the reactor.

To enhance the stability and reusability of *At*PAL2 the enzyme was fused to a C-terminal CBM and immobilized on the cellulose carrier Avicel. The immobilizates were used in different reactor modes for the production of 2-Cl-L-Phe.

Immobilization via CBMs to cellulose as a cheap and environmentally friendly carrier is easy and fast. The binding can be done directly from crude extract in about 10 minutes, and the immobilized enzyme can directly be used for biotransformation after short washing with the reaction buffer to remove unbound impurities. The carrier can be easily removed from

the reaction solution (by centrifugation in batch mode or by retaining with a membrane in plug-flow mode), thereby simplifying the downstream processing.

The highest product formation was observed using the fed-batch mode (20 $g_{product}/g_{DCW}$).

4.3 Aminomutases

For the production of β-amino acids three aminomutase were used: a bacterial TAM from C. *crocatus* (*Cc*TAM) and two enzymes, *Tca*PAM and *Tch*PAM, from *Taxus* species. All three enzymes are (*R*)-selective with regard to the β-amino acid, leading to a product mixture of (*S*)-α-Phe and (*R*)-β-Phe or the respective derivatives, either through amination of cinnamic acid derivatives or through isomerization of the respective (*S*)-α or (*R*)-β-amino acids. The PAM enzymes share a sequence identity of 97 %. Therefore the substrate range was expected to be similar, but only for *Tch*PAM the amination reaction has been investigated intensively in previous studies[94,122,123]. In this thesis only the direct amination of CAs in ammonium carbonate buffer was studied, because CA is an intermediate of the reaction mechanism (see Figure 9) and can be therefore used as a substrate for the direct addition of ammonia to yield a range of the respective α- and β-amino acids. All initial experiments described here were conducted with lyophilized whole cells. The ratio between α- and β-amino acids and the *ee* for the desired (*S*)-α- and (*R*)-β-amino acid product was calculated.

4.3.1 **Amination of cinnamic acid derivatives with PAM in whole cells**

4.3.1.1 *Tch*PAM

For the production of β-amino acids with *Tch*PAM the same substrates and concentrations were used as previously described for the PALs (3.5.6). Solutions containing the respective CA in 2.5 M ammonium carbonate buffer, pH 8.9, were incubated with lyophilized whole cells containing *Tch*PAM. The product formation was monitored with HPLC (3.4.4.2). The product distribution after 71 h reaction is shown in Figure 43. The *ee* values of formed products are listed in Table 17.

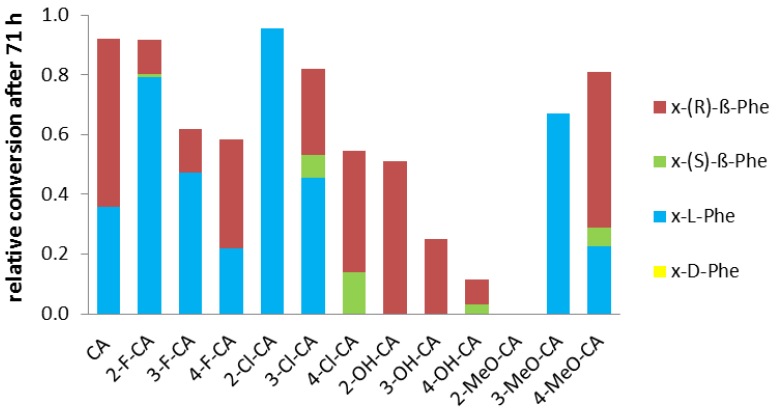

Figure 43: Amino acid isomer distribution after 71 h amination reaction with lyophilized whole cells containing *Tch*PAM. Reaction conditions: 2.5-50 mM CA derivative (see 3.5.6) in 2.5 M $(NH_4)_2CO_3$, pH 8.9, 30 °C, 1 ml volume, 1200 rpm, cell load: 100 mg/ml. The product formation was monitored with HPLC (3.4.4.2), single measurements.

With 2-MeO-CA and 2,3-diMeO-CA no product formation could be detected, which might be due to steric hindrance of the methoxy group in *ortho*-position of the aromatic ring. Depending on the kind of substituent and the position at the phenylring, a distribution of three regio- and stereoisomers ranging from enantiopure (*S*)-α-amino acid (with 2-Cl-CA) to enantiopure β-amino acid (with 2-OH-CA) could be found. No (*R*)-α-amino acids (D-Phe derivatives) were detected. Some general trends could be identified for fluoro-, chloro-, and hydroxy-substituted CAs: the total conversion decreased with increasing distance between substituent and the double bond, which corresponds to an increasing bulkiness of the substrate. The same effect was observed by Weise *et al.* [124] in the amination of different fluoro- and chloro-CAs with the bacterial ammonia lyase EncP, which exhibits aminomutase activity at higher temperatures. Another factor investigated by the same group was the influence of electronic effects on the regioselectivity of the ammonia addition. Strong electron-withdrawing groups led to mainly α-amino acid formation whereas electron-donating groups (e.g. like methoxy) led to the formation of mainly β-amino acids using EncP. The position of the substituent at the ring had also an influence: the formation of β-amino acids increased with fluoro and chloro-substituents in the order *ortho* < *meta* < *para* [124]. This effect on the β-amino acid formation can also be seen in our results obtained with *Tch*PAM and fluoro-CAs [14 % (2-F) < 23 % (3-F) < 63 % (4-F) β-product) and chloro-CAs [0 % (2-Cl) < 44 % (3-Cl) < 100 % (4-Cl)] but not for methoxy-CAs. Szymanski *et al*. [122] also reported the exclusive formation of the (*S*)-α-isomer during the amination of CAs with chloro-, fluoro-, bromo-, and methyl substituents in *ortho*-position using *Tch*PAM. They assume that a shielding of the β-position occurs due to steric hindrance.

Table 17: *Tch*PAM catalyzed amination reaction: ratio of formed α- and β-amino acids depending on the substituent after 71 h and *ee* of the isomers. Samples were analyzed with chiral HPLC (3.4.4.2), single measurements; n.d. = *ee* not determined; - = not detected. The retention times of the products are in agreement with the references ordered from Peptech. With di-substituted CAs (2,4-diMeO; 3,4-diMeO; 3-MeO-4-OH) products were formed, which could not be identified as the respective amino acids, due to missing reference compounds for HPLC. Reaction conditions see Figure 43.

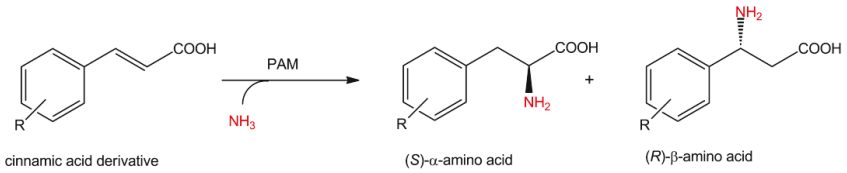

cinnamic acid derivative (*S*)-α-amino acid (*R*)-β-amino acid

substituent	α:β ratio	*ee* (*S*)-α-amino acid [%]	*ee* (*R*)-β-amino acid [%]
H	39:61	> 99	> 99
2-F	86:14	> 99	84
3-F	77:23	> 99	>99
4-F	37:63	> 99	>99
2-Cl	100:0	n.d.	-
3-Cl	56:44	n.d.	58
4-Cl	0:100	-	48
2-OH	0:100	-	> 99
3-OH	0:100	-	> 99
4-OH	0:100	-	41
3-OCH_3	100:0	n.d.	-
4-OCH_3	28:72	n.d.	78

Except for 4-F-CA in all cases the formation of the undesired (*S*)-β-product was observed with a substituent in the *para*-position, leading to decreased *ee* values for the (*R*)-β-amino acid (Table 17), probably owing to a less preferred orientation of the substrate in the hydrophobic binding pocket (see Figure 11).

All in all the results obtained with whole cells in this thesis are in agreement with those obtained by Szymanski *et al*. [122] for purified *Tch*PAM. However, in the present study the transformation of hydroxy-CAs and 3-MeO-CA was detected, which were not found to be converted in the previous studies [122]. This is most probably due to a 10-fold higher substrate concentration (50 mM) in our experiments. After 71 h 17.3 mM (2-OH), 7.9 mM (3-OH) and 2.9 mM (4-OH) of the respective (*R*)-β-amino acid was detected. Using 30 mM 3-MeO-CA only the L-α-amino acids was produced (15.4 mM).

4.3.1.2 *Tca*PAM

The substrate range of *Tca*PAM was analyzed analogously to the experiments with *Tch*PAM. To our knowledge the direct amination of cinnamic acid derivatives using PAM from *T. canadensis* was not reported before. Solutions containing the respective CA in 2.5 M ammonium carbonate buffer were incubated with lyophilized whole cells containing *Tca*PAM. The product formation was monitored with HPLC (3.4.4.2). The product distribution after 71 h reaction is shown below (Figure 44). The *ee* values of formed products are listed in Table 18.

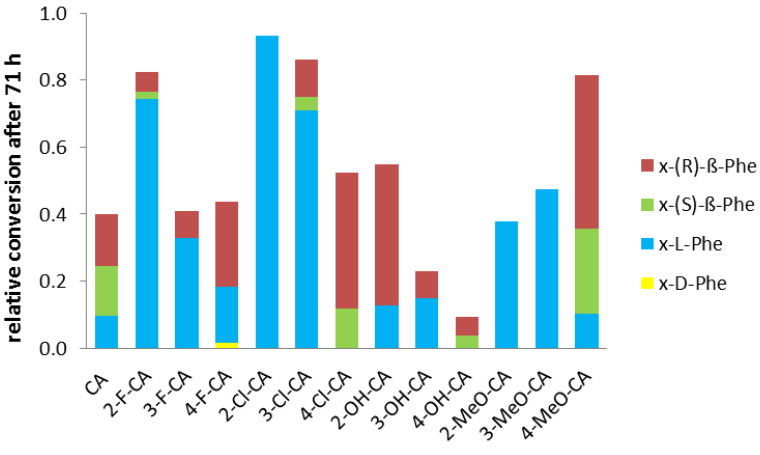

Figure 44: Amino acid isomer distribution after 71 h amination reaction with lyophilized whole cells containing *Tca*PAM. Reaction conditions: 2.5-50 mM CA derivative (see 3.5.6) in 2.5 M $(NH_4)_2CO_3$, pH 8.9, 30 °C, 1 ml volume, 1200 rpm, cell load: 100 mg/ml. The product formation was monitored with HPLC (3.4.4.2), single measurements.

As expected based on the high sequence identity of 97 % between the two PAMs (see Appendix), their substrate range is similar. All the effects described above with *Tch*PAM regarding conversions, regioselectivity and increasing racemization with *para*-substituents can be also observed with *Tca*PAM. Therefore only the differences will be highlighted here. Total conversions with *Tca*PAM after 71 h are in general lower than with *Tch*PAM, which corresponds to the lower expression level of *Tca*PAM (see Figure 19). With *Tca*PAM and unsubstituted CA as substrate a racemic mixture of β-Phe was obtained, whereas *ortho*- and *meta*-methoxy substituents resulted in the respective α-amino acid. This shows that small differences in the amino acid sequence may result in big changes in product scope, even if they were not located in the active site. It is important to note that *Tca*PAM catalyzes the conversion of 2-MeO-CA, which was not converted by *Tch*PAM at all (Table 17).

2,3-diMeO-CA and 3,4-diMeO-CA are no substrates for *Tca*PAM. With 2,4-diMeO-CA two products appeared and with 3-MeO-4-OH-CA three products, which might be the expected

amino acids, but could not yet be finally identified due to missing standards. One of the three products elutes at the same retention time as the available 3-MeO-4-OH-L-Phe reference, which supports this assumption (data not shown).

Table 18: *Tca*PAM catalyzed amination reaction: ratio of formed α- and β-amino acids depending on the substituent after 71 h and *ee* of the isomers. Samples were analyzed with chiral HPLC (3.4.4.2), single measurements; n.d. = *ee* not determined; - = not detected. The retention times of the products are in agreement with the respective reference compounds ordered from Peptech. Reaction conditions see Figure 44.

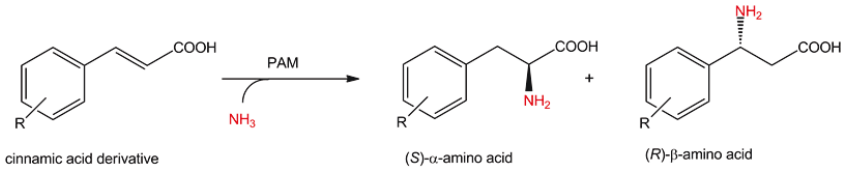

cinnamic acid derivative (*S*)-α-amino acid (*R*)-β-amino acid

substituent	α:β ratio	*ee* (*S*)-α-amino acid [%]	*ee* (*R*)-β-amino acid [%]
H	24:76	>99	2
2-F	90:10	>99	45
3-F	80:20	>99	>99
4-F	42:58	81	>99
2-Cl	100:0	n.d.	-
3-Cl	83:17	n.d.	48
4-Cl	0:100	-	55
2-OH	23:77	>99	>99
3-OH	65:35	>99	>99
4-OH	0:100	-	21
2-OCH_3	100:0	n.d.	-
3-OCH_3	100:0	n.d.	-
4-OCH_3	13:87	n.d.	28

Comparing both PAMs, the enzyme from *T. chinensis* is the more suitable catalyst for the production of β-amino acid, because of the higher expression and overall conversion and due to the lower amount of side-products in some reactions (Table 17: CA, 2-OH-CA, 3-OH-CA). But with *Tch*PAM still a hugh amount of the α-amino acid is formed, which complicates product recovery. For industrial applications enzymes with higher β-amino acid selectivity and also with higher stereoselectivity would be desirable.

Whole cells containing *Tch*PAM show higher conversions, due to a higher expression level, and less side-products compared to *Tca*PAM.

Both PAMs catalyze the formation of mixtures of α- and β-amino acids, which complicates the downstream processing.

4.3.2 **Amination of cinnamic acid derivatives with *Cc*TAM in whole cells**

To our knowledge, the addition of ammonia to a variety of CA derivatives using *Cc*TAM was not investigated in detail until now. To compare the substrate range of *Cc*TAM to PAMs the same experimental conditions were used. Solutions containing the respective CA in 2.5 M ammonium carbonate buffer were incubated with lyophilized whole cells containing *Cc*TAM (3.5.6). The product formation was monitored with HPLC (3.4.4.2). The product distribution after 72 h reaction is shown in Figure 45. The *ee* values of formed products are listed in Table 19.

The number of substrates accepted by *Cc*TAM is lower compared to PAMs. CAs with substituents in *para*-positions were generally not accepted, except for the natural substrate tyrosine with a hydroxy-group in this position. In case of a small fluoro-substituent most probably electronic effects between the electronegative fluoro atom and the amino acids in this region of the active site (see Figure 11) are relevant, rather than steric hindrance. In case of larger substituents like 4-methoxy-groups, steric hindrance most probably prevents product formation (Table 19, Figure 45). Another reason may be that the respective substrate concentrations are not high enough to achieve reasonable enzyme activity and conversions after this reaction time.

The disruption of H-bridges between the para-hydroxy group and amino acids in the active site, as they occur in TALs between the *para*-hydroxy-group of the substrate and His89 (see 2.3.1), seems not to be a problem, because *Cc*TAM shows good conversions of CA without a *para*-hydroxy-group. The 4-hydroxy-group seemed to impair the stereoselectivity of *Cc*TAM, since only in this case the respective β-Phe derivate was formed as a racemate, which was not observed with other products. Increasing bulkiness of the substituent in *meta*-position had a negative influence on conversions with 3-F > 3-Cl > 3-MeO. Interestingly with 3-MeO-4-OH-CA two products appeared, which could not yet be fully analyzed. The products might be the two β-isomers, because the retention times of these products (13.1 min and 16.4 min) are comparable to the similar (commercially available) reference compounds 3,4-diMeO-(*S*)-β-Phe (14.8 min) and 3,4-diMeO-(*R*)-β-Phe (16.2 min), but not to the respective α-amino acid 3-MeO-4-OH-L-α-Phe (9.8 min). The deprotection of these products under acidic conditions would lead to β-Dopa [119].

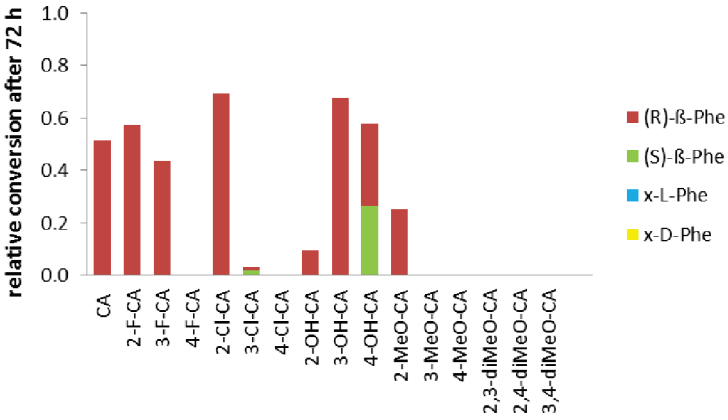

Figure 45: Amino acid isomer distribution after 72 h amination reaction with lyophilized whole cells containing *Cc*TAM. Reaction conditions: 2.5-50 mM CA derivative (see 3.5.6) in 2.5 M $(NH_4)_2CO_3$, pH 8.9, 30 °C, 1 ml volume, 1200 rpm, cell load: 100 mg/ml. The product formation was monitored with HPLC (3.4.4.2), single measurements.

Table 19: *Cc*TAM catalyzed amination reaction: ratio of formed α- and β-amino acids depending on the substituent after 72 h and *ee* of the product isomers. Samples were analyzed with chiral HPLC (3.4.4.2), single measurements; n.d. = *ee* not determined; - = not detected. The retention times of the products are in agreement with the references ordered from Peptech. Reaction conditions see Figure 45.

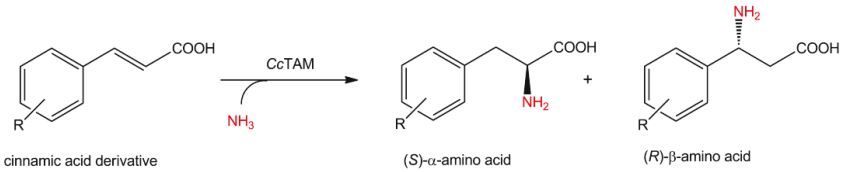

substituent	α:β ratio	*ee* (*R*)-β-amino acid [%]
H	0:100	> 99
2-F	0:100	> 99
3-F	0:100	> 99
2-Cl	0:100	> 99
3-Cl	0:100	85
2-OH	0:100	> 99
3-OH	0:100	> 99
4-OH	0:100	-
2-OCH_3	0:100	> 99

Although the substrate range of *Cc*TAM is limited compared to the PAMs (4.3.1), it is a very useful catalyst, because every accepted substrate was exclusively converted to the desired (*R*)-β-isomer with excellent *ee* values. No α-amino acids could be detected. Either they were not formed at all under these conditions or their concentrations were below the detection limits of the HPLC.

With *Cc*TAM a new enzyme was found that catalyzed the formation of exclusively (*R*)-β-Phe-derivatives with excellent *ee* by direct ammination of cheap cinnamic acid derivatives. This makes *Cc*TAM a valuable catalyst for the enzyme toolbox.

4.3.2.1 Immobilization of *Cc*TAM-CBM

*Cc*TAM is a useful catalyst, due to the formation of exclusively the desired (*R*)-β-amino acid, but all aminomutases in this thesis suffer from low expression levels compared to ALs. Therefore high cell loads are necessary, which complicates sampling and product isolation due to cell lysis. To simplify downstream processing, the immobilization concept through a CBM-fusion, which was successfully used for *At*PAL2 (4.2.9) should be transferred to *Cc*TAM. The *Cc*TAM gene was amplified using PCR to introduce an NcoI restriction site and cloned into the pET28 vector containing a C-terminal CBM of the exoglucanase/xylanase Cex from *C. fimi* (3.1.4). Due to the generation of the NcoI resctriction site, a point mutation at position 2 (Lys -> Glu) was introduced. *Cc*TAM K2E-CBM was expressed in *E. coli* BL21 (3.3.1) and immobilizates on Avicel were prepared (3.5.7) and used for the amination of 2-Cl-CA (Figure 46).

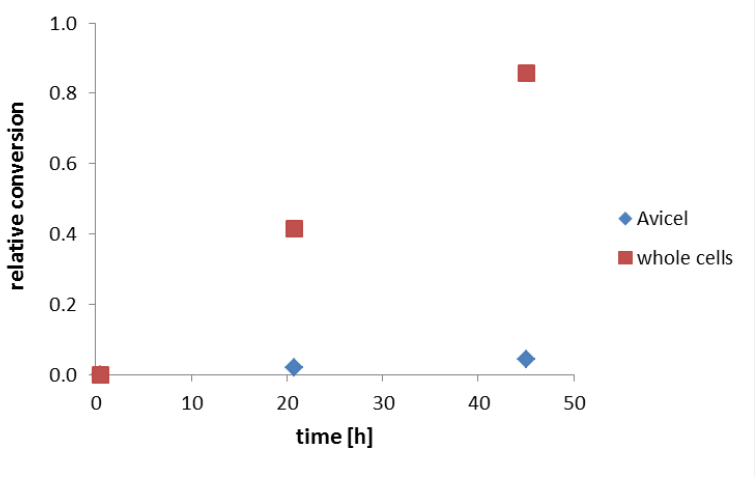

Figure 46: Conversion during the amination of 2-Cl-CA using *Cc*TAM K2E immobilized onto Avicel or wet whole cells. Reaction conditions: 1.5 g wet whole cells in 5 ml Tris-HCl buffer, 10 x 30 s sonification on ice, centrifugation. 3.4 ml CCE were incubated with 1 g Avicel for 1 h at 30 °C. Immobilizate and 1.5 g wet cells were washed twice with $(NH_4)_2CO_3$ buffer. 20 mM 2-Cl-CA in 2.5 M $(NH_4)_2CO_3$, pH 8.9, 30 °C, 4 ml volume, 45 h, 20 rpm, over head shaker.

After 45 h a conversion of only 4 % was reached with *Cc*TAM K2E immobilized on Avicel, whereas whole cells reached 86 % in this time. The reaction was repeated several times. The reason for the low activity using Avicel, is the low soluble expression of *Cc*TAM fused with CBM (Figure 47).

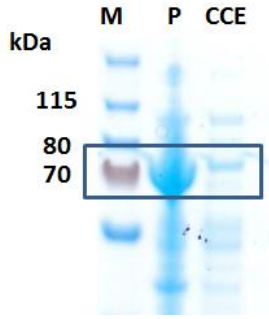

Figure 47: Pellet fraction (P) and CCE after sonification of 1.5 g wet *E. coli* cells containing *Cc*TAM K2E-CBM in 5 ml Tris-HCl buffer, 10 x 30 s sonification on ice, centrifugation; 1µl sample, 12 µl buffer, 5 µl NuPage LDS Sample Buffer 4x, 2 µl NuPage Reducing Agent 10x; 2 min 99°C, 10 µl loaded onto gel; 200 V, 100 mM 15 W, 60 min; 1 h in Coomassie staining, destaining in water.

Due to the negative effect of this CBM on the soluble production of *Cc*TAM, this immobilization strategy is not suitable for this enzyme with the chosen CBM. Fusion of this CBM to the N-terminus or the fusion to another CBM may increase the soluble expression. Furthermore, the limited binding capacity of Avicel may be a problem in the immobilization of AMs, because ALs and AMs are all tetramers of similar size, but ALs are 100-fold more active when comparing the cell load in amination reactions (1 mg/ml *At*PAL2, 100 mg/ml *Cc*TAM). Therefore, a cellulose carrier with higher binding capacity would be useful. To circumvent low binding capacities of the carrier, the decreased soluble expression level of some CBM fusion proteins could be used for the production of catalytically active inclusion bodies as alternative carrier-free immobilization strategy. This technique was already demonstrated for sialic acid aldolase fused to a CBM from *C. cellulovorans* [125].

*Cc*TAM K2E-CBM can be immobilized from crude cell extract onto Avicel and directly used for biotransformation.

Due to a decreased expression level of *Cc*TAM K2E caused by the fusion to the CBM, the activity was low. Fusion to another CBM could improve the expression.

5 Conclusion and future perspectives

Unnatural amino acids are valuable building blocks for the production of chemicals and pharmaceuticals. To get access to this class of compounds a toolbox of MIO-dependent ammonia lyases and aminomutases was generated including four wild type ammonia lyases (*Pc*PAL1, *At*PAL2, *Rt*PAL and *Rs*TAL), one variant with altered substrate specificity (*At*PAL2 F136H) and three wild type aminomutases (*Cc*TAM, *Tch*PAM, *Tca*PAM). The enzymes were cloned, expressed in *E. coli* and purified.

Kinetic parameters, pH- and temperature optima for the amination and deamination reaction of natural substrates were determined for the ammonia lyases. Aqueous ammonia as solvent, was exchanged to volatile ammonium carbonate buffer, which can be easily removed by evaporation, enhanced the stability of the enzymes, and simplified product isolation, sampling and product analysis. The substrate range of *At*PAL2 wt in the amination of cinnamic acid derivatives, which was not investigated until know, was examined and compared to the well characterized enzymes *Pc*PAL1 and *Rt*PAL. *At*PAL2 shows significant increased conversion of 3-F-cinnamic acid (91.2 %), 4-F-cinnamic acid (84.7 %) and 2-Cl-cinnamic acid (96.4 %) in batch reactions compared to the reference enzymes *Pc*PAL1 and *Rt*PAL. Due to the importance of 2-Cl-L-phenylalanine as a key intermediate for the production of hypertension drugs [61], this reaction was further investigated in larger scale using different rector types and reaction modes. With a continuous enzyme membrane reactor the space-time-yield and productivity could be enhanced from 11.8 g/L*d and 10.8 g/g_{DCW} in batch to 67.8 g/L*d and 46.8 g/g_{DCW}. The product 2-Cl-L-phenylalanine could be isolated by simple volume reduction and crystallization with a yield of 57 % and high purity.

To increase the stability and reusability of the enzymes in industrial applications an immobilization strategy using carbohydrate binding modules (CBM) from *C. fimi* was investigated. *At*PAL2 fused with a C-terminal CBM and immobilized on Avicel showed 81.5 % remaining activity in the amination of 2-Cl-cinnamic acid after eleven 1 h batch reaction cycles and 3 days storage at 4 °C. Furthermore *At*PAL2-CBM was immobilized on Avicel directly in a plug-flow reactor by simply pumping crude cell extract through an Avicel-filled column and was afterwards directly used for biotransformation by pumping the substrate through the reactor. Space-time-yield reached 248.6 g/L*d and the productivity was 18.5 g/g_{DCW}.

Similar to the ammonia lyases, the amination of cinnamic acid derivatives using aminomutases in whole cells was investigated. The substrate range of *Cc*TAM and *Tca*PAM, which was not described in detail yet, was investigated and compared to the well known enzyme *Tch*PAM. *Tca*PAM is less active as a whole cell catalyst, due to a lower expression level compared to *Tch*PAM and catalyzes the formation of more side products. Both PAMs mediated the formation of a mixture of α- and β-amino acids, which is difficult to separate.

Compared to the PAMs *Cc*TAM showed a higher substrate selectivity and produced only the desired (*R*)-β-amino acids in initial measurements. Therefore *Cc*TAM was used for immobilization studies to increase the enzyme stability. The fusion protein *Cc*TAM-CBM was immobilized directly from crude cell extract onto Avicel, but owing to a decreased expression level, the activity was low.

In the future ammonia lyases and aminomutases with broader substrate ranges would be desireable, which convert not only cinnamic acid and derivatives, but also the respective aldehydes or substrates which are not analogous to the natural substrate. Furthermore, the acceptance of other N-scources for example substituted amines would be benefical. To broaden the application of aminomutases in industry, enzymes with higher activity would be necessary. Furthermore, more aminomutases with increased regioselectivity for the addition of ammonia to the β-position of cinnamic acid would be useful or further methods for the easy separation of amino acid isomer mixtures.

The cheap and easy immobilization of aminomutases from crude cell extract without purification is target of further investigations in our group in the future using various CBMs and other immobilization strategies like Halo-tag or aldehyde tags [126,127]. The application of PALs immobilized to cellulose carrier can be an opportunity for the treatment of phenylketonuria by oral administration in the future.

6 References

[1] Pollak P, Vouillamoz R. (2013) Fine chemicals. Ullmann´s encyclopedia of industrial chemistry. WILEY-VCH Verlag, Weinheim.

[2] Aleu J, Bustillo AJ, Hernandez-Galan R, Collado IG. (2006) Biocatalysis applied to the synthesis of agrochemicals. Curr. Org. Chem. **10**, 2037–2054.

[3] Bornscheuer UT, Huisman GW, Kazlauskas RJ, Lutz S, Moore JC, Robins K. (2012) Engineering the third wave of biocatalysis. Nature. **485**, 185–194.

[4] Choi J-M, Han S-S, Kim H-S. (2015) Industrial applications of enzyme biocatalysis: Current status and future aspects. Biotechnol. Adv. **33**, 1443–1453.

[5] Otte KB, Hauer B. (2015) Enzyme engineering in the context of novel pathways and products. Curr. Opin. Biotechnol. **35**, 16–22.

[6] Pollard DJ, Woodley JM. (2006) Biocatalysis for pharmaceutical intermediates: the future is now. Trends Biotechnol. **25**, 66–73.

[7] Schmid A, Dordick JS, Hauer B, Kiener A, Wubbolts M, Witholt B. (2001) Industrial biocatalysis today and tomorrow. Nature. **409**, 258–266.

[8] Faber K. (2011) Biotransformations in organic chemistry. Springer-Verlag, Berlin;

[9] Zheng GW, Xu JH. (2011) New opportunities for biocatalysis: Driving the synthesis of chiral chemicals. Curr. Opin. Biotechnol. **22**, 784–792.

[10] Zhang Z-J, Pan J, Ma B-D, Xu JH. (2014) Efficient biocatalytic synthesis of chiral chemicals. Adv. Biochem. Eng. Biotechnol. **155**, 55–106.

[11] U.S. Food and Drug Administration. (1992) Development of new stereoisomeric drugs. Available from: http://www.fda.gov/Drugs/GuidanceComplianceRegulatoryInformation/Guidances/ucm122883.htm

[12] Hollmann F, Arends IWCE, Holtmann D. (2011) Enzymatic reductions for the chemist. Green Chem. **13**, 2285–2314.

[13] Torrelo G, Hanefeld U, Hollmann F. (2014) Biocatalysis. Catal. Lett. **145**, 309–345.

[14] DiCosimo R, McAuliffe J, Poulose AJ, Bohlmann G. (2013) Industrial use of immobilized enzymes. Chem. Soc. Rev. **42**, 6437–6474.

[15] Woodley JM. (2006) Choice of biocatalyst form for scalable processes. Biochem. Soc. Trans. **34**, 301–303.

[16] Zhao X, Qi F, Yuan C, Du W, Liu D. (2015) Lipase-catalyzed process for biodiesel production: Enzyme immobilization, process simulation and optimization. Renew. Sustain. Energy Rev. **44**, 182–197.

[17] Sheldon RA, van Pelt S. (2013) Enzyme immobilisation in biocatalysis: why, what and how. Chem. Soc. Rev. **42**, 6223–6235.

[18] Datta S, Christena LR. (2013) Enzyme immobilization : an overview on techniques and support materials. **3**, 1–9.

[19] Cui JD, Li LL, Bian HJ. (2013) Immobilization of cross-linked phenylalanine ammonia lyase aggregates in microporous silica gel. PLoS One. **8**, 1–8.

[20] Talekar S, Waingade S, Gaikwad V, Patil S, Nagavekar N. (2012) Preparation and characterization of cross linked enzyme aggregates (CLEAs) of *Bacillus amyloliquefaciens* alpha amylase. J. Biochem. Tech. **3**, 349–353.

[21] Velasco-Lozano S, López-Gallego F, Mateos-Díaz JC, Favela-Torres E. (2016) Cross-linked enzyme aggregates (CLEA) in enzyme improvement – a review. Biocatalysis. **1**, 166–177.

[22] Cui JD, Cui LL, Zhang SP, Zhang YF, Su ZG, Ma GH. (2014) Hybrid magnetic cross-linked enzyme aggregates of phenylalanine ammonia lyase from *Rhodotorula glutinis*. PLoS One. **9**, 1–8.

[23] Carrea G, Riva S. (2008) Organic synthesis with enzymes in non-aqueous media. Wiley-VCH Verlag, Weinheim; 2008.

[24] Mohamad NR, Marzuki NHC, Buang NA, Huyop F, Wahab RA. (2015) An overview of technologies for immobilization of enzymes and surface analysis techniques for immobilized enzymes. Biotechnol. Biotechnol. Equip. **29**, 205–220.

[25] Bezerra CS, De Farias Lemos CMG, De Sousa M, Goncalves LRB. (2015) Enzyme immobilization onto renewable polymeric matrixes: Past, present, and future trends. J. Appl. Polym. Sci. **132**, 1–15.

[26] Linko Y, Pohjola L. (1976) A simple entrapment method for immobilizing enzymes. **62**, 77–80.

[27] Shah RM, D'mello AP. (2008) Strategies to maximize the encapsulation efficiency of phenylalanine ammonia lyase in microcapsules. Int. J. Pharm. **356**, 61–68.

[28] Cui J, Liang L, Han C, Liu R lin. (2015) Stabilization of phenylalanine ammonia lyase from *Rhodotorula glutinis* by encapsulation in polyethyleneimine-mediated biomimetic silica. Appl. Biochem. Biotechnol. **176**, 999–1011.

[29] Marconi W, Bartoli F, Gianna R, Morisi F, Spotorno G. (1980) Phenylalanine ammonia-lyase entrapped in fibers. Biochimie. **62**, 575–580.

[30] Bucke C. (1987) Cell immobilization in calcium alginate. Methods Enzymol. **135**, 175–189.

[31] Fernandez-Lafuente R, Armisen P, Sabuquillo P, Fernández-Lorente G, Guisan JM. (1998) Immobilization of lipases by selective adsorption on hydrophobic supports. Chem. Phys. Lipids. **93**, 185–197.

[32] Waugh DS. (2005) Making the most of affinity tags. Trends Biotechnol. **23**, 316–320.

[33] Oliveira C, Carvalho V, Domingues L, Gama FM. (2015) Recombinant CBM-fusion technology - Applications overview. Biotechnol. Adv. **33**, 358–369.

[34] Boraston AB, Bolam DN, Gilbert HJ, Davies GJ. (2004) Carbohydrate-binding modules: fine-tuning polysaccharide recognition. Biochem. J. **382**, 769–781.

[35] Tomme P, Boraston A, McLean B, Kormos J, Creagh AL, Sturch K, et al. (1998) Characterization and affinity applications of cellulose-binding domains. J. Chromatogr. B Biomed. Sci. Appl. **715**, 283–296.

[36] Terpe K. (2003) Overview of tag protein fusions: from molecular and biochemical fundamentals to commercial systems. Appl. Microbiol. Biotechnol. **60**, 523–533.

[37] Bolam DN, Ciruela A, McQueen-Mason S, Simpson P, Williamson MP, Rixon JE, et al. (1998) *Pseudomonas* cellulose-binding domains mediate their effects by increasing enzyme substrate proximity. Biochem. J. **331**, 775–781.

[38] Shoseyov O, Shani Z, Levy I. (2006) Carbohydrate binding modules: biochemical properties and novel applications. Microbiol. Mol. Biol. Rev. **70**, 283–95.

[39] Wan W, Wang D, Gao X, Hong J. (2011) Expression of family 3 cellulose-binding module (CBM3) as an affinity tag for recombinant proteins in yeast. Appl. Microbiol. Biotechnol. **91**, 789–798.

[40] Wang S, Cui GZ, Song XF, Feng Y, Cui Q. (2012) Efficiency and stability enhancement of Cis-epoxysuccinic acid hydrolase by fusion with a carbohydrate binding module and immobilization onto cellulose. Appl. Biochem. Biotechnol. **168**, 708–717.

[41] Velikodvorskaya GA, Tikhonova T V., Gurvits ID, Karyagina AS, Lavrova N V., Sergienko O V., et al. (2010) Chimeric lactase capable of spontaneous and strong immobilization on cellulose and development of a continuous-flow system for lactose hydrolysis at high temperatures. Appl. Environ. Microbiol. **76**, 8071–8075.

[42] Kopka B, Diener M, Wirtz A, Pohl M, Jaeger KE, Krauss U. (2015) Purification and simultaneous immobilization of *Arabidopsis thaliana* hydroxynitrile lyase using a family 2 carbohydrate-binding module. Biotechnol. J. **10**, 811–819.

[43] Liese A, Seelbach K, Wandrey C. (2006) Industrial biotransformation, second edition. Wiley-VCH Verlag, Weinheim; 2006.

[44] Gujer W. (2008) Systems analysis for water technology. Springer Verlag, Berlin Heidelberg; 2008.

[45] Caccavale F. (2011) Control and monitoring of chemical batch reactors, advances in industrial control. Springer Verlag, London; 2011.

[46] Rios GM, Belleville MP, Paolucci D, Sanchez J. (2004) Progress in enzymatic membrane reactors - a review. J. Memb. Sci. **242**, 189–196.

[47] Straathof AJ, Panke S, Schmid A. (2002) The production of fine chemicals by biotransformation. Curr. Opin. Biotechnol. **13**, 548–556.

[48] Blaser HU. (2003) Enantioselective catalysis in fine chemicals production. Chem.Commun. , 293–296.

[49] Verband der Chemischen Industrie. Chemiewirtschaft in Zahlen 2012. Available from: https://www.vci.de/Downloads/Publikation/Chemiewirtschaft in Zahlen 2012.pdf

[50] Ager DJ. (2008) Unnatural amino acids. In: Process chemistry in the pharmaceutical industry. CRC Press, Taylor and Francis group, Boca Raton; 2008. p. 157–179.

[51] Karau A, Grayson I. (2014) Amino acids in human and animal nutrition. Adv. Biochem. Eng. Biotechnol. **143**, 189–228.

[52] Kircher M, Pfefferle W. (2001) The fermentative production of L-lysine as an animal feed additive. Chemosphere. **43**, 27–31.

[53] Hermann T. (2003) Industrial production of amino acids by coryneform bacteria. J. Biotechnol. **104**, 155–172.

[54] Bahl CP, Rose JE, White TJ. (1981) Process for producing aspartame, patent EP0036258 A2.

[55] Baez-Viveros JL, Osuna J, Hernandez-Chavez G, Soberon X, Bolivar F, Gosset G. (2004) Metabolic engineering and protein directed evolution increase the yield of L-phenylalanine synthesized from glucose in *Escherichia coli*. Biotechnol. Bioeng. **87**, 516–524.

[56] Weaver BA. (2014) How Taxol/paclitaxel kills cancer cells. Mol. Biol. Cell. **25**, 2677–2681.

[57] Kudo F, Miyanaga A, Eguchi T. (2014) Biosynthesis of natural products containing β-amino acids. Nat. Prod. Rep. **31**, 1056–1073.

[58] Patil SA, Surwase SN, Jadhav SB, Jadhav JP. (2013) Optimization of medium using response surface methodology for L-DOPA production by *Pseudomonas sp. SSA*. Biochem. Eng. J. **74**, 36–45.

[59] Mercuri NB, Bernardi G. (2005) The magic of L-Dopa: why is it the gold standard Parkinson´s disease therapy? Trends Pharmacol. Sci. **26**, 341–344.

[60] Lloyd KG, Davidson L, Hornykiewicz O. (1975) The neurochemistry of Parkinson´s disease: effect of L-Dopa therapy. J. Pharmacol. Exp. Ther. **195**, 453–464.

[61] DeLange B, Hyett DJ, Maas PJD, Mink D, van Assema FBJ, Sereinig N, et al. (2011) Asymmetric synthesis of (S)-2-indolinecarboxylic acid by combining biocatalysis and homogeneous catalysis. ChemCatChem. **3**, 289–292.

[62] Cardillo G, Tomasini C. (1996) Asymmetric synthesis of β-amino acids and α-substituted β-amino acids. Chem. Soc. Rev. **25**, 117–128.

[63] Leuchtenberger W, Huthmacher K, Drauz K. (2005) Biotechnological production of amino acids and derivatives: Current status and prospects. Appl. Microbiol. Biotechnol. **69**, 1–8.

[64] Rudat J, Brucher BR, Syldatk C. (2012) Transaminases for the synthesis of enantiopure beta-amino acids. AMB Express. **2**, 11–20.

[65] Höhne M, Bornscheuer UT. (2009) Biocatalytic routes to optically active amines. ChemCatChem. **1**, 42–51.

[66] Turner NJ. (2011) Ammonia lyases and aminomutases as biocatalysts for the synthesis of α-amino and β-amino acids. Curr. Opin. Chem. Biol. **15**, 234–240.

[67] Heberling MM, Wu B, Bartsch S, Janssen DB. (2013) Priming ammonia lyases and aminomutases for industrial and therapeutic applications. Curr. Opin. Chem. Biol. **17**, 250–260.

[68] Poppe L, Paizs C, Kovacs K, Irimie FD, Vertessy B. (2008) Preparation of unnatural amino acids with ammonia-lyases and 2,3-aminomutases. Methods Mol. Biol. **794**, 3–19.

[69] Breuer M, Ditrich K, Habicher T, Hauer B, Keßeler M, Stürmer R, et al. (2004) Industrial methods for the production of optically active intermediates. Angew. Chemie - Int. Ed. **43**, 788–824.

[70] Asano Y, Kato Y, Levy C, Baker P, Rice D. (2004) Structure and function of amino acid ammonia-lyases. Biocatal. Biotransformation. **22**, 133–140.

[71] Ritter H. (2004) Structural basis for the entrance into the phenylpropanoid metabolism catalyzed by phenylalanine ammonia-lyase. Plant Cell Online. **16**, 3426–3436.

[72] Wang K, Hou Q, Liu Y. (2013) Insight into the mechanism of aminomutase reaction: A case study of phenylalanine aminomutase by computational approach. J. Mol. Graph. Model. **46**, 65–73.

[73] Christianson C V, Montavon TJ, Festin GM, Cooke HA, Shen B, Bruner SD. (2007) The mechanism of MIO-based aminomutases in beta-amino acid biosynthesis. J. Am. Chem. Soc. **129**, 15744–15745.

[74] Cooke HA, Christianson C V., Bruner SD. (2009) Structure and chemistry of 4-methylideneimidazole-5-one containing enzymes. Curr. Opin. Chem. Biol. **13**, 453–461.

[75] Poppe L, Retey J. (2005) Friedel-crafts-type mechanism for the enzymatic elimination of ammonia from histidine and phenylalanine. Angew. Chemie - Int. Ed. **44**, 3668–3688.

[76] MacDonald MJ, D'Cunha GB. (2007) A modern view of phenylalanine ammonia lyase. Biochem. Cell Biol. **85**, 273–282.

[77] Fraser CM, Chapple C. (2011) The phenylpropanoid pathway in *Arabidopsis*. Am. Soc. Plant Biol. **9**, e0152.

[78] Cochrane FC, Davin LB, Lewis NG. (2004) The *Arabidopsis* phenylalanine ammonia lyase gene family: Kinetic characterization of the four PAL isoforms. Phytochemistry. **65**, 1557–1564.

[79] Louie G V., Bowman ME, Moffitt M, Baiga TJ, Moore B, Noel JP. (2006) Structural determinants and modulation of substrate specificity in phenylalanine-tyrosine ammonia-lyases. Chem. Biol. **13**, 1327–1338.

[80] Bartsch S, Bornscheuer UT. (2010) Mutational analysis of phenylalanine ammonia lyase to improve reactions rates for various substrates. Protein Eng. Des. Sel. **23**, 929–933.

[81] Watts KT, Mijts BN, Lee PC, Manning AJ, Schmidt-Dannert C. (2006) Discovery of a substrate selectivity switch in tyrosine ammonia-lyase, a member of the aromatic amino acid lyase family. Chem. Biol. **13**, 1317–1326.

[82] Havir EA, Hanson KR. (1968) L-phenylalanine ammonia-lyase. II. mechanism and kinetic properties of the enzyme from potato tubers. Biochemistry. **7**, 1904–1914.

[83] Paizs C, Katona A, Rétey J. (2006) The interaction of heteroaryl-acrylates and alanines with phenylalanine ammonia-lyase from parsley. Chem. Eur. J. **12**, 2739–2744.

[84] Wu B, Symanski W, Heberling MM, Feringa BL, Janssen DB. (2011) Aminomutases: Mechanistic diversity, biotechnological applications and future perspectives. Trends Biotechnol. **29**, 352–362.

[85] Mutatu W, Klettke KL, Foster C, Walker KD. (2007) Unusual mechanism for an aminomutase rearrangement: Retention of configuration at the migration termini. Biochemistry. **46**, 9785–9794.

[86] Lohman JR, Shen B. (2012) 4-Methylideneimidazole-5-one-containing aminomutases in enediyne biosynthesis. 1st ed. Elsevier Inc.; 2012.

[87] Christenson SD, Wu W, Spies MA, Shen B, Toney MD. (2003) Kinetic analysis of the 4-methylideneimidazole-5-one-containing tyrosine aminomutase in enediyne antitumor antibiotic C-1027 biosynthesis. Biochemistry. **42**, 12708–12718.

[88] Feng L, Wanninayake U, Strom S, Geiger J, Walker KD. (2011) Mechanistic, mutational, and structural evaluation of a *Taxus* phenylalanine aminomutase. Biochemistry. **50**, 2919–2930.

[89] Christianson C V, Montavon TJ, Lanen SG Van, Shen B, Bruner SD. (2007) The structure of L-tyrosine 2,3-aminomutase from the C-1027 enediyne antitumor antibiotic biosynthetic pathway. Biochemistry. **46**, 7205–7214.

[90] Bartsch S, Wybenga GG, Jansen M, Heberling MM, Wu B, Dijkstra BW, et al. (2013) Redesign of a phenylalanine aminomutase into a phenylalanine ammonia lyase.

ChemCatChem. **5**, 1797–1802.

[91] Kovacs K, Banoczi G, Varga A, Szabo I, Holczinger A, Hornyanszky G, et al. (2014) Expression and properties of the highly alkalophilic phenylalanine ammonia-lyase of thermophilic *Rubrobacter xylanophilus*. PLoS One. **9**, 1–10.

[92] Pilbak S, Tomin A, Retey J, Poppe L. (2006) The essential tyrosine-containing loop conformation and the role of the C-terminal multi-helix region in eukaryotic phenylalanine ammonia-lyases. FEBS J. **273**, 1004–1019.

[93] Wu B, Szymański W, Wijma HJ, Crismaru CG, de Wildeman S, Poelarends GJ, et al. (2010) Engineering of an enantioselective tyrosine aminomutase by mutation of a single active site residue in phenylalanine aminomutase. Chem. Commun. **46**, 8157–8159.

[94] Wu B, Szymanski W, Wietzes P, de Wildeman S, Poelarends GJ, Feringa BL, et al. (2009) Enzymatic synthesis of enantiopure α- and β-amino acids by phenylalanine aminomutase-catalysed amination of cinnamic acid derivatives. ChemBioChem. **10**, 338–344.

[95] Wu B, Szymanski W, Heberling MM, Feringa BL, Janssen DB. (2011) Aminomutases: Mechanistic diversity, biotechnological applications and future perspectives. Trends Biotechnol. **29**, 352–362.

[96] Heberling MM, Masman MF, Bartsch S, Wybenga GG, Dijkstra BW, Marrink SJ, et al. (2015) Ironing out their differences: Dissecting the structural determinants of a phenylalanine aminomutase and ammonia lyase. ACS Chem. Biol. **10**, 989–997.

[97] Rachid S, Krug D, Weissman KJ, Müller R. (2007) Biosynthesis of (*R*)-β-tyrosine and its incorporation into the highly cytotoxic chondramides produced by *Chondromyces crocatus*. J. Biol. Chem. **282**, 21810–21817.

[98] Schruber JJ, Vollmer PJ, Montgomery JP. (1984) Verfahren zur Herstellung und Rückgewinnung von L-Phenylalanin, patent EP0140713 A2.

[99] Hidesaki T. (2008) Phenylalanine aminomutase with selectivity for S-form, DNA encoding the same, method for producing (*S*)-β-phenylalanine and method for producing (*S*)-β-phenylalanine analogs, patent WO2008129873 A1.

[100] Hauer B, Schneider N, Drew D, Ditrich K, Turner N, Nestl BM. (2011) Biocatalyst for catalytic hydroamination, patent WO2011012632 A2.

[101] Weiner DP, Varvak A, Richardson T, Podar M, Burke E, Healey S. (2015) Lyase enzymes, nucleic acids encoding them and methods for making and using them, patent application 20160068832.

[102] Mohammad Wadud Bhuiya, Chen H, CAI X, Han J, Xiaoda Y. (2013) Enzymes and methods for styrene synthesis, patent EP2864491.

[103] Ramaen O, Sauveplane V, Rudy P. (2012) Recombinant host cell for biosynthetic

production of vanillin, patent EP2749644 A1.

[104] Katz M, Smits HP, Forster J, Jens Bredel N. (2015) Metabolically engineered cells for the production of resveratrol or an oligomeric or glycosidically-bound derivative thereof, patent US20150361455 A1.

[105] Huisman GW, Agard NJ, Elgart D, Xiyun Z. (2015) Engineered tyrosine ammonia lyase, patent US20150299689.

[106] Al-Hafid N, Christodoulou J, Tong XZ. (2014) Genetically-modified probiotic for treatment of phenylketonuria, patent WO2014066945 A1.

[107] Hafid N Al, Christodoulou J. Phenylketonuria : a review of current and future treatments. **4**, 304–317.

[108] Hilberath T. (2015) Expanding the biocatalytic toolbox: Engineering a phenylalanine ammonia-lyase by site-directed mutagenesis and fusion to a carbohydrate-binding module, master thesis, Heinrich-Heine Universität Düsseldorf.

[109] Jia SR, Cui JD, Li Y, Sun AY. (2008) Production of L-phenylalanine from trans-cinnamic acids by high-level expression of phenylalanine ammonia lyase gene from *Rhodosporidium toruloides* in *Escherichia coli*. Biochem. Eng. J. **42**, 193–197.

[110] Kyndt JA, Meyer TE, Cusanovich MA, Van Beeumen JJ. (2002) Characterization of a bacterial tyrosine ammonia lyase, a biosynthetic enzyme for the photoactive yellow protein. FEBS Lett. **512**, 240–244.

[111] Krug D, Müller R. (2009) Discovery of additional members of the tyrosine aminomutase enzyme family and the mutational analysis of CmdF. ChemBioChem. **10**, 741–750.

[112] Calabrese JC, Jordan DB, Boodhoo A, Sariaslani S, Vannelli T. (2004) Crystal structure of phenylalanine ammonia lyase: Multiple helix dipoles implicated in catalysis. Biochemistry. **43**, 11403–11416.

[113] Wybenga GG, Szymanski W, Wu B, Feringa BL, Janssen DB, Dijkstra BW. (2014) Structural investigations into the stereochemistry and activity of a phenylalanine-2,3-aminomutase from *Taxus chinensis*. Biochemistry. **53**, 3187–3198.

[114] Appert C, Logemann E, Hahlbrock K, Schmid J, Amrhein N. (1994) Structural and catalytic properties of the four phenylalanine ammonia-lyase isoenzymes from parsley (*Petrosselinum crispum Nym*.). Eur. J. Biochem. **225**, 491–498.

[115] Xue Z, McCluskey M, Cantera K, Sariaslani FS, Huang L. (2007) Identification, characterization and functional expression of a tyrosine ammonia-lyase and its mutants from the photosynthetic bacterium *Rhodobacter sphaeroides*. J. Ind. Microbiol. Biotechnol. **34**, 599–604.

[116] Bartsch S, Bornscheuer UT. (2009) A single residue influences the reaction mechanism of ammonia lyases and mutases. Angew. Chemie - Int. Ed. **48**, 3362–3365.

[117] Lovelock SL, Turner NJ. (2014) Bacterial *Anabaena variabilis* phenylalanine ammonia lyase: A biocatalyst with broad substrate specificity. Bioorganic Med. Chem. **22**, 5555–5557.

[118] Lippold BC, Jaeger I. (1972) Stabilität sowie Dissoziationskonstanten von L-Dopa und α-L-Methyldopa. Arch.Pharmaz. **4**, 106–117.

[119] Knowles WS. (2002) Asymmetric hydrogenations (Nobel lecture). Angew. Chem. Int. Ed. **41**, 1998–2007.

[120] Gloge A, Zon J, Kövari A, Poppe L, Retey J. (2000) Phenylalanine ammonia-lyase : The use of its broad substrate specificity for mechanistic investigations and biocatalysis-Synthesis of L-arylalanines. **6**, 3386–3390.

[121] Cui J, Jia S, Liang L, Zhao Y, Feng Y. (2015) Mesoporous CLEAs-silica composite microparticles with high activity and enhanced stability. Sci. Rep. **5**, 14203–14216.

[122] Szymanski W, Wu B, Weiner B, De Wildeman S, Feringa BL, Janssen DB. (2009) Phenylalanine aminomutase-catalyzed addition of ammonia to substituted cinnamic acids: A route to enantiopure α- and β-amino acids. J. Org. Chem. **74**, 9152–9157.

[123] Wu B, Szymanski W, Wybenga GG, Heberling MM, Bartsch S, Dewildeman S, et al. (2012) Mechanism-inspired engineering of phenylalanine aminomutase for enhanced β-regioselective asymmetric amination of cinnamates. Angew. Chemie - Int. Ed. **51**, 482–486.

[124] Weise NJ, Parmeggiani F, Ahmed ST, Turner NJ. (2015) The bacterial ammonia lyase EncP: A tunable biocatalyst for the synthesis of unnatural amino acids. J. Am. Chem. Soc. **137**, 12977–12983.

[125] Nahálka J, Vikartovská A, Hrabárová E. (2008) A crosslinked inclusion body process for sialic acid synthesis. J. Biotechnol. **134**, 146–153.

[126] Los G V, Encell LP, McDougal MG, Hartzell DD, Karassina N, Zimprich C, et al. (2008) Halo tag: a novel protein labeling technology for cell imaging and protein analysis. ACS Chem. Biol. **3**, 373–382.

[127] Rabuka D, Rush JS, DeHart GW, Wu P, Bertozzi CR. (2012) Site-specific chemical protein conjugation using genetically encoded aldehyde tags. Nat. Protoc. **7**, 1052–1067.

7 Appendix

7.1 Plasmid cards, protein and DNA sequences

pET22b-*Pc*PAL1

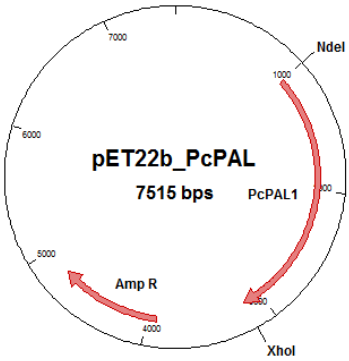

Proteine sequence with His_6 tag

MENGNGATTNGHVNGNGMDFCMKTEDPLYWGIAAEAMTGSHLDEVKKMVAEYRKPVVKLGGETLTISQVAAISARDGSGVTVELSEAARAGVKASSDWVM
DSMNKGTDSYGVTTGFGATSHRRTKQGGALQKELIRFLNAGIFGNGSDNTLPHSATRAAMLVRINTLLQGYSGIRFEILEAITKFLNQNITPCLPLRGTITASGDLVP
LSYIAGLLTGRPNSKAVGPTGVILSPEEAFKLAGVEGGFFELQPKEGLALVNGTAVGSGMASMVLFEANILAVLAEVMSAIFAEVMQGKPEFTDHLTHKLKHHPG
QIEAAAIMEHILDGSAYVKAAQKLHEMDPLQKPKQDRYALRTSPQWLGPQIEVIRSSTKMIEREINSVNDNPLIDVSRNKAIHGGNFQGTPIGVSMDNTRLAIAAI
GKLMFAQFSELVNDFYNNGLPSNLSGGRNPSLDYGFKGAEIAMASYCSELQFLANPVTNHVQSAEQHNQDVNSLGLISSRKTSEAVEILKLMSTTFLVGLCQAIDL
RHLEENLKSTVKNTVSSVAKRVLTMGVNGELHPSRFCEKDLLRVVDREYIFAYIDDPCSATYPLMQKLRQTLVEHALKNGDNERNLSTSIFQKIATFEDELKALLPKE
VESARAALESGNPAIPNRIEECRSYPLYKFVRKELGTEYLTGEKVTSPGEEFEKVFIAMSKGEIIDPLLECLESWNGAPLPICLEHHHHHH

DNA sequence with His_6tag:

ATGGAAAATGGTAATGGTGCAACCACCAATGGTCATGTTAATGGCAATGGTATGGACTTCTGTATGAAAACCGAAGATCCGCTGTATTGGGGTATTGCAG
CAGAAGCAATGACCGGTAGCCATCTGGATGAAGTGAAAAAAATGGTTGCCGAATATCGTAAACCGGTTGTTAAACTGGGTGGTGAAACCCTGACCATTAG
CCAGGTTGCAGCAATTAGCGCACGTGATGGTAGCGGTGTTACCGTTGAACTGAGCGAAGCAGCACGTGCCGGTGTTAAAGCAAGCAGCGATTGGGTTAT
GGATAGCATGAATAAAGGCACCGATAGTTATGGTGTTACCACCGGTTTTGGTGCGACCAGCCATCGTCGTACCAAACAGGGTGGTGCACTGCAAAAAGAA
CTGATTCGTTTTCTGAATGCCGGTATTTTTGGTAATGGCAGCGATAATACCCTGCCGCATAGCGCAACCCGTGCAGCAATGCTGGTTCGCATTAATACACTG
CTGCAAGGTTATAGCGGTATCCGTTTTGAAATTCTGGAAGCCATTACGAAATTTCTGAACCAGAATATTACCCCGTGTCTGCCGCTGCGTGGTACAATTACC
GCAAGCGGTGATCTGGTTCCGCTGAGCTATATTGCAGGTCTGCTGACCGGTCGTCCGAATAGCAAAGCAGTTGGTCCGACCGGTGTTATTCTGAGTCCGGA
AGAAGCATTTAAACTGGCAGGCGTTGAAGGTGGTTTTTTTGAACTGCAACCGAAAGAAGGTCTGGCACTGGTTAATGGTACAGCAGTGGGTAGCGGTATG
GCAAGCATGGTTCTGTTTGAAGCAAACATTCTGGCAGTTCTGGCCGAAGTTATGAGCGCAATTTTTGCAGAAGTTATGCAGGGTAAACCGGAATTTACCGA
TCATCTGACCCATAAACTGAAACATCATCCGGGTCAGATTGAAGCAGCAGCCATTATGGAACATATTCTGGATGGTAGTGCCTATGTTAAAGCCGCACAGA
AACTGCATGAAATGGACCCGCTGCAAAAACCGAAACAGGATCGTTATGCACTGCGTACCAGTCCGCAGTGGCTGGGTCCGCAGATCGAAGTTATTCGTAG
CAGCACCAAAATGATTGAACGCGAAATTAACAGCGTGAATGATAACCCGCTGATTGATGTTAGCCGTAATAAAGCAATTCACGGTGGTAATTTTCAGGGCA
CCCCGATTGGTGTTAGCATGGATAATACACGTCTGGCAATTGCAGCCATTGGTAAACTGATGTTTGCACAGTTTAGCGAACTGGTGAACGATTTCTATAATA
ACGGTCTGCCGAGCAATCTGAGCGGTGGTCGTAATCCGAGCCTGGATTATGGTTTTAAAGGTGCAGAAATTGCAATGGCCAGCTATTGCAGCGAACTGCA
ATTCCTGGCAAATCCGGTTACCAATCATGTTCAGAGCGCAGAACAGCATAATCAGGATGTTAATAGCCTGGGTCTGATTAGCAGCCGTAAAACCAGCGAAG
CCGTGGAAATTCTGAAACTGATGAGCACCACCTTTCTGGTTGGTCTGTGTCAGGCAATTGATCTGCGTCATCTGGAAGAAAATCTGAAAAGCACCGTTAAA
AACACCGTTAGCAGCGTTGCAAAACGTGTTCTGACAATGGGTGTTAATGGTGAACTGCATCCGTCACGTTTTTGTGAAAAAGATCTGCTGCGTGTTGTTGAT
CGCGAATATATCTTTGCCTATATTGATGATCCGTGTAGCGCCACCTATCCGCTGATGCAAAAACTGCGTCAGACCCTGGTTGAACATGCACTGAAAAATGGT
GATAATGAACGTAATCTGAGCACCAGCATCTTTCAGAAAATTGCCACCTTTGAAGATGAACTGAAAGCACTGCTGCCTAAAGAAGTTGAAAGCGCACGCGC
AGCACTGGAAAGCGGTAATCCGGCAATTCCGAATCGTATTGAAGAATGTCGTAGCTACCCGCTGTATAAATTCGTTCGTAAAGAACTGGGCACCGAATATC
TGACCGGTGAAAAAGTTACCTCACCGGGTGAAGAATTTGAAAAAGTGTTTATCGCAATGAGCAAAGGCGAAATTATTGATCCGCTGCTGGAATGTCTGGA
AAGCTGGAATGGTGCACCGCTGCCGATTTGTCTCGAGCACCACCACCACCACCAC

pET22b_*At*PAL2

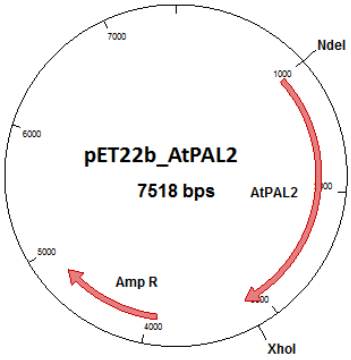

Proteine sequence with His_6 tag:

MDQIEAMLCGGGEKTKVAVTTKTLADPLNWGLAADQMKGSHLDEVKKMVEEYRRPVVNLGGETLTIGQVAAISTVGGSVKVELAETSRAGVKASSDWVMES
MNKGTDSYGVTTGFGATSHRRTKNGTALQTELIRFLNAGIFGNTKETCHTLPQSATRAAMLVRVNTLLQGYSGIRFEILEAITSLLNHNISPSLPLRGTITASGDLVPL
SYIAGLLTGRPNSKATGPDGESLTAKEAFEKAGISTGFFDLQPKEGLALVNGTAVGSGMASMVLFEANVQAVLAEVLSAIFAEVMSGKPEFTDHLTHRLKHHPGQI
EAAAIMEHILDGSSYMKLAQKVHEMDPLQKPKQDRYALRTSPQWLGPQIEVIRQATKSIEREINSVNDNPLIDVSRNKAIHGGNFQGTPIGVSMDNTRLAIAAIG
KLMFAQFSELVNDFYNNGLPSNLTASSNPSLDYGFKGAEIAMASYCSELQYLANPVTSHVQSAEQHNQDVNSLGLISSRKTSEAVDILKLMSTTFLVGICQAVDLR
HLEENLRQTVKNTVSQVAKKVLTTGINGELHPSRFCEKDLLKVVDREQVFTYVDDPCSATYPLMQRLRQVIVDHALSNGETEKNAVTSIFQKIGAFEEELKAVLPKE
VEAARAAYGNGTAPIPNRIKECRSYPLYRFVREELGTKLLTGEKVVSPGEEFDKVFTAMCEGKLIDPLMDCLKEWNGAPIPICLEHHHHHH

DNA sequence with His_6 tag:

ATGGATCAGATTGAAGCAATGCTGTGTGGTGGTGGTGAAAAAACCAAAGTTGCAGTTACCACCAAAACCCTGGCAGATCCGCTGAATTGGGGTCTGGCAG
CAGATCAGATGAAAGGTAGCCATCTGGATGAAGTGAAAAAAATGGTGGAAGAATATCGTCGTCCGGTTGTTAATCTGGGTGGCGAAACCCTGACCATTGG
CCAGGTTGCAGCAATTAGCACCGTTGGTGGTAGCGTTAAAGTTGAACTGGCAGAAACCAGCCGTGCCGGTGTTAAAGCAAGCAGCGATTGGGTTATGGAA
AGCATGAATAAAGGCACCGATAGTTATGGTGTTACCACCGGTTTTGGCGCAACCAGCCATCGTCGTACCAAAAATGGCACCGCACTGCAAACCGAACTGAT
TCGTTTTCTGAATGCAGGCATTTTTGGCAACACCAAAGAAACCTGTCATACCCTGCCGCAGAGCGCAACCCGTGCAGCCATGCTGGTTCGTGTTAATACCCT
GCTGCAAGGTTATAGCGGTATTCGTTTTGAAATTCTGGAAGCAATTACCAGCCTGCTGAATCATAACATTAGCCCGAGCCTGCCGCTGCGTGGCACCATTAC
CGCAAGCGGTGATCTGGTTCCGCTGAGCTATATTGCAGGTCTGCTGACCGGTCGTCCGAATAGCAAAGCAACCGGTCCGGATGGTGAAAGCCTGACCGCA
AAAGAAGCATTTGAAAAAGCAGGTATTAGCACGGGCTTTTTTGATCTGCAACCGAAAGAAGGTCTGGCACTGGTTAATGGTACAGCAGTTGGTAGCGGTA
TGGCAAGCATGGTTCTGTTTGAAGCAAATGTTCAGGCAGTTCTGGCAGAAGTTCTGAGCGCAATTTTTGCCGAAGTTATGAGCGGTAAACCGGAATTTACC
GATCATCTGACCCATCGTCTGAAACATCATCCGGGTCAGATCGAAGCAGCAGCCATTATGGAACATATTCTGGATGGTAGCAGCTATATGAAACTGGCACA
GAAAGTTCATGAAATGGACCCGCTGCAAAAACCGAAACAGGATCGTTATGCACTGCGTACCAGTCCGCAGTGGCTGGGTCCGCAGATTGAGGTTATTCGT
CAGGCAACCAAAAGCATTGAACGTGAAATTAACAGCGTGAATGATAACCCGCTGATTGATGTTAGCCGTAATAAAGCAATTCACGGTGGTAATTTTCAGGG
CACCCCGATTGGTGTTAGCATGGATAATACCCGTCTGGCAATTGCAGCCATTGGTAAACTGATGTTTGCACAGTTTAGCGAACTGGTGAACGATTTCTATAA
TAACGGTCTGCCGAGCAATCTGACCGCCAGCAGCAATCCGAGCCTGGATTATGGTTTTAAAGGTGCAGAAATTGCAATGGCCAGCTATTGCAGCGAACTG
CAATATCTGGCAAATCCGGTTACCAGCCATGTTCAGAGCGCAGAACAGCATAATCAGGATGTTAATAGCCTGGGTCTGATTAGCAGCCGTAAAACCAGCGA
AGCAGTTGATATTCTGAAACTGATGAGCACCACCTTTCTGGTTGGTATTTGTCAGGCCGTTGATCTGCGTCATCTGGAAGAAAACCTGCGTCAGACCGTGA
AAAATACCGTTAGCCAGGTGGCAAAAAAAGTTCTGACCACCGGTATTAATGGTGAACTGCATCCGAGCCGTTTTTGTGAAAAAGATCTGCTGAAAGTTGTG
GATCGTGAACAGGTTTTTACCTATGTTGATGATCCGTGTAGCGCAACCTATCCGCTGATGCAGCGTCTGCGTCAGGTTATTGTTGATCATGCACTGAGCAAT
GGTGAAACCGAAAAAAACGCCGTTACCAGCATTTTTCAGAAAATCGGTGCATTTGAAGAGGAACTGAAAGCAGTTCTGCCTAAAGAAGTTGAAGCAGCAC
GCGCAGCCTATGGTAATGGTACGGCACCGATTCCGAATCGTATTAAAGAATGTCGTAGTTATCCGCTGTATCGTTTTGTTCGTGAAGAACTGGGCACCAAA
CTGCTGACAGGTGAAAAAGTTGTTAGTCCGGGTGAAGAGTTTGATAAAGTTTTTACCGCAATGTGCGAAGGCAAACTGATTGATCCTCTGATGGATTGTCT
GAAAGAATGGAATGGTGCACCGATCCCGATTTGCCTCGAGCACCACCACCACCACCAC

pET22b_*Rt*PAL

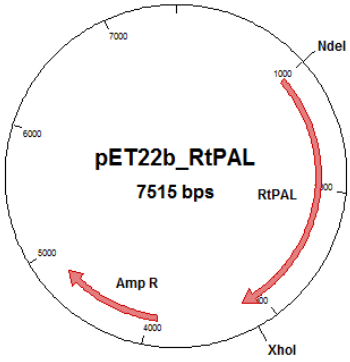

Proteine sequence with His_6 tag:

MAPSLDSISHSFANGVASAKQAVNGASTNLAVAGSHLPTTQVTQVDIVEKMLAAPTDSTLELDGYSLNLGDVVSAARKGRPVRVKDSDEIRSKIDKSVEFLRSQLS
MSVYGVTTGFGGSADTRTEDAISLQKALLEHQLCGVLPSSFDSFRLGRGLENSLPLEVVRGAMTIRVNSLTRGHSAVRLVVLEALTNFLNHGITPIVPLRGTISASGD
LSPLSYIAAAISGHPDSKVHVVHEGKEKILYAREAMALFNLEPVVLGPKEGLGLVNGTAVSASMATLALHDAHMLSLLSQSLTAMTVEAMVGHAGSFHPFLHDVT
RPHPTQIEVAGNIRKLLEGSRFAVHHEEEVKVKDDEGILRQDRYPLRTSPQWLGPLVSDLIHAHAVLTIEAGQSTTDNPLIDVENKTSHHGGNFQAAAVANTMEK
TRLGLAQIGKLNFTQLTEMLNAGMNRGLPSCLAAEDPSLSYHCKGLDIAAAAYTSELGHLANPVTTHVQPAEMANQAVNSLALISARRTTESNDVLSLLLATHLYC
VLQAIDLRAIEFEFKKQFGPAIVSLIDQHFGSAMTGSNLRDELVEKVNKTLAKRLEQTNSYDLVPRWHDAFSFAAGTVVEVLSSTSLSLAAVNAWKVAAAESAISLT
RQVRETFWSAASTSSPALSYLSPRTQILYAFVREELGVKARRGDVFLGKQEVTIGSNVSKIYEAIKSGRINNVLLKMLALEHHHHHH

DNA sequence with His_6 tag:

ATGGCACCCTCGCTCGACTCGATCTCGCACTCGTTCGCAAACGGCGTCGCATCCGCAAAGCAGGCTGTCAATGGCGCCTCGACCAACCTCGCAGTCGCAGG
CTCGCACCTGCCCACAACCCAGGTCACGCAGGTCGACATCGTCGAGAAGATGCTCGCCGCGCCGACCGACTCGACGCTCGAACTCGACGGCTACTCGCTCA
ACCTCGGAGACGTCGTCTCGGCCGCGAGGAAGGGCAGGCCTGTCCGCGTCAAGGACAGCGACGAGATCCGCTCAAAGATTGACAAATCGGTCGAGTTCT
TGCGCTCGCAACTCTCCATGAGCGTCTACGGCGTCACGACTGGATTTGGCGGATCCGCAGACACCCGCACCGAGGACGCCATCTCGCTCCAGAAGGCTCTC
CTCGAGCACCAGCTCTGCGGTGTTCTCCCTTCGTCGTTCGACTCGTTCCGCCTCGGCCGCGGTCTCGAGAACTCGCTTCCCCTCGAGGTTGTTCGCGGCGCC
ATGACAATCCGCGTCAACAGCTTGACCCGCGGCCACTCGGCTGTCCGCCTCGTCGTCCTCGAGGCGCTCACCAACTTCCTCAACCACGGCATCACCCCCATC
GTCCCCCTCCGCGGCACCATCTCTGCGTCGGGCGACCTCTCTCCTCTCTCCTACATTGCAGCGGCCATCAGCGGTCACCCGGACAGCAAGGTGCACGTCGTC
CACGAGGGCAAGGAGAAGATCCTGTACGCCCGCGAGGCGATGGCGCTCTTCAACCTCGAGCCCGTCGTCCTCGGCCCGAAGGAAGGTCTCGGTCTCGTCA
ACGGCACCGCCGTCTCAGCATCGATGGCCACCCTCGCTCTGCACGACGCACACATGCTCTCGCTCCTCTCGCAGTCGCTCACGGCCATGACGGTCGAAGCG
ATGGTCGGCCACGCCGGCTCGTTCCACCCCTTCCTTCACGACGTCACGCGCCCTCACCCGACGCAGATCGAAGTCGCGGGAAACATCCGCAAGCTCCTCGA
GGGAAGCCGCTTTGCTGTCCACCATGAGGAGGAGGTCAAGGTCAAGGACGACGAGGGCATTCTCCGCCAGGACCGCTACCCCTTGCGCACGTCTCCTCAG
TGGCTCGGCCCGCTCGTCAGCGACCTCATTCACGCCCACGCCGTCCTCACCATCGAGGCCGGCCAGTCGACGACCGACAACCCTCTCATCGACGTCGAGAA
CAAGACTTCGCACCACGGCGGCAATTTCCAGGCTGCCGCTGTGGCCAACACCATGGAGAAGACTCGCCTCGGGCTCGCCCAGATCGGCAAGCTCAACTTC
ACGCAGCTCACCGAGATGCTCAACGCCGGCATGAACCGCGGCCTCCCCTCCTGCCTCGCGGCCGAAGACCCCTCGCTCTCCTACCACTGCAAGGGCCTCGA
CATCGCCGCTGCGGCGTACACCTCGGAGTTGGGACACCTCGCCAACCCTGTGACGACGCATGTCCAGCCGGCTGAGATGGCGAACCAGGCGGTCAACTCG
CTTGCGCTCATCTCGGCTCGTCGCACGACCGAGTCCAACGACGTCCTTTCTCTCCTCCTCGCCACCCACCTCTACTGCGTTCTCCAAGCCATCGACTTGCGCG
CGATCGAGTTCGAGTTCAAGAAGCAGTTCGGCCCAGCCATCGTCTCGCTCATCGACCAGCACTTTGGCTCCGCCATGACCGGCTCGAACCTGCGCGACGAG
CTCGTCGAGAAGGTGAACAAGACGCTCGCCAAGCGCCTCGAGCAGACCAACTCGTACGACCTCGTCCCGCGCTGGCACGACGCCTTCTCCTTCGCCGCCGG
CACCGTCGTCGAGGTCCTCTCGTCGACGTCGCTCTCGCTCGCCGCCGTCAACGCCTGGAAGGTCGCCGCCGCCGAGTCGGCCATCTCGCTCACCCGCCAAG
TCCGCGAGACCTTCTGGTCCGCCGCGTCGACCTCGTCGCCCGCGCTCTCGTACCTCTCGCCGCGCACTCAGATCCTCTACGCCTTCGTCCGCGAGGAGCTTG
GCGTCAAGGCCCGCCGCGGAGACGTCTTCCTCGGCAAGCAAGAGGTGACGATCGGCTCGAACGTCTCCAAGATCTACGAGGCCATCAAGTCGGGCAGGA
TCAACAACGTCCTCCTCAAGATGCTCGCTCTCGAGTAGCACCACCACCACCACCAC

pET22b_*Rs*TAL

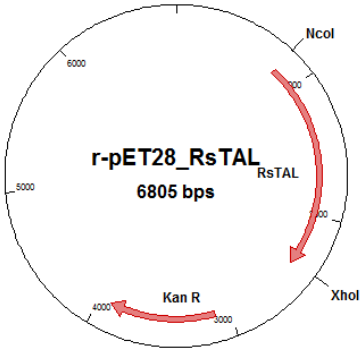

Proteine sequence with His_6 tag:

MGLAMSPPKPAVELDRHIDLDQAHAVASGGARIVLAPPARDRCRASEARLGAVIREARHVYGLTTGFGPLANRLISGENVRTLQANLVHHLASGVGPVLDWTTA
RAMVLARLVSIAQGASGASEGTIARLIDLLNSELAPAVPSRGTVGASGDLTPLAHMVLCLQGRGDFLDRDGTRLDGAEGLRRGRLQPLDLSHRDALALVNGTSAM
TGIALVNAHACRHLGNWAVALTALLAECLRGRTEAWAAALSDLRPHPGQKDAAARLRARVDGSARVVRHVIAERRLDAGDIGTEPEAGQDAYSLRCAPQVLGA
GFDTLAWHDRVLTIELNAVTDNPVFPPDGSVPALHGGNFMGQHVALTSDALATAVTVLAGLAERQIARLTDERLNRGLPPFLHRGPAGLNSGFMGAQVTATAL
LAEMRATGPASIHSISTNAANQDVVSLGTIAARLCREKIDRWAEILAILALCLAQAAELRCGSGLDGVSPAGKKLVQALREQFPPLETDRPLGQEIAAALATHLLQQSP
VLEHHHHHH

DNA sequence with His_6 tag:

CCATGGGTCTGGCTATGAGTCCTCCTAAACCGGCAGTTGAACTGGATCGTCATATTGATCTGGATCAGGCACATGCAGTTGCAAGCGGTGGTGCACGTATT
GTTCTGGCACCGCCTGCACGTGATCGTTGTCGTGCAAGCGAAGCACGTCTGGGTGCAGTTATTCGTGAAGCCCGTCATGTTTATGGTCTGACCACCGGTTTT
GGTCCGCTGGCAAATCGTCTGATTAGCGGTGAAAATGTTCGTACCCTGCAGGCAAATCTGGTTCATCATCTGGCCAGCGGTGTGGGTCCGGTTCTGGATTG
GACCACCGCACGTGCAATGGTGCTGGCACGCCTGGTTAGCATTGCACAGGGTGCGAGCGGTGCAAGTGAAGGTACAATTGCACGTCTGATTGATCTGCTG
AATAGCGAACTGGCACCGGCAGTGCCGAGCCGTGGCACCGTTGGTGCATCAGGTGATCTGACTCCGCTGGCCCATATGTTCTGTGTCTGCAGGGTCGTGG
TGATTTTCTGGATCGTGATGGCACCCGTCTGGATGGTGCCGAAGGTCTGCGTCGTGGTCGTCTGCAGCCGCTGGATCTGAGCCATCGTGATGCACTGGCAC
TGGTTAATGGCACCAGCGCAATGACAGGTATTGCACTGGTGAATGCACATGCCTGTCGTCATCTGGGTAATTGGGCAGTTGCACTGACCGCACTGCTGGCA
GAATGTCTGCGTGGTCGTACCGAAGCATGGGCAGCAGCACTGAGCGATCTGCGTCCGCATCCGGGTCAGAAAGATGCAGCAGCCCGTCTGCGTGCACGT
GTTGATGGTAGCGCACGTGTGGTTCGTCATGTTATTGCAGAACGTCGCCTGGATGCCGGTGATATTGGCACCGAACCGGAAGCAGGTCAGGATGCATATA
GCCTGCGTTGTGCACCGCAGGTTCTGGGTGCCGGTTTTGATACCCTGGCATGGCATGATCGTGTTCTGACCATTGAACTGAATGCAGTTACCGATAATCCG
GTTTTTCCTCCGGATGGTAGTGTTCCGGCACTGCATGGTGGCAATTTTATGGGTCAGCATGTTGCCCTGACCTCAGATGCCCTGGCAACCGCAGTGACCGTT
CTGGCAGGTCTGGCCGAACGTCAGATTGCCCGTCTGACCGATGAACGTCTGAATCGTGGTCTGCCTCCGTTTCTGCACCGTGGTCCGGCAGGCCTGAATAG
TGGCTTTATGGGTGCACAGGTTACCGCAACAGCCCTGCTGGCCGAAATGCGTGCAACCGGTCCGGCAAGCATTCATAGCATTAGCACCAATGCAGCAAATC
AGGATGTTGTTAGCCTGGGTACGATTGCCGCACGTCTGTGTCGTGAAAAAATTGATCGTTGGGCAGAAATTCTGGCCATTCTGGCACTGTGTCTGGCACAG
GCAGCAGAACTGCGTTGCGGTAGTGGCCTGGATGGCGTTTCACCGGCAGGTAAAAAACTGGTTCAGGCACTGCGCGAACAGTTTCCGCCTCTGGAAACCG
ATCGTCCGCTGGGTCAAGAAATTGCAGCACTGGCAACCCATCTGCTGCAACAGAGTCCAGTTCTCGAGCACCACCACCACCACCACTGA

pET28_*At*PAL2-CBM

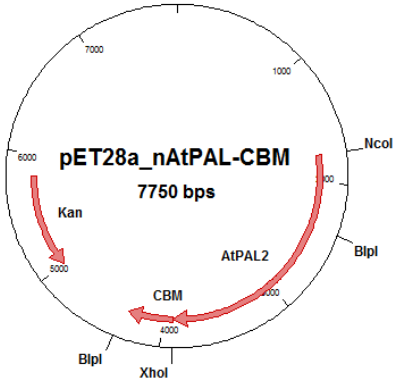

natural proline-threonine-linker of the exoglucanase/xylanase Cex from *C. fimi*
C-terminal CBM of the exoglucanase/xylanase Cex from *C.fimi*

Proteine sequence with linker and CBM:

MDQIEAMLCGGGEKTKVAVTTKTLADPLNWGLAADQMKGSHLDEVKKMVEEYRRPVVNLGGETLTIGQVAAISTVGGSVKVELAETSRAGVKASSDWVMES
MNKGTDSYGVTTGFGATSHRRTKNGTALQTELIRFLNAGIFGNTKETCHTLPQSATRAAMLVRVNTLLQGYSGIRFEILEAITSLLNHNISPSLPLRGTITASGDLVPL
SYIAGLLTGRPNSKATGPDGESLTAKEAFEKAGISTGFFDLQPKEGLALVNGTAVGSGMASMVLFEANVQAVLAEVLSAIFAEVMSGKPEFTDHLTHRLKHHPGQI
EAAAIMEHILDGSSYMKLAQKVHEMDPLQKPKQDRYALRTSPQWLGPQIEVIRQATKSIEREINSVNDNPLIDVSRNKAIHGGNFQGTPIGVSMDNTRLAIAAIG
KLMFAQFSELVNDFYNNGLPSNLTASSNPSLDYGFKGAEIAMASYCSELQYLANPVTSHVQSAEQHNQDVNSLGLISSRKTSEAVDILKLMSTTFLVGICQAVDLR
HLEENLRQTVKNTVSQVAKKVLTTGINGELHPSRFCEKDLLKVVDREQVFTYVDDPCSATYPLMQRLRQVIVDHALSNGETEKNAVTSIFQKIGAFEEELKAVLPKE
VEAARAAYGNGTAPIPNRIKECRSYPLYRFVREELGTKLLTGEKVVSPGEEFDKVFTAMCEGKLIDPLMDCLKEWNGAPIPICLEPTPTPTTPTPTPTTPTPTPTSGPA
GCQVLWGVNQWNTGFTANVTVKNTSSAPVDGWTLTFSFPSGQQVTQAWSSTVTQSGSAVTVRNAPWNGSIPAGGTAQFGFNGSHTGTNAAPTAFSLNGTP
CTVG

DNA sequence with linker and CBM:

CCATGGATCAGATTGAAGCAATGCTGTGTGGTGGTGGTGAAAAAACCAAAGTTGCAGTTACCACCAAAACCCTGGCAGATCCGCTGAATTGGGGTCTGGC
AGCAGATCAGATGAAAGGTAGCCATCTGGATGAAGTGAAAAAAATGGTGGAAGAATATCGTCGTCCGGTTGTTAATCTGGGTGGCGAAACCCTGACCATT
GGCCAGGTTGCAGCAATTAGCACCGTTGGTGGTAGCGTTAAAGTTGAACTGGCAGAAACCAGCCGTGCCGGTGTTAAAGCAAGCAGCGATTGGGTTATG
GAAAGCATGAATAAAGGCACCGATAGTTATGGTGTTACCACCGGTTTTGGCGCAACCAGCCATCGTCGTACCAAAAATGGCACCGCACTGCAAACCGAACT
GATTCGTTTTCTGAATGCAGGCATTTTTGGCAACACCAAAGAAACCTGTCATACCCTGCCGCAGAGCGCAACCCGTGCAGCCATGCTGGTTCGTGTTAATAC
CCTGCTGCAAGGTTATAGCGGTATTCGTTTTGAAATTCTGGAAGCAATTACCAGCCTGCTGAATCATAACATTAGCCCGAGCCTGCCGCTGCGTGGCACCAT
TACCGCAAGCGGTGATCTGGTTCCGCTGAGCTATATTGCAGGTCTGCTGACCGGTCGTCCGAATAGCAAAGCAACCGGTCCGGATGGTGAAAGCCTGACC
GCAAAAGAAGCATTTGAAAAAGCAGGTATTAGCACGGGCTTTTTTGATCTGCAACCGAAAGAAGGTCTGGCACTGGTTAATGGTACAGCAGTTGGTAGCG
GTATGGCAAGCATGGTTCTGTTTGAAGCAAATGTTCAGGCAGTTCTGGCAGAAGTTCTGAGCGCAATTTTTGCCGAAGTTATGAGCGGTAAACCGGAATTT
ACCGATCATCTGACCCATCGTCTGAAACATCATCCGGGTCAGATCGAAGCAGCAGCCATTATGGAACATATTCTGGATGGTAGCAGCTATATGAAACTGGC
ACAGAAAGTTCATGAAATGGACCCGCTGCAAAAACCGAAACAGGATCGTTATGCACTGCGTACCAGTCCGCAGTGGCTGGGTCCGCAGATTGAGGTTATT
CGTCAGGCAACCAAAAGCATTGAACGTGAAATTAACAGCGTGAATGATAACCCGCTGATTGATGTTAGCCGTAATAAAGCAATTCACGGTGGTAATTTTCA
GGGCACCCCGATTGGTGTTAGCATGGATAATACCCGTCTGGCAATTGCAGCCATTGGTAAACTGATGTTTGCACAGTTTAGCGAACTGGTGAACGATTTCT
ATAATAACGGTCTGCCGAGCAATCTGACCGCCAGCAGCAATCCGAGCCTGGATTATGGTTTTAAAGGTGCAGAAATTGCAATGGCCAGCTATTGCAGCGA
ACTGCAATATCTGGCAAATCCGGTTACCAGCCATGTTCAGAGCGCAGAACAGCATAATCAGGATGTTAATAGCCTGGGTCTGATTAGCAGCCGTAAAACCA
GCGAAGCAGTTGATATTCTGAAACTGATGAGCACCACCTTTCTGGTTGGTATTTGTCAGGCCGTTGATCTGCGTCATCTGGAAGAAAACCTGCGTCAGACC
GTGAAAAATACCGTTAGCCAGGTGGCAAAAAAAGTTCTGACCACCGGTATTAATGGTGAACTGCATCCGAGCCGTTTTTGTGAAAAAGATCTGCTGAAAGT
TGTGGATCGTGAACAGGTTTTTACCTATGTTGATGATCCGTGTAGCGCAACCTATCCGCTGATGCAGCGTCTGCGTCAGGTTATTGTTGATCATGCACTGAG
CAATGGTGAAACCGAAAAAAACGCCGTTACCAGCATTTTTCAGAAAATCGGTGCATTTGAAGAGGAACTGAAAGCAGTTCTGCCTAAAGAAGTTGAAGCA
GCACGCGCAGCCTATGGTAATGGTACGGCACCGATTCCGAATCGTATTAAAGAATGTCGTAGTTATCCGCTGTATCGTTTTGTTCGTGAAGAACTGGGCAC
CAAACTGCTGACAGGTGAAAAAGTTGTTAGTCCGGGTGAAGAGTTTGATAAAGTTTTTACCGCAATGTGCGAAGGCAAACTGATTGATCCTCTGATGGATT
GTCTGAAAGAATGGAATGGTGCACCGATCCCGATTTGCCTCGAGCCTACTCCGACTCCTACCACCCCAACCCCAACACCGACCACGCCCACTCCGACTCCCA
CCTCTGGTCCAGCTGGTTGCCAAGTTCTGTGGGGAGTAAACCAGTGGAATACGGGCTTTACTGCGAACGTCACAGTGAAGAATACCAGTTCTGCCCCGGTG
GATGGCTGGACCTTAACGTTCTCGTTTCCGTCAGGTCAGCAAGTCACTCAAGCCTGGTCGTCCACGGTAACGCAATCCGGTAGTGCGGTGACCGTTCGTAA
CGCACCGTGGAATGGAAGCATTCCCGCTGGTGGTACGGCTCAGTTCGGGTTCAATGGCAGCCATACGGGGACCAATGCAGCACCGACCGCCTTTAGCCTC
AATGGCACACCGTGTACCGTGGGCTAA

pET28_*Tch*PAM

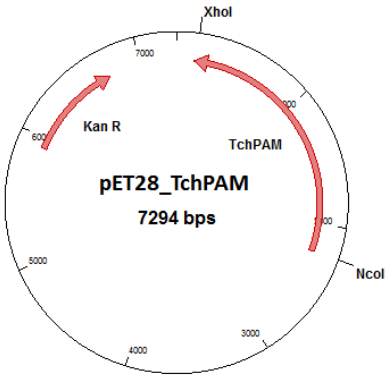

Proteine sequence with His_6 tag:

MGFAVESRSHVKDILGLINAFNEVKKITVDGTTPITVAHVAALARRHDVKVALEAEQCRARVETCSSWVQRKAEDGADIYGVTTGFGACSSRRTNRLSELQESLIR
CLLAGVFTKGCAPSVDELPATATRSAMLLRLNSFTYGCSGIRWEVMEALEKLLNSNVSPKVPLRGSVSASGDLIPLAYIAGLLIGKPSVIARIGDDVEVPAPEALSRVG
LRPFKLQAKEGLALVNGTSFATAVASTVMYDANVLLLLVETLCGMFCEVIFGREEFAHPLIHKVKPHPGQIESAELLEWLLRSSPFQELSREYYSIDKLKKPKQDRYAL
RSSPQWLAPLVQTIRDATTTVETEVNSANDNPIIDHANDRALHGANFQGSAVGFYMDYVRIAVAGLGKLLFAQFTELMIEYYSNGLPGNLSLGPDLSVDYGLKGL
DIAMAAYSSELQYLANPVTTHVHSAEQHNQDINSLALISARKTEEALDILKLMIASHLTAMCQAVDLRQLEEALVKVVENVVSTLADECGLPNDTKARLLYVAKAV
PVYTYLESPCDPTLPLLLGLKQSCFDTILALHKKDGIETDTLVDRLAEFEKRLSDRLENEMTAVRVLYEKKGHKTADNNDALVRIQGSKFLPFYRFVREELDTGVMSA
RREQTPQEDVQKVFDAIADGRITVPLLHCLQGFLGQPNGCANGVLEHHHHHH

DNA sequence with His_6 tag:

CCATGGGGTTTGCCGTGGAATCGCGTTCTCACGTAAAGGATATATTGGGGCTGATCAACGCGTTCAACGAGGTGAAGAAAATTACAGTAGACGGTACGAC
CCCCATCACGGTGGCCCATGTCGCGGCGCTGGCCCGGAGGCATGACGTGAAGGTTGCGTTGGAGGCGGAGCAATGCAGAGCCCGTGTGGAAACCTGCTC
TTCGTGGGTGCAGCGCAAGGCGGAAGACGGCGCCGACATATACGGCGTCACCACGGGCTTCGGCGCGTGCTCGAGCCGGAGGACCAACCGGCTGAGCG
AGCTGCAGGAGTCGCTCATACGCTGCCTGCTCGCGGGGGTGTTTACTAAAGGATGCGCTCCCTCCGTCGACGAGCTCCCCGCGACCGCCACCCGCAGCGCC
ATGCTGCTCCGCCTTAATAGTTTTACCTATGGATGTTCCGGCATCCGGTGGGAGGTCATGGAAGCGCTGGAAAAGCTTCTCAACAGCAATGTCTCTCCTAAA
GTGCCTCTCCGGGGGTTCTGTGAGCGCTTCGGGAGACCTCATCCCGCTCGCCTACATTGCAGGGCTCCTGATCGGGAAGCCTAGCGTAATCGCTCGCATAGG
CGACGATGTCGAGGTCCCTGCGCCCGAGGCGTTGAGCAGGGTGGGGCTTCGGCCATTCAAGCTCCAGGCCAAAGAAGGGCTGGCGCTCGTCAACGGCAC
CTCCTTCGCCACCGCGGTCGCCTCCACCGTCATGTACGACGCCAATGTTCTGTTGCTGCTCGTCGAAACGCTTTGCGGAATGTTCTGCGAGGTGATCTTTGG
AAGGGAGGAGTTCGCGCATCCGCTGATCCATAAAGTGAAGCCGCACCCGGGCCAGATCGAATCGGCGGAGCTGCTCGAGTGGCTGCTGCGGTCGAGCCC
GTTTCAGGAGCTGTCGAGGGAGTATTACAGTATTGATAAGCTGAAGAAACCGAAACAGGATCGCTATGCTCTGAGGTCGAGCCCGCAGTGGTTGGCTCCT
CTGGTGCAGACAATCAGAGACGCCACCACTACAGTGGAGACGGAGGTCAATTCCGCCAATGATAACCCCATCATTGACCACGCCAATGACAGGGCTCTCC
ATGGTGCGAATTTCCAGGGCAGCGCCGTCGGTTTCTACATGGACTACGTGCGCATCGCAGTAGCCGGGCTGGGGAAACTCTTGTTCGCTCAGTTCACGGA
GCTGATGATCGAATATTACAGCAACGGCCTACCGGGGAACCTCTCCCTGGGGCCGGACCTGAGCGTGGACTACGGCCTCAAGGGGCTCGACATCGCCATG
GCCGCCTACAGCTCCGAGCTTCAGTACCTGGCGAATCCCGTGACCACACACGTGCACAGCGCGGAACAGCACAACCAGGACATCAACTCTCTGGCGCTCAT
CTCCGCCCGCAAGACGGAGGAGGCGTTGGATATCTTAAAGCTCATGATCGCCTCGCATTTAACAGCAATGTGCCAGGCGGTGGACCTTCGGCAGCTCGAA
GAAGCCCTAGTAAAAGTCGTGGAGAATGTCGTTTCCACCCTTGCAGACGAATGCGGCCTCCCTAACGACACAAAGGCGAGGCTTTTATATGTAGCCAAAGC
GGTGCCTGTTTACACATACCTGGAATCCCCCTGCGACCCCACGCTTCCCCTCTTGTTAGGCCTGAAACAGTCCTGTTTCGATACCATTCTGGCTCTCCACAAA
AAAGACGGCATTGAGACGGACACCTTGGTCGATCGGCTCGCCGAGTTCGAGAAGCGGCTGTCCGACCGCCTGGAAAACGAGATGACGGCAGTGAGGGTT
TTGTACGAAAAGAAAGGGCATAAAACGGCAGACAACAACGACGCCCTCGTGAGAATCCAGGGTTCCAAATTCCTTCCTTTTTACAGATTTGTTCGGGAAGA
GCTCGACACAGGTGTGATGAGTGCGAGAAGAGAGCAGACGCCGCAAGAGGACGTGCAGAAAGTGTTCGATGCAATTGCCGACGGCAGAATTACGGTGC
CTCTACTGCACTGCCTGCAAGGGTTTCTCGGCCAACCAAATGGGTGCGCCAACGGCGTCCTCGAGCACCACCACCACCACCACTGA

pET28_*Tca*PAM

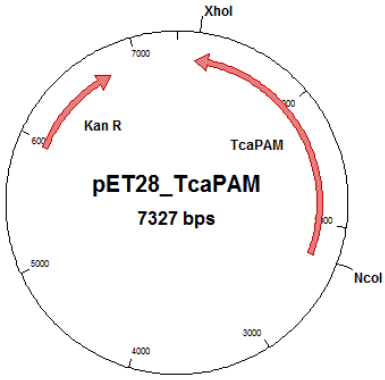

Proteine sequence with His_6 tag:

MGFAVESRSHVKDILGLINTFNEVKKITVDGTTPITVAHVAALARRHDVKVALEAEQCRARVETCSSWVQRKAEDGADIYGVTTGFGACSSRRTNQLSELQESLIR
CLLAGVFTKGCASSVDELPATATRSAMLLRLNSFTYGCSGIRWEVMEALEKLLNSNVSPKVPLRGSVSASGDLIPLAYIAGLLIGKPSVVARIGDDVEVPAPEALSRV
GLRPFKLQAKEGLALVNGTSFATALASTVMYDANVLLLLVETLCGMFCEVIFGREEFAHPLIHKVKPHPGQIESAELLEWLLRSSPFQDLSREYYSIDKLKKPKQDRY
ALRSSPQWLAPLVQTIRDATTTVETEVNSANDNPIIDHANDRALHGANFQGSAVGFYMDYVRIAVAGLGKLLFAQFTELMIEYYSNGLPGNLSLGPDLSVDYGLK
GLDIAMAAYSSELQYLANPVTTHVHSAEQHNQDINSLALISARKTEEALDILKLMIASHLTAMCQAVDLRQLEEALVKVVENVVSTLADECGLPNDTKARLLYVAK
AVPVYTYLESPCDPTLPLLLGLEQSCFGSILALHKKDGIETDTLVDRLAEFEKRLSDRLENEMTAVRVLYEKKGHKTADNNDALVRIQGSRFLPFYRFVREELDTGVM
SARREQTPQEDVQKVFDAIADGRITVPLLHCLQGFLGQPNGCANGVESFQSVWNKSALEHHHHHH

DNA sequence with His_6 tag:

CCATGGGGTTTGCCGTGGAATCGCGTTCTCACGTAAAGGATATATTGGGGCTGATCAACACGTTCAACGAGGTGAAGAAAATTACAGTAGACGGTACGAC
CCCCATCACGGTGGCCCATGTCGCGGCGCTGGCCCGGAGGCATGACGTGAAGGTTGCGTTGGAGGCGGAGCAATGCAGAGCCCGTGTGGAAACCTGCTC
TTCGTGGGTGCAGCGCAAGGCGGAAGACGGCGCCGACATATACGGCGTCACCACGGGCTTTGGCGCGTGCTCGAGCCGTAGGACCAACCAGCTGAGCGA
GCTGCAGGAGTCGCTTATACGCTGCCTGCTCGCGGGGGTGTTTACTAAAGGATGCGCTTCCTCCGTCGACGAGCTCCCTGCGACCGCCACCCGCAGCGCCA
TGCTGCTCCGCCTTAATAGTTTTACCTATGGATGTTCCGGCATCCGGTGGGAGGTCATGGAAGCGCTGGAAAAGCTTCTCAACAGCAATGTCTCTCCTAAAG
TGCCTCTCCGAGGATCTGTGAGCGCTTCGGGAGACCTCATCCCGCTCGCCTACATTGCAGGGCTCCTGATTGGGAAGCCTAGCGTAGTCGCTCGCATAGGC
GACGATGTCGAGGTCCCTGCGCCCGAAGCGTTGAGCAGGGTGGGGCTGCGGCCATTCAAGCTCCAGGCCAAAGAAGGGCTGGCGCTCGTCAACGGCACC
TCCTTCGCCACCGCGCTCGCCTCCACCGTCATGTACGACGCCAATGTTCTGTTGCTGCTCGTCGAAACGCTTTGCGGAATGTTCTGCGAGGTGATCTTTGGA
AGGGAGGAGTTCGCGCATCCGCTGATCCATAAAGTGAAGCCGCACCCAGGCCAGATCGAATCGGCGGAGCTGCTCGAGTGGCTGCTGCGGTCGAGCCCG
TTTCAGGACCTGTCGAGGGAGTATTACAGTATTGATAAGCTGAAGAAACCGAAACAGGATCGCTATGCTCTGAGGTCGAGCCCGCAGTGGTTGGCTCCTCT
GGTGCAGACAATCAGAGACGCCACCACTACAGTGGAGACGGAGGTCAATTCCGCCAATGATAACCCCATCATTGACCACGCCAATGACAGGGCTCTCCAT
GGTGCGAATTTCCAGGGCAGCGCCGTCGGCTTCTACATGGACTACGTGCGCATCGCAGTCGCCGGGCTGGGGAAACTCTTGTTCGCTCAGTTCACGGAGC
TGATGATCGAATATTACAGCAACGGCCTACCGGGGAACCTCTCCCTGGGGCCGGACCTGAGCGTGGACTACGGCCTCAAGGGGCTCGACATCGCCATGGC
CGCCTACAGCTCCGAGCTTCAGTACCTGGCGAATCCCGTGACCACACACGTGCACAGCGCGGAACAGCACAACCAGGACATCAACTCTCTGGCGCTCATCT
CCGCCCGCAAGACGGAGGAAGCGTTGGATATCTTAAAGCTCATGATCGCCTCGCATTTAACAGCAATGTGCCAGGCGGTGGACCTTCGGCAGCTCGAAGA
AGCCCTAGTAAAAGTCGTGGAGAATGTCGTTTCCACCCTTGCAGACGAATGCGGCCTCCCTAACGACACAAAGGCGAGGCTTTTATATGTAGCCAAAGCG
GTGCCTGTTTACACATACCTGGAATCCCCCTGCGACCCTACGCTTCCCCTCTTGTTAGGCCTGGAACAGTCCTGTTTCGGTTCCATTCTGGCTCTCCACAAAA
AAGACGGCATTGAGACGGACACCTTGGTCGATCGGCTCGCCGAGTTCGAGAAGCGGCTGTCCGACCGCCTGGAAAACGAGATGACGGCAGTGAGGGTTT
TGTACGAAAAGAAAGGGCATAAAACTGCAGACAACAACGACGCCCTCGTGAGAATCCAGGGTTCCAGATTCCTTCCTTTTTACAGATTTGTTCGGGAAGAG
CTCGACACAGGTGTGATGAGTGCGAGAAGAGAGCAGACGCCGCAAGAGGACGTGCAGAAAGTGTTCGATGCAATTGCCGACGGCAGAATTACGGTGCCT
CTGCTGCACTGCCTGCAAGGGTTTCTCGGCCAACCAAATGGGTGCGCCAACGGCGTCGAGTCGTTCCAAAGTGTTTGGAACAAATCTGCGCTCGAGCACCA
CCACCACCACCACTGA

pET22_*Cc*TAM

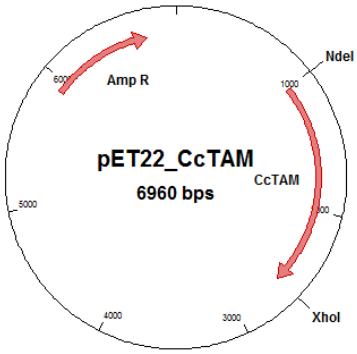

Proteine sequence with His_6 tag:

MKITGSNLSIYDVADVCMKRATVELDPSQLERVAVAHERTQAWGEAQHPIYGVNTGFGELVPVMIPRQHKRELQENLIRSHAAGGGEPFADDVVRAIMLARLN
CLMKGYSGASVETVKLLAEFINRGIHPVIPQQGSLGASGDLSPLSHIALALIGEGTVSFKGQVRKTGDVLREEGLKPLELGFKGGLTLINGTSAMTGAACVALGRAY
HLFRLALLATADFVQCLGGSTGPFEERGHLPKNHSGQVIVAREIRKLLAGSQLTSDHQDLMKEMVARSGVGNDVVDTGVYLQDAYTLRAVPQILGPVLDTLDFAR
KLIEEELNSTNDNPLIFDVPEQTFHGANFHGQYVAMACDYLNIAVTEIGVLAERQLNRLVDPNINGKLPPFLASAHSGLLCGFEGGQYLATSIASENLDLAAPSSIKS
LPSNGSNQDVVSMGTTSARKSLRLCENVGTIVSTLIAACNQAGHILGNERFSPPIRELHGELSRSVPLYQDDSPIFELFQTVRAFVGGDGFRAHLVTHLDLAATTASS
LEHHHHHH

DNA sequence with His_6 tag:

CATATGAAAATTACCGGCAGCAACCTGAGCATTTATGATGTGGCGGATGTGTGCATGAAACGCGCGACCGTGGAACTGGATCCGAGCCAGCTGGAACGC
GTGGCGGTGGCGCATGAACGCACCCAGGCGTGGGGCGAAGCGCAGCATCCGATTTATGGCGTGAACACCGGCTTTGGCGAACTGGTGCCGGTGATGATT
CCGCGCCAGCATAAACGCGAACTGCAGGAAAACCTGATTCGCAGCCATGCGGCGGGCGGCGGCGAACCGTTTGCGGATGATGTGGTGCGCGCGATTATG
CTGGCGCGCCTGAACTGCCTGATGAAAGGCTATAGCGGCGCGAGCGTGGAAACCGTGAAACTGCTGGCGGAATTTATTAACCGCGGCATTCATCCGGTGA
TTCCGCAGCAGGGCAGCCTGGGCGCGAGCGGCGATCTGAGCCCGCTGAGCCATATTGCGCTGGCGCTGATTGGCGAAGGCACCGTGAGCTTTAAAGGCC
AGGTGCGCAAAACCGGCGATGTGCTGCGCGAAGAAGGCCTGAAACCGCTGGAACTGGGCTTTAAAGGCGGCCTGACCCTGATTAACGGCACCAGCGCGA
TGACCGGCGCGGCGTGCGTGGCGCTGGGCCGCGCGTATCATCTGTTTCGCCTGGCGCTGCTGGCGACCGCGGATTTTGTGCAGTGCCTGGGCGGCAGCAC
CGGCCCGTTTGAAGAACGCGGCCATCTGCCGAAAAACCATAGCGGCCAGGTGATTGTGGCGCGCGAAATTCGCAAACTGCTGGCGGGCAGCCAGCTGAC
CAGCGATCATCAGGATCTGATGAAAGAAATGGTGGCGCGCAGCGGCGTGGGCAACGATGTGGTGGATACCGGCGTGTATCTGCAGGATGCGTATACCCT
GCGCGCGGTGCCGCAGATTCTGGGCCCGGTGCTGGATACCCTGGATTTTGCGCGCAAACTGATTGAAGAAGAACTGAACAGCACCAACGATAACCCGCTG
ATTTTTGATGTGCCGGAACAGACCTTTCATGGCGCGAACTTTCATGGCCAGTATGTGGCGATGGCGTGCGATTATCTGAACATTGCGGTGACCGAAATTGG
CGTGCTGGCGGAACGCCAGCTGAACCGCCTGGTGGATCCGAACATTAACGGCAAACTGCCGCCGTTTCTGGCGAGCGCGCATAGCGGCCTGCTGTGCGGC
TTTGAAGGCGGCCAGTATCTGGCGACCAGCATTGCGAGCGAAAACCTGGATCTGGCGGCGCCGAGCAGCATTAAAAGCCTGCCGAGCAACGGCAGCAAC
CAGGATGTGGTGAGCATGGGCACCACCAGCGCGCGCAAAAGCCTGCGCCTGTGCGAAAACGTGGGCACCATTGTGAGCACCCTGATTGCGGCGTGCAAC
CAGGCGGGCCATATTCTGGGCAACGAACGCTTTAGCCCGCCGATTCGCGAACTGCATGGCGAACTGAGCCGCAGCGTGCCGCTGTATCAGGATGATAGCC
CGATTTTTGAACTGTTTCAGACCGTGCGCGCGTTTGTGGGCGGCGATGGCTTTCGCGCGCATCTGGTGACCCATCTGGATCTGGCGGCGACCACCGCGAGC
AGCCTCGAGCACCACCACCACCACCACTGA

pET28_*Cc*TAM K2E-CBM

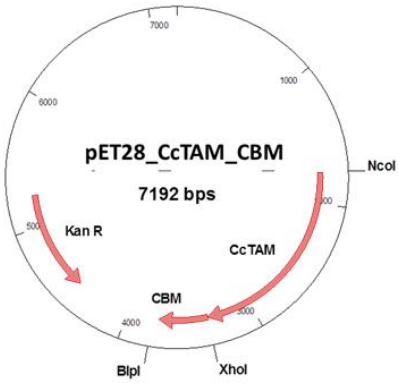

natural proline-threonine-linker of the exoglucanase/xylanase Cex from *C. fimi*
C-terminal CBM of the exoglucanase/xylanase Cex from *C.fimi*

Proteine sequence with linker and CBM:

MEITGSNLSIYDVADVCMKRATVELDPSQLERVAVAHERTQAWGEAQHPIYGVNTGFGELVPVMIPRQHKRELQENLIRSHAAGGGEPFADDVVRAIMLARLN
CLMKGYSGASVETVKLLAEFINRGIHPVIPQQGSLGASGDLSPLSHIALALIGEGTVSFKGQVRKTGDVLREEGLKPLELGFKGGLTLINGTSAMTGAACVALGRAY
HLFRLALLATADFVQCLGGSTGPFEERGHLPKNHSGQVIVAREIRKLLAGSQLTSDHQDLMKEMVARSGVGNDVVDTGVYLQDAYTLRAVPQILGPVLDTLDFAR
KLIEEELNSTNDNPLIFDVPEQTFHGANFHGQYVAMACDYLNIAVTEIGVLAERQLNRLVDPNINGKLPPFLASAHSGLLCGFEGGQYLATSIASENLDLAAPSSIKS
LPSNGSNQDVVSMGTTSARKSLRLCENVGTIVSTLIAACNQAGHILGNERFSPPIRELHGELSRSVPLYQDDSPIFELFQTVRAFVGGDGFRAHLVTHLDLAATTASS
PTPTPTTPTPTPTTPTPTPTSGPAGCQVLWGVNQWNTGFTANVTVKNTSSAPVDGWTLTFSFPSGQQVTQAWSSTVTQSGSAVTVRNAPWNGSIPAGGTAQ
FGFNGSHTGTNAAPTAFSLNGTPCTVG

DNA sequence with linker and CBM:

CCATGGAAATTACCGGCAGCAACCTGAGCATTTATGATGTGGCGGATGTGTGCATGAAACGCGCGACCGTGGAACTGGATCCGAGCCAGCTGGAACGCG
TGGCGGTGGCGCATGAACGCACCCAGGCGTGGGGCGAAGCGCAGCATCCGATTTATGGCGTGAACACCGGCTTTGGCGAACTGGTGCCGGTGATGATTC
CGCGCCAGCATAAACGCGAACTGCAGGAAAACCTGATTCGCAGCCATGCGGCGGGCGGCGGCGAACCGTTTGCGGATGATGTGGTGCGCGCGATTATGC
TGGCGCGCCTGAACTGCCTGATGAAAGGCTATAGCGGCGCGAGCGTGGAAACCGTGAAACTGCTGGCGGAATTTATTAACCGCGGCATTCATCCGGTGAT
TCCGCAGCAGGGCAGCCTGGGCGCGAGCGGCGATCTGAGCCCGCTGAGCCATATTGCGCTGGCGCTGATTGGCGAAGGCACCGTGAGCTTTAAAGGCCA
GGTGCGCAAAACCGGCGATGTGCTGCGCGAAGAAGGCCTGAAACCGCTGGAACTGGGCTTTAAAGGCGGCCTGACCCTGATTAACGGCACCAGCGCGAT
GACCGGCGCGGCGTGCGTGGCGCTGGGCCGCGCGTATCATCTGTTTCGCCTGGCGCTGCTGGCGACCGCGGATTTTGTGCAGTGCCTGGGCGGCAGCACC
GGCCCGTTTGAAGAACGCGGCCATCTGCCGAAAAACCATAGCGGCCAGGTGATTGTGGCGCGCGAAATTCGCAAACTGCTGGCGGGCAGCCAGCTGACC
AGCGATCATCAGGATCTGATGAAAGAAATGGTGGCGCGCAGCGGCGTGGGCAACGATGTGGTGGATACCGGCGTGTATCTGCAGGATGCGTATACCCTG
CGCGCGGTGCCGCAGATTCTGGGCCCGGTGCTGGATACCCTGGATTTTGCGCGCAAACTGATTGAAGAAGAACTGAACAGCACCAACGATAACCCGCTGA
TTTTTGATGTGCCGGAACAGACCTTTCATGGCGCGAACTTTCATGGCCAGTATGTGGCGATGGCGTGCGATTATCTGAACATTGCGGTGACCGAAATTGGC
GTGCTGGCGGAACGCCAGCTGAACCGCCTGGTGGATCCGAACATTAACGGCAAACTGCCGCCGTTTCTGGCGAGCGCGCATAGCGGCCTGCTGTGCGGCT
TTGAAGGCGGCCAGTATCTGGCGACCAGCATTGCGAGCGAAAACCTGGATCTGGCGGCGCCGAGCAGCATTAAAAGCCTGCCGAGCAACGGCAGCAACC
AGGATGTGGTGAGCATGGGCACCACCAGCGCGCGCAAAAGCCTGCGCCTGTGCGAAAACGTGGGCACCATTGTGAGCACCCTGATTGCGGCGTGCAACC
AGGCGGGCCATATTCTGGGCAACGAACGCTTTAGCCCGCCGATTCGCGAACTGCATGGCGAACTGAGCCGCAGCGTGCCGCTGTATCAGGATGATAGCCC
GATTTTTGAACTGTTTCAGACCGTGCGCGCGTTTGTGGGCGGCGATGGCTTTCGCGCGCATCTGGTGACCCATCTGGATCTGGCGGCGACCACCGCGAGCA
GCCTCGAGCCTACTCCGACTCCTACCACCCCAACCCCAACACCGACCACGCCCACTCCGACTCCCACCTCTGGTCCAGCTGGTTGCCAAGTTCTGTGGGGAG
TAAACCAGTGGAATACGGGCTTTACTGCGAACGTCACAGTGAAGAATACCAGTTCTGCCCCGGTGGATGGCTGGACCTTAACGTTCTCGTTTCCGTCAGGT
CAGCAAGTCACTCAAGCCTGGTCGTCCACGGTAACGCAATCCGGTAGTGCGGTGACCGTTCGTAACGCACCGTGGAATGGAAGCATTCCCGCTGGTGGTA
CGGCTCAGTTCGGGTTCAATGGCAGCCATACGGGGACCAATGCAGCACCGACCGCCTTTAGCCTCAATGGCACACCGTGTACCGTGGGCTAA

7.2 Stability of wt PALs in ammonium carbonate and ammonium sulfate buffers

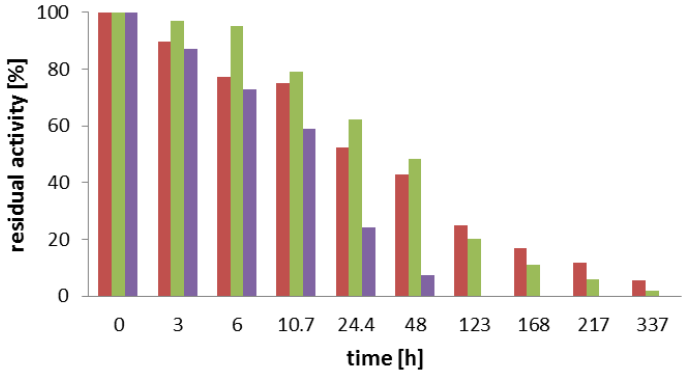

Figure 48: Residual volumetric activity after incubation of purified *Pc*PAL2 in ammonium carbonate buffer, pH 8.9 (red) and ammonium sulfate buffer pH 9.2 (green) or pH 10.6 (purple). Incubation conditions: 8-9 mg lyophilized enzyme in 1.5 ml of the respective buffer at 30 °C and 300 rpm.

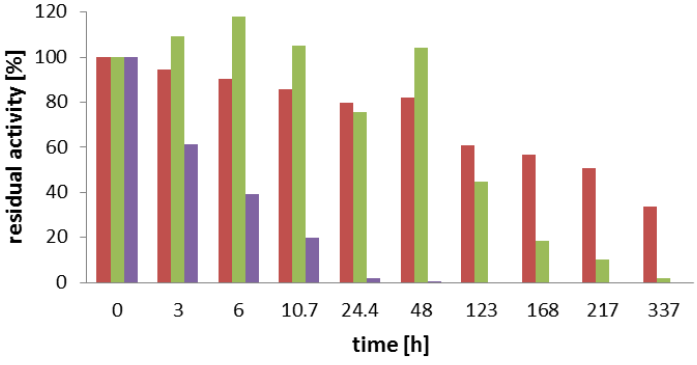

Figure 49: Residual volumetric activity after incubation of purified *Rt*PAL in ammonium carbonate buffer, pH 8.9 (red) and ammonium sulfate buffer pH 9.2 (green) or pH 10.6 (purple). Incubation conditions: 8-9 mg lyophilized enzyme in 1.5 ml of the respective buffer at 30 °C and 300 rpm.

7.3 Amination of cinnamic acid and derivatives

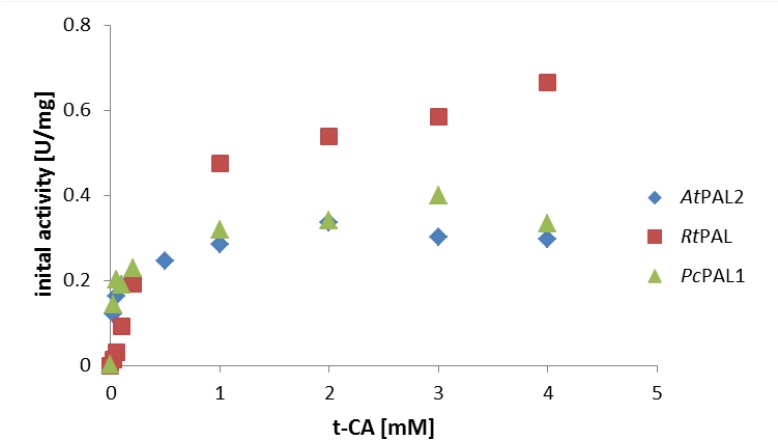

Figure 50: Michaelis Menten kinetics for the amination of t-CA catalyzed by purified wt PALs. Assay conditions: 30 °C, 0.2-10 mm cuvette, 5 M NH_3, pH 10, 5-20 µl enzyme solution, 0.5 - 1 ml assay volume, 1- 2 min measuring time; 0-4 mM t-CA, 275 nm.

Table 20: Decrease in *ee* at time point of maximum conversion in the amination of CAs with wt PALs in lyophilized *E. coli* whole cells.

c) 3-F-CA, 50 mM
f) 3-Cl-CA, 5 mM
h) 2-OH-CA, 5 mM
i) 3-OH-CA, 5 mM

	***Pc*PAL1**			***At*PAL2**			***Rt*PAL**		
	conv.	time [h]	*ee**	conv.	time [h]	*ee**	conv.	time [h]	*ee**
c							89.3	21.6	98
f							89.7	2.9	96
h	42.7	23.9	98	57.7	23.9	98			
i	87.0	23.9	97	87.7	23.9	97	75.5	23.9	96

Reaction conditions: x mM x-CA in 2.5 M $(NH_4)_2CO_3$, pH 8.9, 30 °C, 1 ml volume, 1200 rpm, cell load: 1 mg/ml (*Pc*PAL1, *At*PAL2) or 5 mg/ml (*Rt*PAL); * *ee* of the L-enantiomer.

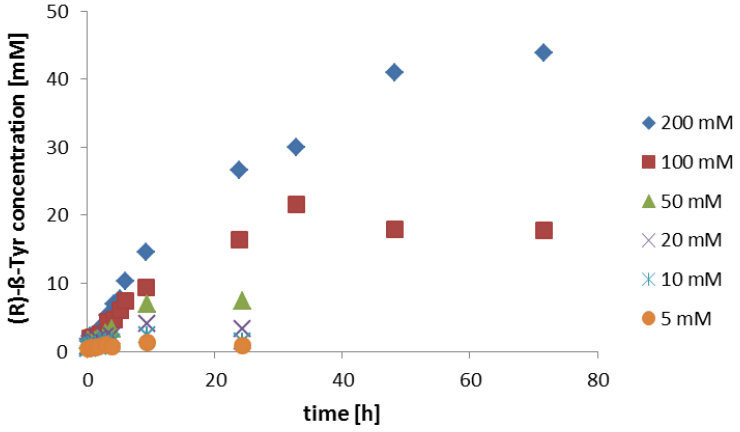

Figure 51: (*R*)-β-Tyr formation from 4-OH-CA with whole cells containing *Cc*TAM. Reaction conditions: 5 - 200 mM 4-OH-CA in 2.5 M $(NH_4)_2CO_3$, pH 8.9, 30 °C, 1 ml volume, 1200 rpm, cell load: 100 mg/ml.

7.4 Sequence alignment PAMs

```
                1       10        20        30        40        50        60        70        80        90       100       110       120       130
                |--------+---------+---------+---------+---------+---------+---------+---------+---------+---------+---------+---------+---------|
TchPAM          MGFAVESRSHVKDILGLINAFNEVKKITVDGTTPITVAHVAALARRHDVKVALEAEQCRARVETCSSWVQRKAEDGADIYGVTTGFGACSSRRTNRLSELQESLIRCLLAGVFTKGCAPSVDELPATATR
TcaPAM          MGFAVESRSHVKDILGLINTFNEVKKITVDGTTPITVAHVAALARRHDVKVALEAEQCRARVETCSSWVQRKAEDGADIYGVTTGFGACSSRRTNQLSELQESLIRCLLAGVFTKGCASSVDELPATATR
Consensus       MGFAVESRSHVKDILGLINaFNEVKKITVDGTTPITVAHVAALARRHDVKVALEAEQCRARVETCSSWVQRKAEDGADIYGVTTGFGACSSRRTNrLSELQESLIRCLLAGVFTKGCApSVDELPATATR

                131     140       150       160       170       180       190       200       210       220       230       240       250       260
                |--------+---------+---------+---------+---------+---------+---------+---------+---------+---------+---------+---------+---------|
TchPAM          SAMLLRLNSFTYGCSGIRWEVMERLEKLLNSNVSPKVPLRGSVSASGDLIPLAYIAGLLIGKPSYIARIGDDVEYPAPEALSRVGLRPFKLQAKEGLALVNGTSFATAVASTVMYDANVLLLLVETLCGM
TcaPAM          SAMLLRLNSFTYGCSGIRWEVMERLEKLLNSNVSPKVPLRGSVSASGDLIPLAYIAGLLIGKPSVYARIGDDVEVPAPEALSRVGLRPFKLQAKEGLALVNGTSFATALASTVMYDANVLLLLVETLCGM
Consensus       SAMLLRLNSFTYGCSGIRWEVMERLEKLLNSNVSPKVPLRGSVSASGDLIPLAYIAGLLIGKPSVyARIGDDVEVPAPEALSRVGLRPFKLQAKEGLALVNGTSFATAlASTVMYDANVLLLLVETLCGM

                261     270       280       290       300       310       320       330       340       350       360       370       380       390
                |--------+---------+---------+---------+---------+---------+---------+---------+---------+---------+---------+---------+---------|
TchPAM          FCEVIFGREEFAHPLIHKVKPHPGQIESAELLEWLLRSSPFQELSREYYSIDKLKKPKQDRYALRSSPQWLAPLVQTIRDATTTVETEVNSANDNPIIDHANDRALHGANFQGSAVGFYMDYVRIAVAGL
TcaPAM          FCEVIFGREEFAHPLIHKVKPHPGQIESAELLEWLLRSSPFQDLSREYYSIDKLKKPKQDRYALRSSPQWLAPLVQTIRDATTTVETEVNSANDNPIIDHANDRALHGANFQGSAVGFYMDYVRIAVAGL
Consensus       FCEVIFGREEFAHPLIHKVKPHPGQIESAELLEWLLRSSPFQ#LSREYYSIDKLKKPKQDRYALRSSPQWLAPLVQTIRDATTTVETEVNSANDNPIIDHANDRALHGANFQGSAVGFYMDYVRIAVAGL

                391     400       410       420       430       440       450       460       470       480       490       500       510       520
                |--------+---------+---------+---------+---------+---------+---------+---------+---------+---------+---------+---------+---------|
TchPAM          GKLLFAQFTELMIEYYSNGLPGNLSLGPDLSVDYGLKGLDIAMAAYSSELQYLANPVTTHVHSAEQHNQDINSLALISARKTEEALDILKLMIASHLTAMCQAVDLRQLEEALYKVVENVVSTLADECGL
TcaPAM          GKLLFAQFTELMIEYYSNGLPGNLSLGPDLSVDYGLKGLDIAMAAYSSELQYLANPVTTHVHSAEQHNQDINSLALISARKTEEALDILKLMIASHLTAMCQAVDLRQLEEALYKVVENVVSTLADECGL
Consensus       GKLLFAQFTELMIEYYSNGLPGNLSLGPDLSVDYGLKGLDIAMAAYSSELQYLANPVTTHVHSAEQHNQDINSLALISARKTEEALDILKLMIASHLTAMCQAVDLRQLEEALYKVVENVVSTLADECGL

                521     530       540       550       560       570       580       590       600       610       620       630       640       650
                |--------+---------+---------+---------+---------+---------+---------+---------+---------+---------+---------+---------+---------|
TchPAM          PNDTKARLLYVAKAVPVYTYLESPCDPTLPLLLGLKQSCFDTILALHKKDGIETDTLVDRLAEFEKRLSDRLENEMTAVRVLYEKKGHKTADNNDALVRIQGSKFLPFYRFVREELDTGVMSARREQTPQ
TcaPAM          PNDTKARLLYVAKAVPVYTYLESPCDPTLPLLLGLEQSCFGSILALHKKDGIETDTLVDRLAEFEKRLSDRLENEMTAVRVLYEKKGHKTADNNDALVRIQGSRFLPFYRFVREELDTGVMSARREQTPQ
Consensus       PNDTKARLLYVAKAVPVYTYLESPCDPTLPLLLGLeQSCFdsILALHKKDGIETDTLVDRLAEFEKRLSDRLENEMTAVRVLYEKKGHKTADNNDALVRIQGSrFLPFYRFVREELDTGVMSARREQTPQ

                651     660       670       680       690       700   706
                |--------+---------+---------+---------+---------+-----|
TchPAM          EDVQKVFDAIADGRITVPLLHCLQGFLGQPNGCANGV----------LEHHHHHH
TcaPAM          EDVQKVFDAIADGRITVPLLHCLQGFLGQPNGCANGVESFQSVWNKSALEHHHHHH
Consensus       EDVQKVFDAIADGRITVPLLHCLQGFLGQPNGCANGV..........LEHHHHHH
```

Figure 52: Sequence alignment of *Tca*PAM and *Tch*PAM performed with the online tool "Multalin version 5.4.1" http://multalin.toulouse.inra.fr/multalin/cgi-bin/multalin.pl

8 Publications

Poster presentations (presenting author underlined)

A. Dreßen, U. Mackfeld, T. Hilberath, M. Pohl (2015)
"Phenylalanine ammonia lyase from *A. thaliana* for the production of unnatural amino acids"
BioTrans 2015, Wien, Austria

A. Dreßen, T. Hilberath, M. Pohl, W. Wiechert (2015)
"Immobilization of phenylalanine ammonia lyase from crude extract on cellulose – An easy concept for enzyme printing"
MIE project meeting 2015, Karlsruhe, Germany

9 Acknowledgment

Prof. Dr. Martina Pohl: Thank you for the opportunity to work on this interesting topic in your working group, for creative ideas and motivating discussions and above all for the extraordinary good supervision.

I want to thank **Prof. Dr. Michael Bott** for taking over the position as co-referee and **Prof. Dr. Wolfgang Wiechert** for the opportunity to write this thesis in the institute.

Dr. Ulrich Krauss, Dr. Jan Marienhagen & Dr. Constantin Vogel: Thank you for the kind provision of plasmids, alignments and an *At*PAL2-homology model.

I want to thank **Ursula Mackfeld und Thomas Hilberath** for the commitment and successful work that has brought this project to progress.

Thanks to the working group **"Biocatalysis and Biosensors"** for the good working atmosphere, the great helpfulness and valuable practical advice. My special thanks go to Victoria Steffen, who has spent a lot of time at the beginning of my work for an introduction into the "secrets of molecular biology".

Thanks also to **Office 126** for providing me nourishment for nerves manufactured by “Lindt & Sprüngli” and encouraging words whenever necessary, and for many valuable discussions and funny moments.

Finally, I want to thank **my family** for their continuous support without which I would not have come this far.

Band / Volume 119
First-principle investigation of displacive response in complex solids
D. A. Klüppelberg (2016), xi, 179 pp
ISBN: 978-395806-123-1

Band / Volume 120
Beam Cooling at COSY and HESR - Theory and Simulation -
Part 1 Theory
H. Stockhorst, T. Katayama and R. Maier (2016), v, 192 pp
ISBN: 978-3-95806-127-9

Band / Volume 121
Scanning tunneling microscopy of single-molecule magnets and hybrid-molecular magnets: Two approaches to molecular spintronics
V. Heß (2016), x, 127 pp
ISBN: 978-3-95806-128-6

Band / Volume 122
Bulk and surface sensitive energy-filtered photoemission microscopy using synchrotron radiation for the study of resistive switching memories
M. C. Patt (2016), viii, 247 pp
ISBN: 978-3-95806-130-9

Band / Volume 123
Group IV Epitaxy for Advanced Nano- and Optoelectronic Applications
S. Wirths (2016), vi, 116, XXX pp
ISBN: 978-3-95806-132-3

Band / Volume 124
Strained Silicon-Germanium/Silicon Heterostructure Tunnel FETs for Low Power Applications
S. Blaeser (2016), iv, 91, xvii pp
ISBN: 978-3-95806-135-4

Band / Volume 125
Nanocavity Arrays for Extracellular Recording and Stimulation of Electroactive Cell Systems
A. Czeschik (2016), x, 162 pp
ISBN: 978-3-95806-144-6

Band / Volume 126
Band Structure Engineering in 3D Topological Insulators Investigated by Angle-Resolved Photoemission Spectroscopy
M. Eschbach (2016), VIII, 153 pp
ISBN: 978-3-95806-149-1

Band / Volume 127
Dynamics in colloid and protein systems: Hydrodynamically structured particles, and dispersions with competing attractive and repulsive interactions
J. Riest (2016), ix, 226 pp
ISBN: 978-3-95806-153-8

Band / Volume 128
Self-purifying $La_{2/3}Sr_{1/3}MnO_3$ epitaxial films: Observation of surface precipitation of Mn_3O_4 particles for excess Mn ratios
A. Steffen (2016), 154 pp
ISBN: 978-3-95806-162-0

Band / Volume 129
Strain and electric field mediated manipulation of magnetism in $La_{(1-x)}Sr_xMnO_3/BaTiO_3$ heterostructures
M. Schmitz (2016), VI, 141 pp
ISBN: 978-3-95806-164-4

Band / Volume 130
High-Throughput Live-Cell Imaging for Investigations of Cellular Heterogeneity in *Corynebacterium glutamicum*
S. Helfrich (2016), xvi, 217 pp
ISBN: 978-3-95806-167-5

Band / Volume 131
Laser-Induced Ultrafast Electron- and Spin-Dynamics in the Electronic Band Structure of Co(001)
M. A. Plötzing (2016), ii, 109, XXXIV pp
ISBN: 978-3-95806-168-2

Band / Volume 132
Robot-Assisted Phenotyping of Genome-Reduced *Corynebacterium glutamicum* Strain Libraries to Draft a Chassis Organism
S. Unthan (2016), 122 pp
ISBN: 978-3-95806-169-9

Band / Volume 133
Characterization of amino acid ammonia lyases & aminomutases for the production of chiral α- and β-amino acids
A. Dreßen (2016), ix, 112 pp
ISBN: 978-3-95806-176-7

Schlüsseltechnologien /
Key Technologies
Band / Volume 133
ISBN 978-3-95806-176-7